Switched System Stability and Stabilization for Fighter Aircraft

Thesis submitted for the degree of

Doctor of Philosophy

at the University of Leicester

by

Emre Kemer

Department of Engineering

University of Leicester

2017

For my family:

Ummahan and Hamza

Switched System Stability and Stabilization for Fighter Aircraft

Emre Kemer

Abstract

This thesis presents stability and performance analyses for switched systems subject to arbitrary and constrained switching signals. Analysis techniques based on common quadratic Lyapunov functions are first introduced as these can be very effective in coping with arbitrary, unconstrained switching signals. However, for systems subject to switching signals which are time constrained, less conservative tools, based on dwell-time analysis, are introduced and extended for the computation of $\mathcal{L}_2$-gain estimates. Robust $\mathcal{L}_2$-gain and $\mathcal{H}_2$ state-feedback controllers syntheses follow from this analysis. An $\mathcal{L}_2$ performance analysis tool, for piecewise linear systems, is also given and used to the design of piecewise linear state-feedback controllers. The performance analysis and controller synthesis techniques mentioned above have been applied to the control of the longitudinal axis of the ADMIRE aircraft fighter benchmark model. Simulations show that a switched state-feedback controller provides better tracking than a simple LQR feedback gain.

Acknowledgements

I am thankful to Almighty ALLAH (c.c) who has provided me with enough energy and the ability to overcome all difficulties encountered during my PhD.

I would like to express my deep gratitude to Dr. Emmanuel Prempain for his valuable time and fruitful discussions. Without his support and guidance, this work would not have been possible. I would like to thank Professor Matt Turner for providing some crucial commentary during my APG transfer and second year assessment. I would also like to thank my fellow lab members. I am thankful for the numerous discussions and comments that I received from my friends, Ali Polat and Hasan Başak. I would like to thank Dr. Mark Watkins who has helped to improve the flow of this thesis.

There are many friends (too many to name, especially Aykan Toma, Veysi Yıldız, Dr Mustafa Köse, M. Şükrü Kurt, Hüsameddin Ateş, etc.) whose support and friendship made my time in UK more enjoyable. I am thankful to all of them. The support of the Ministry of National Education, Republic of Turkey is gratefully acknowledged.

Most especially, I would like to thank my wife Ummahan, my son Hamza, my parents and all my family members for their boundless love, support and patience.

Contents

List of Figures

List of Tables

Nomenclature and Abbreviations

$\mathbb{N}$	set of natural numbers
$\mathbb{R}$	set of real numbers
$\mathbb{R}^n$	set of n-tuples of elements belonging to the set $\mathbb{R}$
$\mathbb{R}^{k\times l}$	set of k-by-l real matrices
$\mathbb{X}_i$	set of regions
$\mathcal{I}$	the index set of regions
$\in$	belongs to
$\forall$	for all
$\Longrightarrow$	implies
A'	transpose of A
$A' = A > 0$	A is symmetric positive definite matrix
$Tr(A)$	Trace of a square matrix A
`diag`	block diagonal matrix
$s \geq 0$	every entry of s is nonnegative
$\dot{x}$	derivative of x with respect to time, $\frac{dx}{dt}$
$\frac{\partial f}{\partial x}$	a partial derivative of a function with respect to x
$\triangleq$	equal to by definition

$f : A \to B$	A function f mapping a set A into a set B	
$\|.\|$	Euclidean norm (vectors) or included spectral norm (matrices)	
$\mathcal{H}_\infty$	Set of asymptotically stable transfer functions G, with $\|\mathrm{G}\|_\infty$	
γ	$\mathcal{L}_2$ performance gain	
υ	$\mathcal{H}_2$ optimal gain	
DC	Direct current	
SISO	Single-Input-Single-Output	
MIMO	Multi-Input-Multi-Outputs	
LMIs	Linear Matrix Inequalities	
LQR	Linear Quadratic Regulator	
LQG	Linear Quadratic Gaussian	
PDLF	Parameter Dependent Lyapunov Function	
PILF	Parameter Independent Lyapunov Function	
PWL	Piecewise Linear	
BRL	Bounded Real Lemma	
ADMIRE	Aero-Data Model in a Research Environment	
FCS	Flight Control System	
M	Mach number	(-)
h	altitude	(m)
α	angle of attack	(deg)
q	pitch rate	(deg/s)
θ	pitch angle	(deg)
V_T	total velocity	(m/s)
n_z	load factor	(g)
u_{dist}	turbulence in x axis	(m/s)
v_{dist}	turbulence in y axis	(m/s)
w_{dist}	turbulence in z axis	(m/s)
p_{dist}	turbulence around roll axis	(rad/s)

t_{ss}	throttle setting	(-)
δ_{loe}	left outer elevon deflection	(deg)
δ_{lie}	left inner elevon deflection	(deg)
δ_{roe}	right outer elevon deflection	(deg)
δ_{rie}	right inner elevon deflection	(deg)
δ_e	symmetric elevon deflection	(deg)
δ_{lc}	left canard deflection	(deg)
δ_{rc}	right canard deflection	(deg)

CHAPTER 1

Introduction

1.1 Background and Motivation

Control theories are generally categorized into two different analytical methods. The first is called "traditional or classical control theory", and was started in the late 1930's. Classical control theory is based on frequency response methods, the root locus technique, Laplace transforms and transfer functions. The main advantages of these methods are their simplicity and their ease of use in control system design in real applications. These features were especially important before the inception of high-speed digital computers. Hence, the analysis techniques, mainly Bode, Nyquist and root-locus, can be used without the need for a computer. Therefore, their major advantage - being simple - disappears when the system becomes more complex (Nelson, 1998).

Traditional control methods are directly applied for only single-input, single-output (SISO) systems, which are linear time invariant. Using these methods, desired time responses and robustness qualities can be achieved by selecting the place of the closed-loop poles with a single feedback gain. Using consecutive closure of single loops, the tradi-

tional control methods treat the system as if it has multi-input, multi-output (MIMO) or multi-control loops. In this case, these methods involve a considerable amount of trial and error. Hence, placing the closed-loop poles in the MIMO systems becomes more complex and difficult than in SISO systems. Thus, using the traditional control methods for MIMO systems becomes more difficult because of the consecutive SISO design method (Stevens and Lewis, 1992).

The other systematic theory is mainly called "modern control", which was developed after the 1960's. This technique attracted more attention after the inception of high-speed digital computers which had the computational resources required to solve complex control problems. This theory is based on the state space form of the system that consists of n first-order differential equations. Then, these equations can be incorporated into a matrix vector equation. In modern control theory, if the systems have been formulated as a differential equation, the computer programs/ toolboxes can be used to solve more complex control problems. To design optimal control systems, the optimisation techniques can be applied with modern control theory. Contrary to classical control theory, modern control theory can be directly applied to MIMO systems, which might be linear or non-linear, time-invariant or time-variant. Therefore, time domain and frequency domain responses can be used, in some cases, in modern control theory, for instance the LQG and $\mathcal{H}_\infty$ control (Ogata, 2010).

Considering the advantages and disadvantages of traditional and modern control approaches mentioned, they have been widely used in control applications according to system requirements. In this thesis, we have preferred to use one of the modern control approaches called the Linear Quadratic Regulator (LQR) method. It is one of the most effective methods currently available and it plays a crucial role in many control design approaches. Most recent modern control methodologies, such as LQG and $\mathcal{H}_\infty$, use nearly the same methodology as the LQR method (Levine, 2011). The LQR approach computes a static state-feedback controller gain with a desired performance. Moreover, a switched feedback controller methodology is offered to improve the control performance of the

systems in this thesis.

The influences of feedback control in aircraft design has been recognized since World War II. As a consequence, feedback control has been playing a more crucial role in determining aircrafts' stability and control. Moreover, it is a key issue to meet the performance objectives for present and future aircraft. Hence, control engineers have developed various control techniques for aircraft applications with many stringent safety requirements and control objectives (Gangsaas et al., 1986).

Due to the improvements in aircraft engines, aircraft speed and altitude envelopes have been dramatically extended. Hence, achieving a desired performance using traditional control methods is becoming more difficult for new generations of aircraft. However, modern control theories may provide better performance and lower development costs. For example, linear parameter varying (LPV), gain scheduling, $\mathcal{H}_\infty$, LQR and sliding mode control (SMC) are the existing methods in the literature. This thesis is motivated by the idea that using a switched feedback controller methodology can improve the control performance over the wide flight envelopes of modern aircraft.

Tracking performance of the closed-loop system is a crucial control objective which can be achieved locally, for example, with integral state-feedback controllers. These controllers focus on the local parameters of the system dynamics and designed according to these parameters. However, the system dynamics can change dramatically inside the wide flight envelope. Thus, a single state-feedback controller will not, in most cases, deliver adequate performance across the entire flight envelope. Better tracking performance can be achieved with a switched controller, which consists of locally designed robust state-feedback controllers.

Switched systems and *switched controllers* appear in many applications such as auto pilot design, heating systems, automatic transmissions, communication networks, DC-DC converters, automotive engine control, and so on. Such switched control systems may consist of locally designed controllers switched according to a logic rule designed to meet the desired control objectives (Liberzon and Morse, 1999). A possible switching

controller architecture is shown in Figure 1.1 where the controller consists of N state-feedback gains which are switched according to a state-dependent rule.

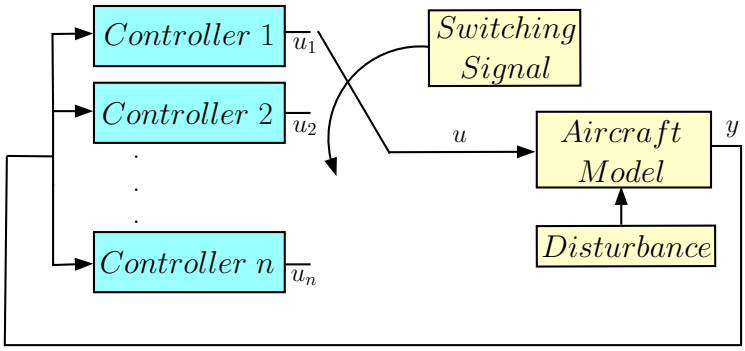

Figure 1.1: Switched controller architecture

Stability analysis techniques have been investigated in the literature. Lyapunov (1892) devised a novel idea relating the energy of dynamic systems to their stability. The stability of any given system can be guaranteed with this idea, so most stability analysis methods use, and try to extend, Lyapunov's idea. This idea claims that if the system initially has a given energy, and the total energy of the system is decreasing with time, then the states of the system will always converge to its equilibrium point.

In *switched systems*, stability cannot be achieved even when each of the subsystems of the total system are stable, or vice versa. Hence, the stability analysis techniques of switched systems are becoming more and more important, and these have been recently addressed in the literature. The switched system stability analysis methods are mostly investigated in two main areas, which are arbitrary switching and constraint switching. The most common methods in the literature are a common quadratic Lyapunov function for arbitrary switching, and time-dependent and state-dependent switching approaches for the constraint switching. In this thesis, these stability analysis methods are investigated and used to prove the stability of the switched system.

Some of the main issues addressed in this thesis are to provide a detailed analysis of the switched system stability and to examine how these analysis techniques can be used to design a switched controller for fighter aircraft.

1.2 Literature Review on the Switched System Stability Analysis

Recently, a considerable amount of literature has been published on the stability of switched systems. Therefore, this section is limited to a review of publications from recent decades.

Branicky (1994) provides some case studies about the stability analysis of switched and hybrid systems. These case studies are focused on the continuous dynamics and the finite dynamics model, which finitely switches among continuous systems. The stability analysis methods, multiple Lyapunov functions (MLF) and iterative function systems (IFS), are introduced to decide the stability of the switched systems. These methods are presented as a tool for analysing Lyapunov stability and proving Lagrange stability, respectively in (Branicky, 1994). Sufficient conditions for continuous dynamics and switching are discussed for both the MLF and IFS cases.

Pettersson and Lennartson (1996b) deal with stability and robustness issues for switched and hybrid systems. The authors examine some drawbacks of the existing theories, which are extensions of classical Lyapunov theory. They have also motivated studies into stability applications that require stronger conditions than the recent theories for hybrid system stability analysis. The candidate Lyapunov functions are formulated as linear matrix inequality (LMI) problems, which can be solved by numerical approaches. They also deal with the problem of how to achieve stability properties. The theory is clarified via an example of a hybrid system. The extended version of their paper is given in (Pettersson and Lennartson, 1996c). The theory suggested in (Pettersson and Lennartson, 1996c) has been extended and applied in the authors' subsequent conference and journal papers. The hybrid systems are specifically examined in (Pettersson and Lennartson, 1996a, 1997b). Pettersson and Lennartson (1999, 2002) have also provided exponential stability and robustness of hybrid systems. Exponential and ordinary stability analysis of non-linear and fuzzy systems are investigated in (Pettersson and Lennartson, 1997a,c).

Johansson and Rantzer (1996) have developed a novel approach for stability analysis of piecewise affine systems. In this technique, a convex optimisation method has been used to find a piecewise quadratic Lyapunov function. This technique has been extended, and improved, the flexibility in the parametrization of Lyapunov functions in (Johansson and Rantzer, 1997a). In addition, these stability analysis methods are extended to performance analysis and optimal controller synthesis for non-linear systems in (Rantzer and Johansson, 1997, 2000). The authors developed this method for a uniform and computationally tractable approach in (Johansson and Rantzer, 1998). Finally, these approaches are collected with a Piecewise Quadratic Lyapunov Function toolbox in Johansson (1999) PhD thesis.

Skafidas et al. (1999) provide the necessary and sufficient conditions to analyse a quadratic, and robust stabilizability of synchronously and asynchronously switched controller systems. The switching occurs at pre-defined switching instants in synchronously switched controller systems. In asynchronously switched controller systems, the switching depends only on the state and can occur at any time. Their paper enhances the results to robust stabilizability via a quadratic storage function. The sufficient conditions for robust output feedback stabilization via synchronously switched controller systems, and the necessary and sufficient conditions for robust stability via synchronously switched controller systems are also given in the authors' previous papers, respectively, (Skafidas et al., 1997; Savkin et al., 1999).

Hespanha (2003) has proposed a new approach to calculate the root mean square (RMS) gain of a switched linear system when there is a large time interval between consecutive switchings. The switching controllers that minimize the closed-loop RMS gain can be designed using these algorithms. Margaliot and Hespanha (2008) have also developed a new method to compute the RMS gain of switched system problems, which tries to characterize the "worst-case" switching law (WCSL). LaSalle's Invariance Principle has been adapted to the specific form of switched linear systems in (Hespanha, 2004a). Asymptotic stability has been proven by using multiple Lyapunov functions. Lie

derivatives of these functions need to be only negative semi-definite. In their paper, the conditions to achieve uniform and exponential stability is also analysed.

Geromel and Colaneri (2005, 2006) have mentioned two different stability strategies for continuous-time switched linear systems used for control synthesis of open-loop (state-independent) and closed-loop (state-dependent) switching rules. The state-independent strategy is based on the determination of a minimum dwell time, whilst the state-dependent strategy is based on the solution of Lyapunov-Metzler inequalities. They have also addressed the determination of a guaranteed cost related to a given control strategy.

Hirata and Hespanha (2009) have introduced non-conservative conditions to compute $\mathcal{L}_2$-induced gain of switched systems. These conditions are given in terms of the common solution of the Hamilton-Jacobi inequalities. Their paper also shows that any switching signal class will give the same induced gain that is attained for the set of all switching signals.

(Shaker et al., 2009) gives a method based on the generalized gramian framework for model reduction to reduce order of switched controllers. In this paper, the stability of closed-loop switched systems for both continuous and discrete time cases is preserved under arbitrary switching signals. The authors have also mentioned one of the drawbacks of their method, which is not assuring the feasibility of a switched system because a common Lyapunov function may not be found consistently.

Wu and Zheng (2009) have reviewed the weighted $\mathcal{H}_\infty$ model for continuous-time linear switched systems via time-variant delay. Sufficient conditions for proving the exponential stability and the weighted $\mathcal{H}_\infty$ performance for the error system has been provided by using the average dwell time method and the piecewise Lyapunov function technique. Illustrative examples have been provided to verify the effectiveness of the given theory.

Zhao, Zhang, and Shi (2013) have addressed the stability problem for a class of switched linear systems with time delays. They have proposed a stability criterion under average dwell time with the extended Lyapunov-Krasovskii functional. In addition,

the stability issue for a class of non-linear switched systems with time delays has been discussed in (Sun and Wang, 2013; Kermani and Sakly, 2014).

Allerhand and Shaked (2010) have pointed out the problem of $\mathcal{H}_\infty$ analysis and controller synthesis for switched linear systems via dwell time. Linear matrix inequalities from robust and optimal control theory have been used in their paper. A piecewise linear quadratic Lyapunov function in time has been used to find and minimize the $\mathcal{L}_2$-gain of uncertain switched systems via dwell time. The proposed Lyapunov function was used to determine the stability of the switched system. The problem of $\mathcal{H}_\infty$ state-feedback control has solved by using this method. This function has also been used to reduce the robust $\mathcal{H}_\infty$ design conservatism in (Boyarski and Shaked, 2009), and solve the problem of stability and stabilization of switched linear systems via dwell time in (Allerhand and Shaked, 2011). Allerhand and Shaked (2013) have applied this proposed function to reduce the design conservatism in linear non-switched systems whose parameters are polytopic uncertainties. The polytope has initially been divided into overlapping subpolytopes, and then the whole system has been treated as a switched system. Illustrative examples have also been given in these papers.

Useful survey papers and books have been published discussing the most important results in the stability of switched systems; for instance, see the survey papers (Michel, 1999; DeCarlo et al., 2000; Hespanha, 2004b; Sun and Ge, 2005; Lin and Antsaklis, 2009) and the books (Brockett, 1993; Morse, 1995; Johansson, 2003; Liberzon, 2003).

1.3 Thesis Organization

The outline of this thesis is graphically illustrated in Figure 1.2. The thesis is divided into six chapters.

- Chapter 2 introduces some basic concepts of Lyapunov analysis and stability analysis of switched systems. *Lyapunov's Indirect and Direct Stability Methods* are presented and a basic definition of switched systems and some stability analysis

methods for the switched systems are given. $\mathcal{H}_2$, LQR controller design methodologies and state-feedback integral controller strategy are also given in this chapter.

- Chapter 3 deals with stability analysis of switched systems which have polytopic parameter uncertainties. A minimum dwell time approach is used to prove the stability of this switched system problem and to find and minimize the $\mathcal{L}_2$-gain of the switched system. State-feedback controller design methodologies have been proposed based on the $\mathcal{L}_2$ performance criteria and the $\mathcal{H}_2$-optimal control technique. Parameter independent Lyapunov functions and parameter dependent Lyapunov functions are also used to derive the methods discussed. Instructive examples are given at the end of each section.

- Chapter 4, based on the existing literature, provides a theoretical background for Chapter 5, and deals with an extended version of state-dependent switching analysis for piecewise linear systems , which are a class of non-linear systems. The piecewise linear systems have different types, such as piecewise linear in input variable u, piecewise linear in time t and piecewise linear in the system state x. In this chapter, the most common case, which is piecewise linear in the system state, is examined. To analyse the stability of the piecewise linear systems, common and piecewise quadratic stability analysis methods have been introduced. These methods are extended to the $\mathcal{L}_2$-gain approach. The lower and upper bounds on cost functions are used to design state-feedback controllers for the piecewise linear systems, and illustrative examples have been given in this chapter.

- Chapter 5 describes the longitudinal control dynamics of the ADMIRE benchmark aircraft model. Constant and switched gain state-feedback controllers have been designed for the ADMIRE model in order to compare the tracking performance between them. The stability and $\mathcal{L}_2$-gain of the ADMIRE aircraft model with the switched state-feedback integral controller is assessed using the methods given in Chapters 3 and 4. Using the control design algorithms of Chapters 3 and 4, the

state-feedback integral controllers are designed for the ADMIRE aircraft model. To see the benefits or drawbacks of the switched controller, constant and switched gain state-feedback controlled ADMIRE models have been simulated. The results of the simulation are discussed at the end of chapter.

- Chapter 6 finally gives concluding remarks on the methods and analysis, and presents a possible future work scheme.

1.4 List of Publications

1. Kemer, Emre, and Emmanuel Prempain. "Switched control for a fighter aircraft." In Control, 2014 UKACC International Conference on, pp. 110-114. IEEE, 2014.

2. Kemer, Emre, and Emmanuel Prempain. "Switched $\mathcal{H}_2$ state-feedback control for polytopic systems based on dwell time" was submitted to the International Journal of Control, Automation and Systems, Springer on 6 June 2016.

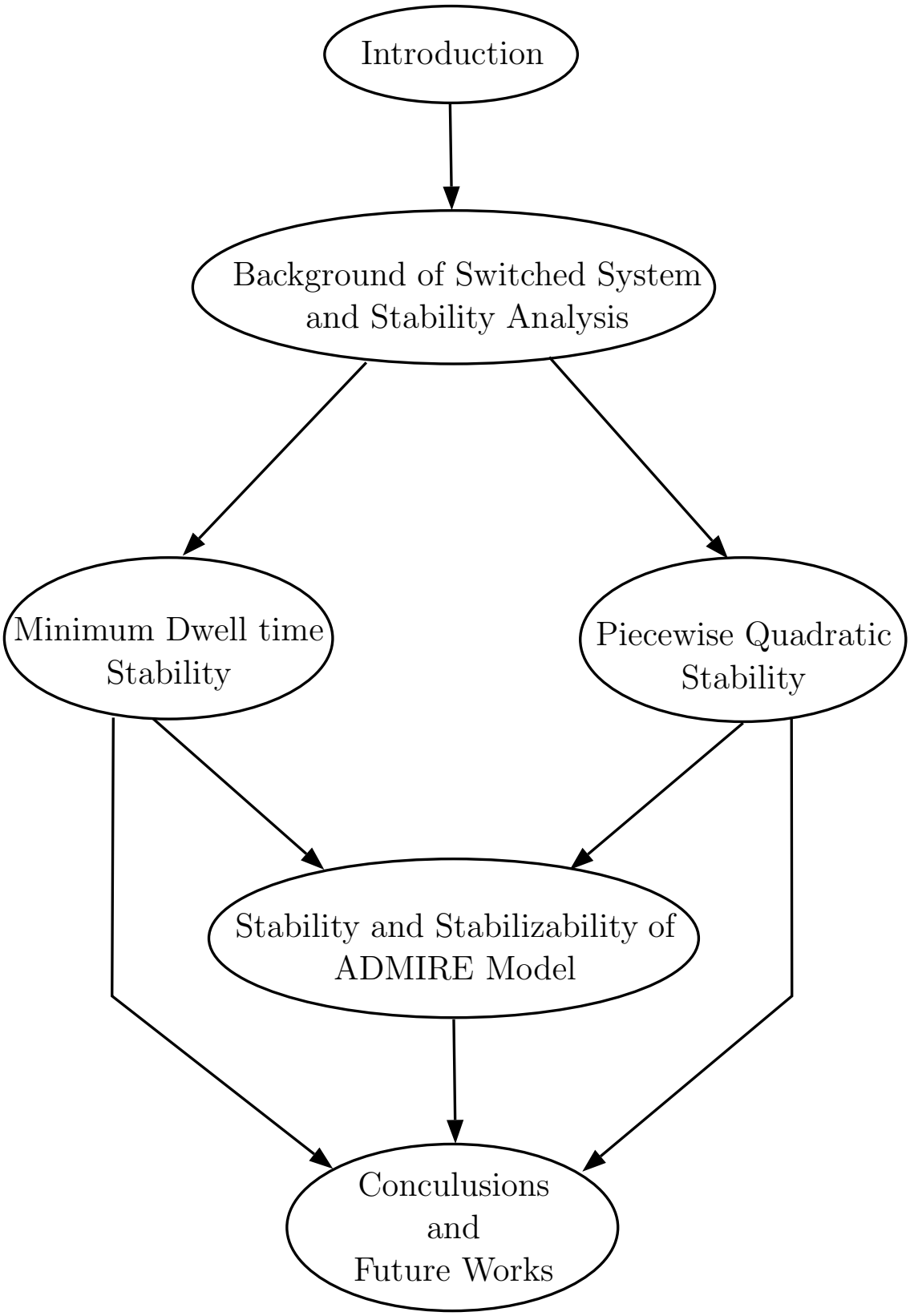

Figure 1.2: Flow chart of the thesis

CHAPTER 2

Background Concepts

2.1 Introduction

This chapter introduces some basic concepts of Lyapunov stability analysis and stability analysis of switched systems. More precisely, the stability of control systems is defined, and Lyapunov approaches are presented to deal with stability. In addition, stability analysis for switched systems is given. The chapter is also concluded with $\mathcal{H}_2$, LQR controller design methodologies and state-feedback integral controller strategy.

2.2 Stability Analysis

Stability analysis plays an important role in control systems. In the literature, different definitions are used for the control system stability. For instance, Khalil (2002) discussed that if a trajectory of the system starts in an initial, constant state called an *equilibrium state*, x_e, and remains in this state without external disturbances, or returns to its equilibrium state after the effect of an external disturbance, then the system is stable.

The stability of systems can be also defined by the time responses of the system in the presence of external step inputs (see Figure 2.1).

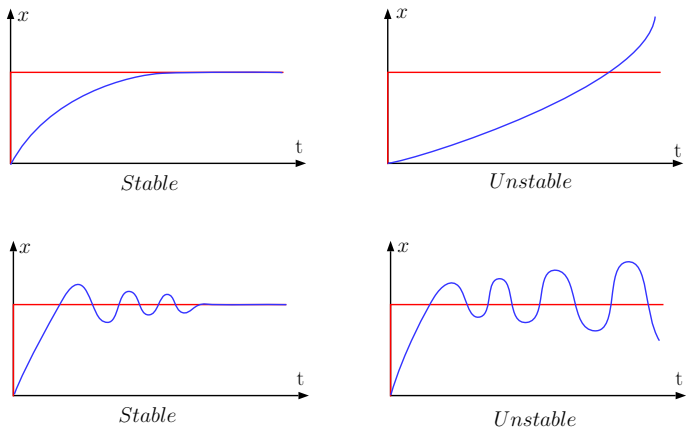

Figure 2.1: System responses in the presence of a step input

In 1892, the Russian mathematician, mechanician and physicist, Aleksandr Mikhailovich Lyapunov, introduced the concept of system stability in his doctoral thesis (Lyapunov, 1892). In this section, we will review some definitions of Lyapunov's stability analysis methods. Stability of equilibrium points is mostly characterized in the sense of Lyapunov which is given in the following definitions.

Definition* 2.2.1*: Consider the non-linear system

$$\dot{x} = f(x) \qquad f : C \to \mathbb{R}^n, \tag{2.1}$$

and x_e is the equilibrium point of (2.1) whenever $f(x_e) = 0$. If there exists $\delta > 0$ for each $\varepsilon > 0$ such that

$$\| x(0) - x_e \| \leq \delta \implies \| x(t) - x_e \| \leq \varepsilon, \text{ for all } t \geq 0$$

then the equilibrium point of (2.1) is stable; otherwise, it is unstable (Ogata, 1990). These conditions assure that system trajectories always remain bounded.

The definition means that an equilibrium point of a system is called stable if all trajectories of the system initially starting at points near the equilibrium point remain nearby; otherwise, it is unstable.

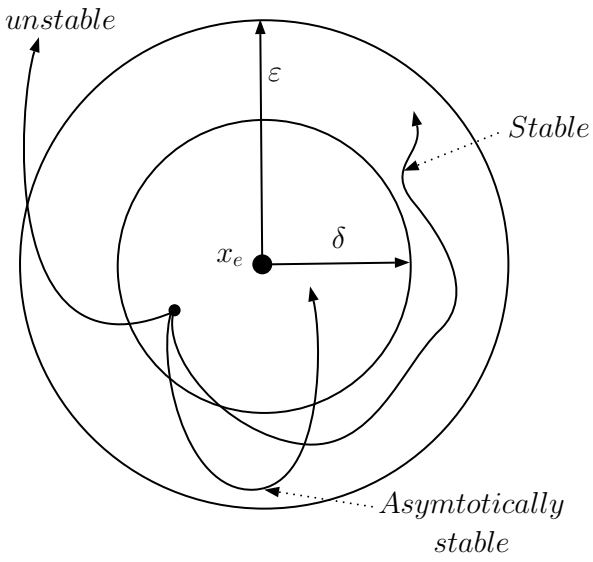

Figure 2.2: System trajectories

***Definition* 2.2.2:** If the equilibrium point of (2.1) is stable according to Definition 2.2.1 and satisfies the condition

$$\| x(0) - x_e \| < \delta \implies \lim_{t \to \infty} x(t) = x_e,$$

then the system (2.1) is *asymptotically stable* for the equilibrium point x_e.

The definition indicates that an equilibrium point of the system is called *asymptotically stable* if all trajectories starting at nearby points of an equilibrium point not only remain nearby but also tend to reach the equilibrium point as time tends to infinity (Khalil, 2002). Both Definitions 2.2.1 and 2.2.2 are illustrated in Figure (2.2).

Note that, if any initial state of the system approaches the equilibrium point, the equilibrium point is called *globally asymptotically stable (or asymptotically stable "in the large")*. Only one equilibrium point in the whole state space can be *globally asymptotically stable* (Ogata, 1990).

Remark: It is assumed that the equilibrium point of the system is always located at the origin, $x_e = 0$. Given any other equilibrium point, $x_e \neq 0$, a change of variables can be applied and a new system having an equilibrium point at $y_e = 0$ can be defined such that

$$
\begin{aligned}
& y = x - x_e \\
& \Rightarrow \dot{y} = \dot{x} = f(x) \\
& \Rightarrow f(x) = f(y + x_e) \triangleq g(y),
\end{aligned}
$$

where the new system is $\dot{y} = g(y)$ and the equilibrium point is $y_e = 0$, as

$$g(0) = f(0 + x_e) = f(x_e) = 0.$$

If $y_e = 0$ is stable for the system $\dot{y} = g(y)$ then x_e is stable for the system (2.1).

2.2.1 Lyapunov's Indirect Method

To determine the local stability of non-linear systems (2.1), Lyapunov's Indirect Method uses the eigenvalues of the linearised system (Slotine and Li, 1991). Consider the non-linear system (2.1) with an equilibrium point $x_e = 0$. The linearised *Jacobian state matrix* is

$$A = \left.\frac{\partial f}{\partial x}\right|_{x_e=0},$$

and the eigenvalues of A are denoted λ_i. The equilibrium point $x_e = 0$ of the system (2.1) can be:

- asymptotically stable if all the real parts of the eigenvalues are negative $(Re\ \lambda_i < 0,\ \forall i)$,
- unstable if one or more of the real parts of the eigenvalues are positive $(Re\ \lambda_i > 0)$,
- either asymptotically stable, stable or unstable if the real part of eigenvalues are negative and at least one of them is zero $(Re\ \lambda_i \leq 0,\ \forall i)$.

Example* 2.1*: Consider the system

$$
\begin{aligned}
\dot{x}_1 &= -x_2 + ax_2^2 - x_1x_2 \\
\dot{x}_2 &= ax_1 - bx_2 + x_1x_2 + x_1^2
\end{aligned}
$$

To investigate stability of the given system at the origin, $x_e = 0$, the Jacobian matrix is defined by

$$\frac{\partial f}{\partial x} = \begin{bmatrix} \frac{\partial f_1}{\partial x_1} & \frac{\partial f_1}{\partial x_2} \\ \frac{\partial f_2}{\partial x_1} & \frac{\partial f_2}{\partial x_2} \end{bmatrix} = \begin{bmatrix} -x_2 & -x_1 + 2ax_2 - 1 \\ 2x_1 + x_2 + a & x_1 - b \end{bmatrix}$$

Evaluating the Jacobian at the origin, $x_e = 0$:

$$A = \frac{\partial f}{\partial x}\Big|_{x_e=0} = \begin{bmatrix} 0 & -1 \\ a & -b \end{bmatrix}$$

The eigenvalues of A are found as

$$\lambda_{1,2} = -\frac{1}{2}(b \pm \sqrt{b^2 - 4a})$$

The equilibrium point, $x_e = 0$, is asymptotically stable when the eigenvalues satisfy the condition $Re\ \lambda_i < 0,\ \forall\ a,\ b > 0$, and it is unstable for all values of a when $b < 0$. If $a > 0$ and b is assumed to be zero, both eigenvalues stay on the imaginary axis, and therefore the stability of the equilibrium point $x_e = 0$ cannot be determined using Lyapunov's indirect method; however, in this case, it can be determined by using Lyapunov's direct (second) method.

2.2.2 Lyapunov's Direct (Second) Method

The stability of the equilibrium point can be determined using the indirect Lyapunov method if the trajectory starts at nearby points. If the trajectory, on the other hand, starts far from the equilibrium point, then the direct Lyapunov method allows us to determine whether the trajectory converges to the equilibrium point, or otherwise, when t approaches ∞.

According to the direct (second) Lyapunov method, concepts of energy and stability are closely related to each other. The important point is that if the total energy of the system continuously decreases with time then the system will eventually reach an equilibrium point regardless of its initial state. To verify the stability of the system, an energy

function is generated and its rate of change is analysed via the direct Lyapunov method (Slotine and Li, 1991).

***Definition* 2.2.3:** Consider the system (2.1) with an equilibrium point $x_e = 0$ and let $V : C \to \mathbb{R}$ be a continuous and differentiable function such that

$$V(0) = 0 \text{ and } V(x) > 0 \to x \in C - \{0\},$$

$$\dot{V}(x) \leq 0 \to x \in C,$$

then the system (2.1) is stable. In addition, if

$$\dot{V}(x) < 0 \to x \in C - \{0\},$$

then the system (2.1) is asymptotically stable (Liberzon, 2003). Here, V can be called the Lyapunov function of the system (2.1). A simple geometrical illustration of the Lyapunov function, $V(x_1, x_2)$ is shown in Figure 2.3.

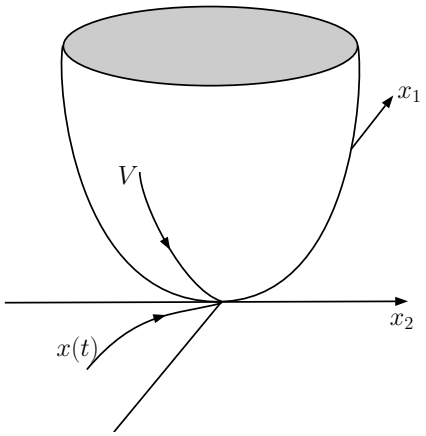

Figure 2.3: Illustration of the Lyapunov function

***Theorem* 2.2.1:** Consider the system (2.1) with an equilibrium point $x_e = 0$ and let $V : \mathbb{R}^n \to \mathbb{R}$ be a continuous and differentiable function such that

$$V(0) = 0 \text{ and } V(x) > 0, \text{ for all } x \neq 0,$$

$$\|x\| \to \infty \Rightarrow V(x) \to \infty,$$

$$\dot{V}(x) \leq 0, \ \forall x,$$

then the system (2.1) is globally stable (Liberzon, 2003). In addition, the system (2.1) is globally asymptotically stable when

$$\dot{V}(x) < 0, \ \forall x \neq 0.$$

Lyapunov stability analysis has drawn considerable amount of attention in literature. There are several articles and books regarding it. Some authors use this method to prove the stability of their application; others try to introduce new approaches based on this method. Switched system stability methods based on the Lyapunov function will be presented in the following section.

2.3 Stability Analysis of Switched Systems

Switched systems appear in many field applications such as heating systems, automatic transmissions, DC-DC converters, and so on. As a consequence, stability analysis and switching stabilization for switched systems has, in recent years, started to take a greater role in research; see (Lin and Antsaklis, 2009, and references therein).

Switched systems are dynamic systems, and are also a simple model of hybrid systems; they are of "variable structure" or are "multi-modal" (Branicky, 1994). Switched systems consist of a finite number of subsystems and logic rules that manage the switching between these subsystems (Pettersson, 2003). Generally, a set of differentials or difference equations describe these subsystems. The switched systems can be categorized according to the dynamics of their subsystems; for instance, continuous-time or discrete-time, linear or non-linear, and so on (Lin and Antsaklis, 2009).

A basic switching controller architecture is shown in Figure 2.4. As can be seen in this figure, the system consists of a number of controllers, and the switching signals orchestrate switching between the controllers in order to obtain stability of the system. The switching signals can be state-dependent, time dependent, or both (Liberzon, 2003).

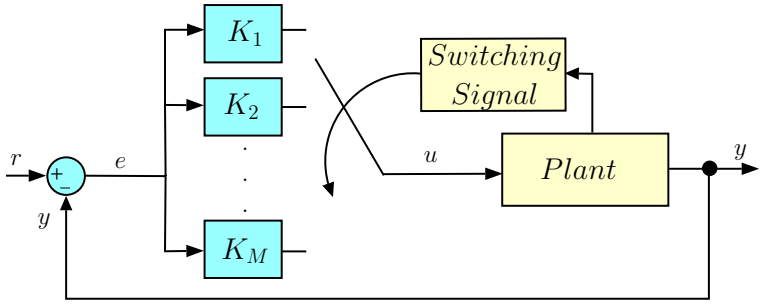

Figure 2.4: Switching Architecture

In this section, we want to define sufficient conditions that can guarantee the stability of a switched system. Stability issues related to switched systems include several interesting results. For instance, the switched systems may be unstable for certain switching signals even when all the subsystems are exponentially stable (Figure 2.5).

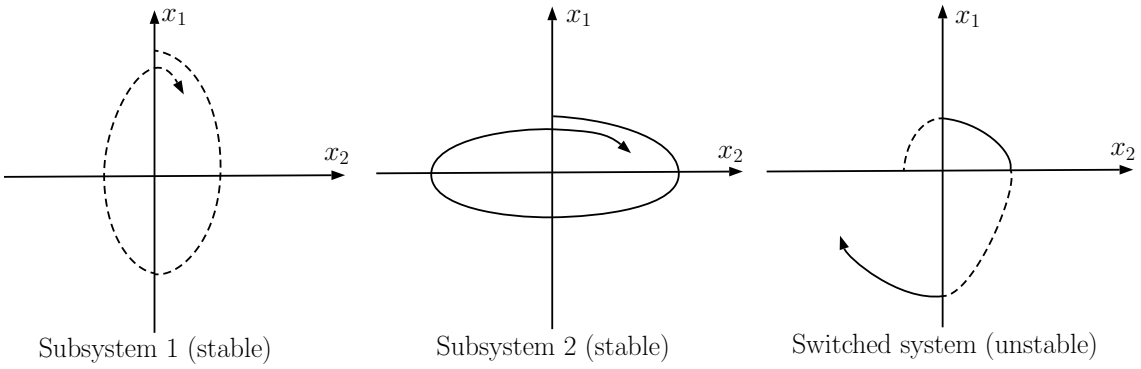

Figure 2.5: Switching between stable systems

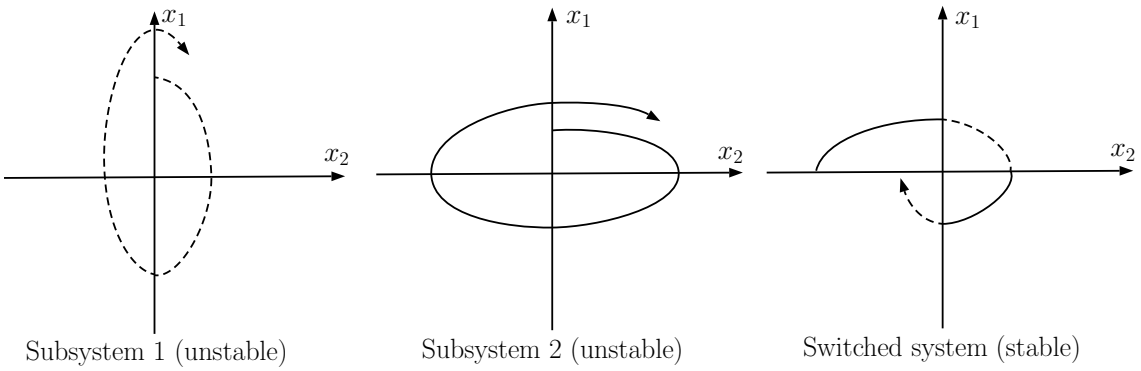

Figure 2.6: Switching between unstable systems

On the other hand, carefully chosen switching signals between unstable subsystems can make the switched system exponentially stable (Figure 2.6). As these examples indicate, the properties of switching signals are just as important as the dynamics of each subsystem for the overall stability of switched systems. So, we roughly analyse the stability of switched systems under two main scenarios. One is the stability analysis of switched systems under arbitrary switching signals; the other is the construction of switching signals for a given collection of subsystems.

2.3.1 Stability of Systems depending on Arbitrary Switching Signals

For the stability analysis problem, we firstly check the stability of the switched system when there is no constraint on the switching signals. All the subsystems have to be asymptotically stable; however, it is still possible to create a divergent trajectory from any initial state even though all the subsystems are exponentially stable. So, generally, the stability assumption of the subsystems is not enough to guarantee stability of switched systems under arbitrary switching conditions. On the other hand, the stability of a switched system is assured under arbitrary switching if a common Lyapunov function exists for all subsystems. Thus, we have focused on the common Lyapunov functions.

Quadratic Stability

Lyapunov (1892) demonstrated that a quadratic Lyapunov function gives a necessary and sufficient condition for the asymptotic stability of linear systems. If a quadratic Lyapunov function exists for all subsystems of the switched system, then the stability of a switched system is guaranteed for any switching rule (Liberzon, 2005). A quadratic Lyapunov function allows us to understand the stability of a switched system under arbitrary switching, so generally the first step is to analyse the linear or non-linear systems. The aim of a quadratic Lyapunov function is to find a common positive definite matrix, P. This matrix satisfies the quadratic Lyapunov function for all individual subsystems.

A linear switched system, mathematically, can be modelled as a differential equation

of the form

$$\dot{x}(t) = A_{\sigma(t)}\, x(t), \quad \forall t \geq 0, \;\; x(0) = x_0 \text{ and } \sigma(t) \in \{1, \ldots, N\} \tag{2.2}$$

where $x(t) \in \mathbb{R}^n$ is the state, x_0 is the initial condition, $\sigma(t) \in \{1, \ldots, N\}$ represents the switching rule between matrices $A_i \in \mathbb{R}^{n \times n},\ i = 1, \ldots, N$. It is known that the requirements for the existence of a common Lyapunov function can be written in terms of LMIs. The following conditions are used by most of the computations:

Lemma* 2.3.1*: To analyse the stability of the switched systems, one possibility is to use a common quadratic Lyapunov function, $V(t) = x(t)'Px(t)$, such that

$$\begin{aligned} &P = P' > 0, \\ &A_i'P + PA_i < 0, \quad \forall i = 1, \ldots, N. \end{aligned} \tag{2.3}$$

If a positive definite matrix, P, exists and satisfies the above Lemma, the switched system (2.2) is globally stable; otherwise, other stability analysis techniques need to be applied to check the stability.

Occasionally, the stability of a switched system can be verified by using the following dual problem: if there exists a set of positive definite matrices, $R_i,\ i \in I$ ($I = \{1, \ldots, N\}$), which satisfy

$$\begin{aligned} R_i = R_i' &> 0, \\ \sum_{i \in I} A_i'\, R_i + R_i A_i &> 0, \end{aligned} \tag{2.4}$$

then (2.3) does not give a feasible solution. The solution of these inequalities shows the inapplicability of the common quadratic function (Johansson and Rantzer, 1998).

Example* 2.2*: Consider a switched linear system, $\dot{x}(t) = A_i x(t)$, with the state matrices

$$A_1 = \begin{bmatrix} -2 & 6 & 1 \\ -1 & -8 & 0 \\ 0 & -1 & -0.1 \end{bmatrix},\ A_2 = \begin{bmatrix} -7 & -1 & 9 \\ -1 & -4 & -1 \\ 0 & 1 & -0.2 \end{bmatrix},\ A_3 = \begin{bmatrix} -8 & -5 & 9 \\ -1 & -4 & -1 \\ 0 & 1 & -4 \end{bmatrix}.$$

Using (2.3) in Lemma 2.3.1, the stability of the switched system is proven with arbitrary switching signals, and a common quadratic Lyapunov matrix is found such that

$$P = \begin{bmatrix} 0.0390 & 0.0107 & -0.0163 \\ 0.0107 & 0.1964 & -0.0072 \\ -0.0163 & -0.0072 & 0.3633 \end{bmatrix}.$$

The common quadratic Lyapunov function approach gives a general solution to the stability problem of a switched system. If the switched system is found to be stable using a common quadratic Lyapunov method, there is no need to apply other stability analysis methods. Hence, the quadratic stability analysis for switched systems is more attractive than other methods since a cell partition and any switching law will not affect the stability of the switched system.

Although the quadratic stability analysis gives a very effective and global solution, it is very conservative for piecewise linear system stability analysis. In some cases, the stability is not guaranteed by the quadratic Lyapunov method even when the switched system is stable. Hence, the switched system stability analysis methods which depend on some constraints can be used to prove stability of a switched system; these methods will be introduced in the following subsection.

2.3.2 Stability of Systems depending on Constrained Switching Signals

Constrained switching may occur naturally due to physical restrictions on the system. Besides this, there are some cases when we have knowledge regarding the reasons under which switching may potentially occur in a switched system, such as state space partitions and their switching rules. By knowing possible switching conditions of the switching signals, we can obtain better stability results for a given system than for arbitrary switching. In this section, we will introduce stability analysis methods for switched systems with constrained switching signals.

Multiple Lyapunov Functions

The multiple Lyapunov functions (MLF's) method is a useful tool for verifying the stability of switched systems (Lin and Antsaklis, 2009). We consider a switched system that can be linear or non-linear, $\dot{x} = f_\sigma(x)$ with the switching signal, $\sigma = \{1, 2\}$, and suppose that both systems $\dot{x} = f_1(x)$ and $\dot{x} = f_2(x)$ are (globally) asymptotically stable. V_1 and V_2 are, respectively, their Lyapunov functions.

When a common Lyapunov function does not exist or is not known, the switched system stability properties depend on σ. We can decide the stability of the system with two different types of MLF's, referred to as continuous and discontinuous.

For the continuous MLF's, each individual subsystem is assumed to be asymptotically stable and the switching times can be defined as $t_n,\ n\ = \{\ 1,\ 2,\ \ldots\}$. If the values of $V_1(t)$ and $V_2(t)$ are equal at each switching time, i.e., $V_{\sigma(t_n-1)}(t_n) = V_{\sigma(t_n)}(t_n)$ for all n, then the system is asymptotically stable. $V_\sigma(t)$ is also a continuous Lyapunov function for the switched system. This condition is shown in Figure 2.7 (left).

On the other hand, the function $V_\sigma(t)$ will more usually be discontinuous. The MLF's, $V_\sigma(t)$, is the combination of the Lyapunov functions of the active subsystem. In this case, each $V_q(t)$, $q = \{1, 2\}$ reduces when the q-th subsystem is active and may increase when the qth subsystem is inactive, as illustrated in Figure 2.7 (right). To prove asymptotic stability of the switched system, the values of $V_q(t)$ are checked at the beginning of each interval when $\sigma\ =\ q$. We can then assure of asymptotic stability if the value of the V_q at the beginning of each interval is greater than the value at the beginning of the next interval on which the q-th subsystem is activated.

Additionally, $V_q(t)$ may increase when the qth subsystem is active as long as this increment is bounded by definite continuous functions, as illustrated in Figure 2.8. See (Liberzon, 2003; Lin and Antsaklis, 2009) and the references therein for details.

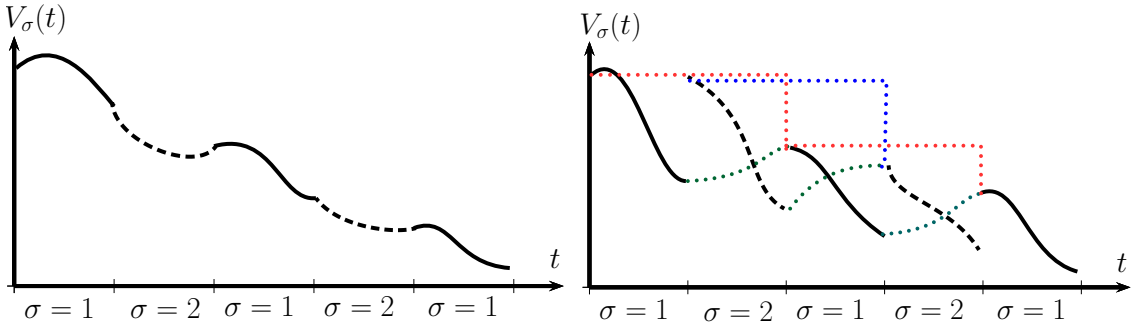

Figure 2.7: Two Lyapunov functions (solid lines represent $V_1(t)$, dashed lines represent $V_2(t)$): continuous $V_\sigma(t)$ (left), discontinuous $V_\sigma(t)$ (right)

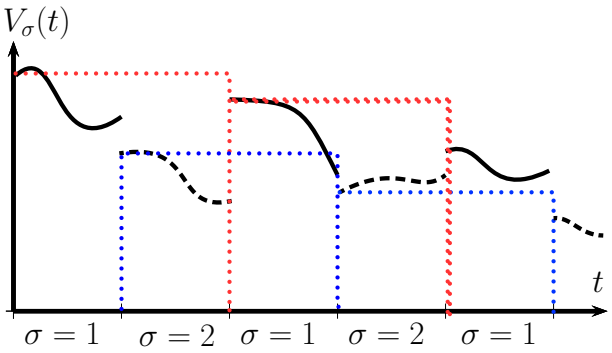

Figure 2.8: Switched systems can be stable even when $V_\sigma(t)$ increases during a definite period.

Stability of Systems depending on Slow Switching Signals

The stability of switched systems can be proven if each subsystem is individually stable and if the switching signals occur sufficiently slowly. This idea was proposed by Liberzon and Morse as a concept of dwell time and average dwell time; see (Liberzon and Morse, 1999).

The conservatism of quadratic stability can be reduced by using a minimum dwell time analysis which consists of introducing a minimum time between switching instants (minimum dwell time, $T > 0$)

$$t_{k+1} - t_k \geq T, \quad \forall k \in \mathbb{N}. \tag{2.5}$$

Definition* 2.3.1*: Dwell time is a time-interval between two switching instants $(t_1, t_2, \ldots)$. It is assumed to be equal or greater than a minimum dwell time T.

$$t_{k+1} - t_k = T_d \geq T, \ \ \forall k \in \mathbb{N}. \tag{2.6}$$

Figure 2.9 shows a geometrical illustration of this notation.

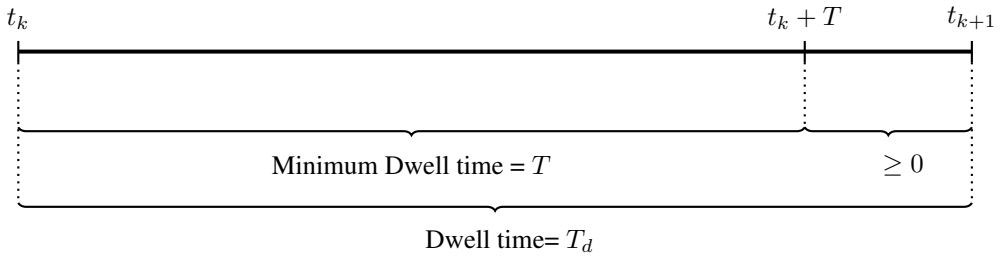

Figure 2.9: Geometrical explanation of the minimum dwell time

The minimum dwell time analysis method is based on MLF's, $V(t) = x(t)'P_i x(t),\ i = \{1, \ldots, N\}$ which can decrease, either continuously or discontinuously, along the state trajectories. Due to this, the minimum dwell time analysis allows discontinuities of the trajectory at the switching instant. The stability of the system can be proved with the following theorem:

Theorem* 2.3.2** (Geromel and Colaneri (2006)):*** Consider a minimum dwell time as defined in (2.5), $T > 0$. If positive definite matrices, P_i, exist and satisfy the condition

$$\begin{aligned} &P_i - e^{A_i' T} P_j e^{A_i T} > 0, \quad i \neq j = 1, \ldots, N \\ &A_i' P_i + P_i A_i < 0, \qquad\quad i = 1, \ldots, N \end{aligned} \tag{2.7}$$

then the system (2.2) is globally asymptotically stable with the switching rule $\sigma(t)$. This theorem gives only a sufficient condition on $\sigma(t)$. Hence, the system (2.2) can be stable even if P_i do not exist. This is because the inequalities in (2.7) are defined as a piecewise quadratic Lyapunov function. Less conservative results can be obtained with more complex Lyapunov functions, as shown in (Chesi et al., 2010; Wirth, 2005).

Proof: Consider the time switching control as $\sigma(t) = i \in \{1, \ldots, N\}$ for all $t \in [t_k, t_{k+1})$, where t_k and t_{k+1} are switching instants satisfying the condition $t_{k+1} = t_k + T_k$ with $T_k \geq T > 0$. The switching control jumps to $\sigma(t) = j \in \{1, \ldots, N\}$ when $t = t_{k+1}$. Using the first inequality (2.7), we have

$$\begin{aligned} V(x(t_{k+1})) &= x(t_{k+1})' P_j x(t_{k+1}) \\ &= x(t_k)' e^{A_i' T_k} P_j e^{A_i T_k} x(t_k) \\ &< x(t_k)' e^{A_i'(T_k - T)} P_i e^{A_i (T_k - T)} x(t_k) \\ &< x(t_k)' P_i x(t_k) = V(x(t_k)), \end{aligned}$$

where we have used the fact, in the second inequality, that $e^{A_i' \zeta} P_i e^{A_i \zeta} \leq P_i$ for all $\zeta = T_k - T \geq 0$. It can be concluded that there exists $\mu \in (0,\, 1)$, such that

$$V(x(t_k)) \leq \mu^k \, V(x_0), \quad \forall k \in \mathbb{N}. \tag{2.8}$$

From the second inequality in (2.7), it can be seen that the time derivative of the Lyapunov function along an arbitrary trajectory of (2.2) satisfies the condition

$$\dot{V}(x(t)) = x(t)'(A_i' P_i + P_i A_i) x(t) < 0, \quad \forall t \in [t_k, t_{k+1}). \tag{2.9}$$

As a result, we conclude that there exist scalars $\alpha > 0$ and $\beta > 0$ such that

$$\|x(t)\|^2 \leq \beta \, e^{-\alpha (t - t_k)} \, V(x(t_k)), \quad \forall t \in [t_k, t_{k+1}), \tag{2.10}$$

which together with (2.8) imply that the equilibrium point, $x_e = 0$, of (2.2) is globally asymptotically stable.

Remark: If all the matrices $\{A_1, \ldots, A_N\}$ are assumed to be stable, the second inequality in (2.7) is consequently always feasible. Then, the first inequality in (2.7) is also satisfied when the dwell time ($T > 0$) is sufficiently large. Note that if $T \to 0$, then $(P_i - P_j) \to 0$, then it follows that $P_i = P_j$ and the quadratic stability conditions (2.3) are thus obtained.

Example 2.3: Consider a switched linear system, $\dot{x}(t) = A_i x(t)$, with the state matrices

$$A_1 = \begin{bmatrix} -2 & 0 & 3 \\ -2 & -1 & 0 \\ 1 & 1 & -1 \end{bmatrix}, \quad A_2 = \begin{bmatrix} -1 & 0.1 & 0 \\ 0 & -2 & 0 \\ 1 & 2 & -1 \end{bmatrix},$$

$$A_3 = \begin{bmatrix} 1 & 1 & 6 \\ -1 & -1 & -5 \\ 0 & 2 & -1 \end{bmatrix}, \quad A_4 = \begin{bmatrix} -1 & 0.2 & 5 \\ -1 & -1 & -4 \\ 0 & 0 & -1 \end{bmatrix}.$$

The quadratic stability method does not give a solution for this switched system. However, the eigenvalues of each of the subsystems lie in the negative half plane, which thus implies stability in each of the individual subsystems. Hence, the stability of the system can be proven if the switching signals occur sufficiently slowly. The inequalities in Theorem 2.3.2 are solved using the LMI control toolbox in MATLAB (Gahinet et al., 1995). Then, the Lyapunov function matrices, P_i, are found to have a minimum dwell time, $T = 2.142\,s$, such that

$$P_1 = \begin{bmatrix} 0.6769 & -0.1042 & 0.5322 \\ -0.1042 & 0.9159 & 0.7425 \\ 0.5322 & 0.7425 & 2.2315 \end{bmatrix}, \quad P_2 = \begin{bmatrix} 0.7945 & 0.3123 & 0.2140 \\ 0.3123 & 0.9407 & 0.2963 \\ 0.2140 & 0.2963 & 0.7923 \end{bmatrix},$$

$$P_3 = \begin{bmatrix} 0.7290 & 0.7834 & 0.3404 \\ 0.7834 & 1.4886 & 0.2472 \\ 0.3404 & 0.2472 & 1.5401 \end{bmatrix}, \quad P_4 = \begin{bmatrix} 0.3110 & 0.1744 & 0.2435 \\ 0.1744 & 0.4149 & -0.1075 \\ 0.2435 & -0.1075 & 5.0188 \end{bmatrix}.$$

Stability of Systems depending on State-Dependent Switching Signals

We have discussed the stability analysis of switched systems depending on slow switching signals. Another example of a method by which to relax the common quadratic function is state-dependent switching. In this case, the state space is divided into a finite or infinite number of regions whose boundaries are called switching surfaces. Whenever the

trajectory of the system hits one of these surfaces, the switching events occur. The stability of the switched system is affected by the properties of the active subsystem when the system is inside the related region. The behaviour of the subsystem does not affect the switched system when the system is outside the related region.

***Example* 2.4:** Consider a switched system, $\dot{x}(t) = A_i x(t)$, which contains two state matrices such that

$$A_1 = \begin{bmatrix} -0.4 & 2 \\ -7 & -0.3 \end{bmatrix}, \quad A_2 = \begin{bmatrix} -0.1 & 6 \\ -2 & -0.5 \end{bmatrix}.$$

A common quadratic Lyapunov function cannot be calculated for this switched system thus we analyse the stability of the system with slow and state-dependent switching methods.

The trajectories of each of the subsystems, which are given in Figure 2.10, are stable individually. Also, if it is assumed that the positive Lyapunov matrix, $P = I$, the Lyapunov function of each subsystem, $V_i(t) = x(t)'Px(t)$, can be found as in Figure 2.11. It implies that the energy of the each subsystems tends to zero as time tends to infinity. Hence, the slow switching method in Section 2.3.2 gives a sufficient result when the dwell time, T, is equal to $1.587\,s$.

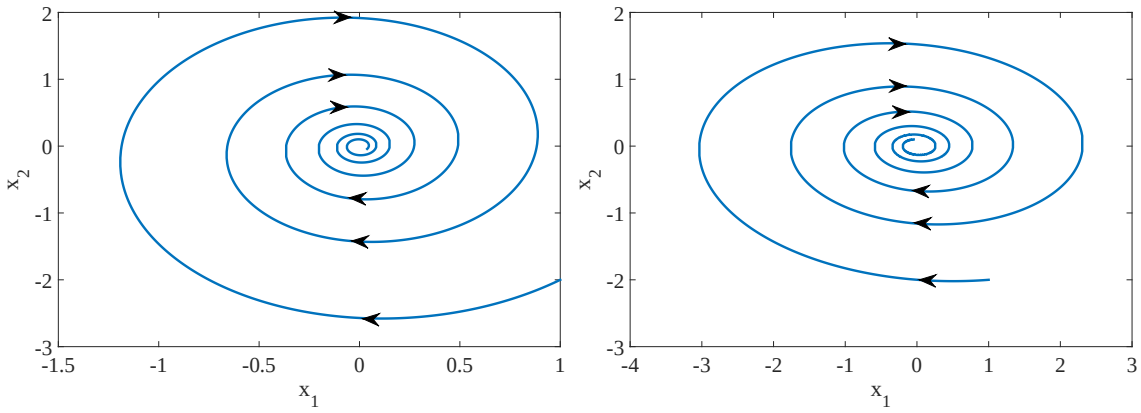

Figure 2.10: Trajectories of each subsystems, left A_1 and right A_2

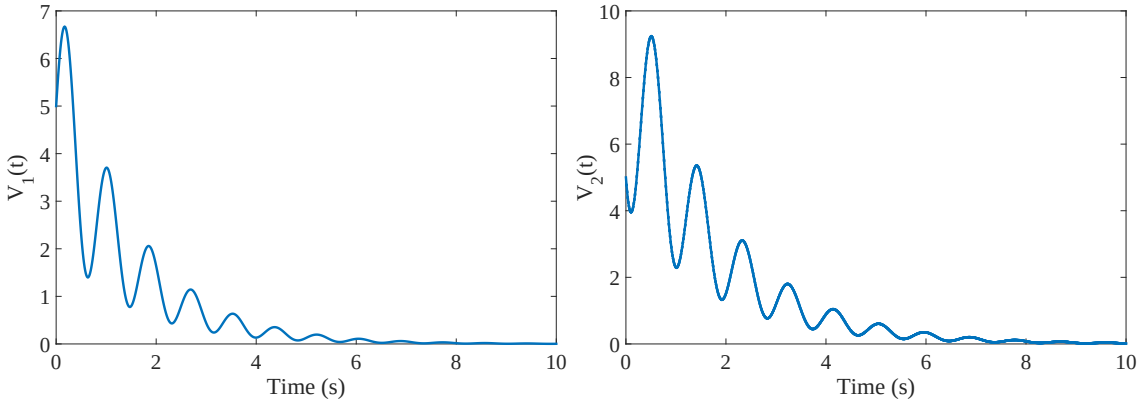

Figure 2.11: Lyapunov functions of each subsystem (left A_1 and right A_2)

According to state-dependent switching, the stability of a switched system can be proven when the following switching law is applied to the system; see Figure 2.12 (left).

$$\dot{x}(t) = \begin{cases} A_1 x, & x_2 > 0 \\ A_2 x, & x_2 \leq 0 \end{cases} \tag{2.13}$$

In addition, if it is assumed that the Lyapunov matrix, $P = I$, takes positive values, then the Lyapunov function of the state-dependent switched system, $V(t) = x(t)'Px(t)$, can be found as shown in Figure 2.12 (right), which proves the stability of the system under the given switching rule (2.13). The vertical dashed lines in the figure show the switching instants.

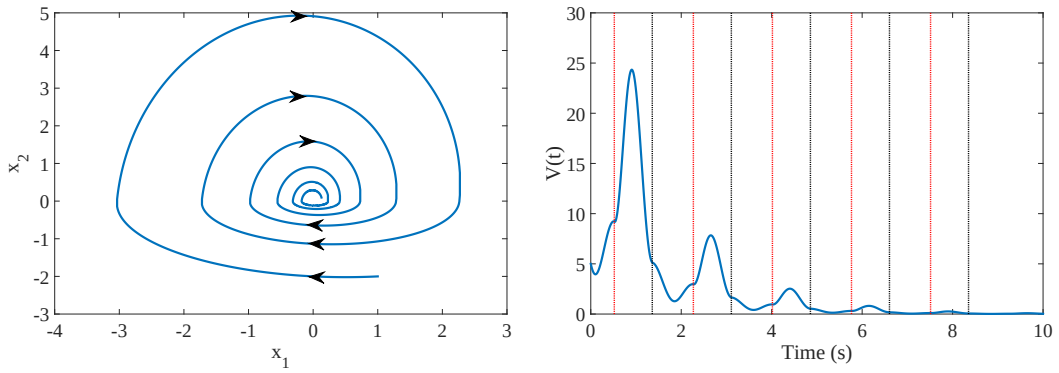

Figure 2.12: Trajectory and Lyapunov function of the state-dependent switched system

On the other hand, the switched system can be unstable for some state-dependent

switching laws such as the following switching rule; see Figure 2.13 (left).

$$\dot{x}(t) = \begin{cases} A_1 x, & x_1 x_2 \leq 0 \\ A_2 x, & x_1 x_2 > 0 \end{cases}$$

Under the above switching rule, the instability of the state-dependent switched system can be seen from the Lyapunov function result in Figure 2.13 (right), where the positive Lyapunov matrix, P, is assumed to be the identity matrix. The vertical dashed lines in the figure show the switching instants.

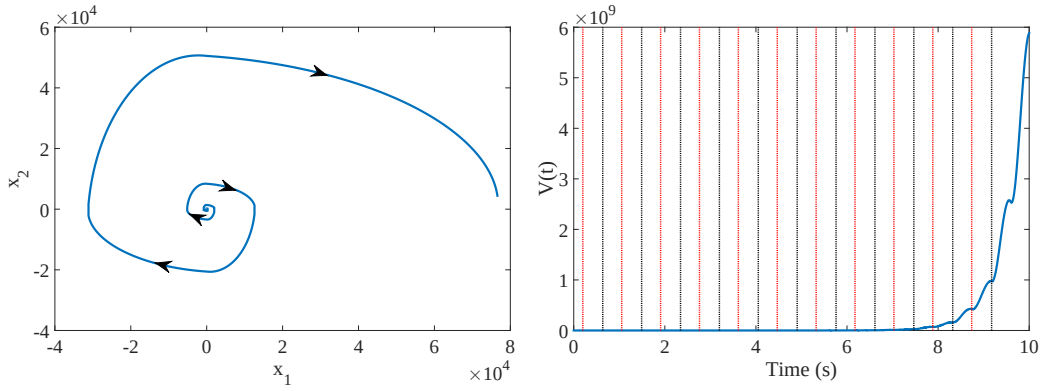

Figure 2.13: Trajectory and Lyapunov function of the state-dependent switched system

In addition to this, the asymptotic stability of each of the subsystems is a strong assumption in the slow switching approach. However, state-dependent switching may prove the stability of switched systems while their subsystems are not individually stable; see Figure 2.6 as an example.

2.4 Controller Design

2.4.1 $\mathcal{H}_2$-optimal control

In this section, the solution of the $\mathcal{H}_2$-optimal control problem is presented. The $\mathcal{H}_2-$optimal control problem finds, for a given plant P, a controller K that stabilizes the system and minimises $\mathcal{H}_2$ norm of the closed-loop transfer function of the system G (Zhou et al., 1996).

The general control configuration is shown in Figure 2.14.

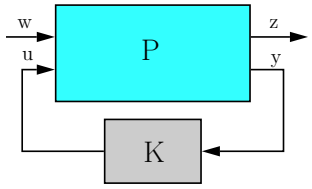

Figure 2.14: General control configuration without uncertainty

Here, the partition of the P can be defined by:

$$\begin{bmatrix} z \\ y \end{bmatrix} = P(s) \begin{bmatrix} w \\ u \end{bmatrix} = \begin{bmatrix} P_{11}(s) & P_{12}(s) \\ P_{21}(s) & P_{22}(s) \end{bmatrix} \begin{bmatrix} w \\ u \end{bmatrix}, \tag{2.14}$$

and the closed-loop system

$$z = F(P, K)w$$

where the generalized controller is K. u is the control inputs of the plant. w are the exogenous inputs which are stochastic and include the measurement of the disturbance signals, noise signals and references inputs (respectively $d,\ n,\ r$).

In addition, the plant contains the sensed, y, and regulated, z, outputs. The generalized plant, P, includes the plant model, G, and weights, W. According to control objectives, the relative signals are penalized by weighting. The transfer function of the system is given by

$$F(P, K) = P_{11} + P_{12}(I - KP_{22})^{-1}KP_{21}.$$

The aim of $\mathcal{H}_2$-optimal control problem is to find a controller K which stabilizes the plant P and minimises the following cost function

$$J(K) = \|F(P, K)\|_2^2$$

where $\|F(P, K)\|_2$ is the $\mathcal{H}_2$-norm of the system (2.14).

Time domain solution is the most convenient way for the control problems. To design a controller, the plant dynamics are assumed to be linear and known, such that

$$\begin{aligned} \dot{x} &= Ax + B_u u + B_w w, \\ y &= C_1 x + D_{1,u} u + D_{1,w} w, \\ z &= C_2 x + D_{2,u} u + D_{2,w} w, \end{aligned} \tag{2.15}$$

A system with the plant model representation can be shown such that

$$\begin{bmatrix} \dot{x} \\ y \\ z \end{bmatrix} = \left[\begin{array}{c|cc} A & \overbrace{B_u}^{B} & B_w \\ \hline C_1 & D_{1,u} & D_{1,w} \\ \underbrace{C_2}_{C} & \underbrace{D_{2,u}}_{D} & D_{2,w} \end{array}\right] \begin{bmatrix} x \\ u \\ w \end{bmatrix} \triangleq G(s) \begin{bmatrix} x \\ u \\ w \end{bmatrix}, \tag{2.16}$$

where the transfer function of the system is $G(s) = C(sI-A)^{-1}B+D$. In order to obtain a finite $\mathcal{H}_2$-norm for the closed-loop system, $D_{2,w}$ is assumed to be zero. In addition, at the infinite frequency, physical systems always have zero gain so $D_{1,u}$ is assumed to be zero.

$\mathcal{H}_2-$norm of the transfer function is the effect of the input w onto the output z. In other words, the $\mathcal{H}_2-$norm of a system stands for the $RMS-$value of the system response to a white noise input. To obtain $\mathcal{H}_2$ optimisation, we can formulate the following theorem.

***Theorem* 2.4.1** ($\mathcal{H}_2$-norm (Scherer and Weiland, 2000))*:* Let $G = C(sI - A)^{-1}B + D$, the following statements are equivalent

- $\mathcal{H}_2-$norm of the system, $\|G\|_2^2 < \upsilon^2$,
- there exist symmetric matrix $P > 0$ such that

$$Tr(B'PB) < \upsilon^2, \qquad A'P + PA + C'C < 0, \tag{2.17}$$

- there exist symmetric matrices, $P > 0$ and R such that

$$Tr(R) < \upsilon^2, \quad \begin{bmatrix} R & B'P \\ * & P \end{bmatrix} > 0, \quad \begin{bmatrix} A'P + PA & C' \\ * & -I \end{bmatrix} < 0, \tag{2.18}$$

- there exist symmetric matrices, $X > 0$ and T such that

$$Tr(T) < \upsilon^2, \quad \begin{bmatrix} T & B' \\ * & X \end{bmatrix} > 0, \quad \begin{bmatrix} XA' + AX & XC' \\ * & -I \end{bmatrix} < 0, \tag{2.19}$$

- there exist symmetric matrix, $Q > 0$ such that

$$Tr(CQC') < \upsilon^2, \qquad AQ + QA' + BB' < 0, \tag{2.20}$$

- there exist symmetric matrices, $Q > 0$ and Z such that

$$Tr(Z) < \upsilon^2, \quad \begin{bmatrix} Z & CQ \\ * & Q \end{bmatrix} > 0, \quad \begin{bmatrix} AQ + QA' & B \\ * & -I \end{bmatrix} < 0, \tag{2.21}$$

- there exist symmetric matrices, $Y > 0$ and N such that

$$Tr(N) < \upsilon^2, \quad \begin{bmatrix} N & C \\ * & Y \end{bmatrix} > 0, \quad \begin{bmatrix} YA + A'Y & YB \\ * & -I \end{bmatrix} < 0. \tag{2.22}$$

Theorem* 2.4.2** ($\mathcal{H}_2-$optimal state-feedback control (Gahinet et al., 1995)):*** If there exist symmetric matrices, $Q > 0$ and Z, then $\mathcal{H}_2$-gain of the system (2.15) with state-feedback, $u = Kx$ is less than υ, if the following conditions hold:

$$\begin{aligned} Tr(Z) &< \upsilon^2, \\ \begin{bmatrix} Z & B'_w \\ * & Q \end{bmatrix} &> 0, \\ \begin{bmatrix} AQ + QA' + B_uY + Y'B'_u & QC'_2 + Y'D'_{2,u} \\ * & -I \end{bmatrix} &< 0, \end{aligned} \tag{2.23}$$

then the closed-loop system is quadratically stable and the $\mathcal{H}_2$-gain from w to z is less than or equal to $\upsilon = \sqrt{Tr(Z)}$.

Remark: Minimising $Tr(Z)$ gives the best upper bound. Then, the state-feedback controller is $K = LQ^{-1}$.

2.4.2 Linear Quadratic Regulator Method

The Linear Quadratic Regulator (LQR) method plays an important role in many control design approaches. The LQR method is an effective control design method and, also, many recent control design methods for the linear multi-input, multi-output (MIMO) systems are based on it. For instance, the controller design methodology of the Linear-Quadratic-Gaussian (LQG) and $\mathcal{H}_\infty$ have nearly the same philosophy as the LQR method. Understanding the philosophy of the LQR method properly is the most convenient route to understand more complicated design methods (Levine, 2011).

Assuming a continuous time linear system (2.15) without disturbance input, if we apply a closed-loop state-feedback rule as $u = -Kx + r$, then the system becomes

$$\dot{x} = (A - B_u K)x + B_u r = A_{cl}x + B_u r, \tag{2.24}$$

where r is a reference input, and it is assumed that r is equal to zero in the following calculations. Moreover, the linear quadratic regulator can be defined as

$$J = \int_0^\infty (x' Q_c x + u' R_c u)\, dt, \tag{2.25}$$

where Q_c - which penalizes the states of the system, x - is a positive semi-definite matrix that means $Q_c \geqslant 0$ and R_c - which penalizes the input signals cost of the system - is a positive definite matrix, such that $R_c > 0$ (Murray, 2009).

The main objective of the LQR method is to minimise the index term J in (2.25). If it is small, then the total energy of the closed-loop system is kept low, so that J can also be called as an energy function. Furthermore, whilst a small J is favourable, neither $u(t)$ or $x(t)$ can be allowed to become too large because both the control input $u(t)$ and the state $x(t)$ are closely related to J. Hence, it is assured that they will definitely be finite. As the time, t, tends to ∞, the state, $x(t)$, tends to zero because the index term, J, is an infinite integral of $x(t)$. Hence, it provides the stability of the closed-loop system (Lewis, 1992).

If a state-feedback $u = -Kx$ is applied to the system in (2.15) and replaced in (2.25), then the equation becomes

$$J = \int_0^\infty x'(Q_c + K'R_cK)x \; dt. \tag{2.26}$$

The aim in optimum design is to select K to minimise the LQR index J. To compute the optimal feedback controller gain K, a constant symmetric positive definite matrix, P, is assumed such that

$$\frac{d}{dt}(x'Px) = -x'(Q_c + K'R_cK)x. \tag{2.27}$$

Then, replacing with (2.26) yields

$$J = -\int_0^\infty \frac{d}{dt}(x'Px) \; dt = x'(0)Px(0) - \lim_{t\to\infty} x'(t)Px(t), \tag{2.28}$$

where $x(0)$ is the initial condition. The closed-loop system is assumed to be stable so that as time t tends to infinity, $x(t)$ tends to zero. It can now be said that J is a constant, it is free of K and it only depends on the initial conditions and the matrix P.

Now, K can be computed using (2.27). To find K, (2.27) is differentiated, and is then replaced with the state-feedback equation in (2.24). Then (2.27) becomes

$$\begin{aligned} 0 &= \dot{x}'Px + x'P\dot{x} + x'Q_cx + x'K'R_cKx, \\ 0 &= x'(A_{cl}'P + PA_{cl} + Q_c + K'R_cK)x. \end{aligned}$$

It can easily be seen that the term in parentheses has to be similarly equivalent to zero. Moreover, for every $x(t)$, the last equation has to be the same. In addition, if the closed-loop matrices A_{cl} are exchanged with $A - BK$, then it becomes a matrix quadratic equation as

$$\begin{aligned} 0 &= (A - BK)'P + P(A - BK) + Q_c + K'R_cK, \\ 0 &= A'P + PA - K'B'P - PBK + Q_c + K'R_cK. \end{aligned} \tag{2.29}$$

K can be chosen such

$$K = R_c^{-1} B' P. \tag{2.30}$$

Then the equation now becomes

$$\begin{aligned} 0 &= A'P + PA + Q_c + (R_c^{-1}B'P)' R_c (R_c^{-1}B'P)(R_c^{-1}B'P)' B'P \\ &\quad - PB(R_c^{-1}B'P), \\ 0 &= A'P + PA + Q_c - PBR_c^{-1}B'P. \end{aligned} \tag{2.31}$$

This equation is called the Algebraic Riccati Equation (ARE), which is extremely important in modern control theory (Lewis, 1992). The positive definite matrix, P, can be computed by solving this equation. Then, the state-feedback controller gain, K, can be calculated using (2.30). The LQR controller gain, K, can be calculated using the lqr function in MATLAB.

Choosing Q_c and R_c matrices for the LQR Method

The control system designers choose the two matrices Q_c and R_c in advance. The closed-loop system will give a different response depending on how these matrices are chosen. More precisely, if R_c is chosen to be a larger value, the control input $u(t)$ will have to be lower to keep the index term, J, small. Moreover, a larger value of R_c implies that the system needs a small control effort, so the closed-loop system poles get slower when the values of state $x(t)$ are increased. Conversely, if Q_c is chosen to be a larger value, it indicates that the state $x(t)$ has to be smaller to keep the index term, J, small. In other words, if Q_c is chosen to be a larger value, then the closed-loop system in the s-plane poles are placed more to the left, so the state $x(t)$ approaches zero more rapidly (Stevens and Lewis, 1992). The LQR is generally defined by

$$J = \int_0^\infty \overbrace{(x'Q_c x + u'R_c u + x'N_c u)}^{S}\, dt. \tag{2.32}$$

But the term N_c in (2.32) is almost always disregarded (Murray, 2009). Q_c and R_c can be determined in the following, different, ways:

1. Basic selection: if we consider $Q_c = I,\ R_c = \rho I$, then S changes as $S = \|(x)\|^2 + \rho\|(u)\|^2$. We can find a good response to change ρ.

2. Selected diagonal: (Hespanha, 2009) Q and R are selected as a diagonal such as

$$Q_c = \text{diag}(q_{11}, \ldots, q_{nn}) \text{ and } R_c = \rho\,\text{diag}(r_{11}, \ldots, r_{mm}).$$

   We can decide q_{ii} and r_{jj} with Brysons rule (Franklin et al., 2010) as

$$\begin{aligned} q_{ii} &= \frac{1}{(\text{ maximum acceptable value of } x_i^2\ )}, \quad i \in \{1, \ldots, n\}, \\ r_{jj} &= \frac{1}{(\text{maximum acceptable value of } u_j^2\ )}, \quad j \in \{1, \ldots, m\}, \end{aligned}$$

   Input/state balance is adjusted using ρ.

3. Output state: if we assume that the controlled output signal is $z = Ex$, and also that we want to keep this small, then (A, E) has to be observable and we choose

$$Q_c = E'E, \quad R_c = \rho I,$$

   where $Q_c \in R^{n\times n}, E \in R^{m\times n}$. It can easily be seen that

$$x'Q_c x = x'E'Ex = z'z.$$

   We can find that S is $S = \|z\|^2 + \rho\|u\|^2$.

Relationship between the LQR method and the $\mathcal{H}_2-$optimal control

LQR method is a special case of the $\mathcal{H}_2-$optimal control. The LQR index of a system, J equals to the $\mathcal{H}_2$ index of a related system and $\mathcal{H}_2-$optimal control can be used to solve LQR problem (Duan and Yu, 2013).

Consider the following assumptions for the system given by (2.15) :

- Assigned $C_2 = \begin{bmatrix} Q_c^{\frac{1}{2}} \\ 0 \end{bmatrix}$, $D_{2,u} = \begin{bmatrix} 0 \\ R_c^{\frac{1}{2}} \end{bmatrix}$ and $B_u = B$
- Full state-feedback, $C_1 = I$ and $D_{1,u} = 0$
- No disturbance input $w = 0$

Then, the objective of the LQR method in (2.25) can be formulated such

$$J = \int_0^\infty (x' C_2' C_2 x + u' D_{2,u}' D_{2,u} u)\, dt. \tag{2.33}$$

Consider the state-feedback law, $u = -Kx$ and unforced response, $x = e^{At} x_0$, then

$$\begin{aligned} J &= \int_0^\infty x_0' (e^{A't} C_2' C_2 e^{At} + e^{A't} K' D_{2,u}' D_{2,u} K e^{At}) x_0 \, dt, \\ &= x_0' \left(\int_0^\infty e^{A't} C_2' C_2 e^{At} + e^{A't} K' D_{2,u}' D_{2,u} K e^{At} \, dt \right) x_0, \\ &= x_0' P x_0, \end{aligned} \tag{2.34}$$

where P is the observability Gramian of the system, with $C_{cl} = C_2 - D_{2,u} K$ that satisfies the following Lyapunov equation

$$\begin{aligned} 0 &= A_{cl}' P + P A_{cl} + C_{cl}' C_{cl} \\ &= A'P + PA - K'B'P - PBK + C_2' C_2 + K' D_{2,u}' D_{2,u} K \\ &= A'P + PA - K'B'P - PBK + Q_c + K' R_c K. \end{aligned} \tag{2.35}$$

Here, it can be seen that (2.29) and (2.35) are equal which shows that conditions of the LQR method can be found using the $\mathcal{H}_2-$optimal control.

2.4.3 State Feedback Integral Control

The values of these variables with the input signals also provide the future state and output of the system (Dorf and Bishop, 2011). The aim of the state-feedback controller is to adjust the output of the system based on the state variables. The output of the system tracks the reference input with reference to the existence of disturbances. Adding an

integral control guarantees obtaining a system that provides zero steady-state tracking error for reference inputs.

To apply the LQR approach discussed above for the state-feedback integral control, some calculations need to be done. The LTI system can be given such that

$$\begin{aligned} \dot{x}_p &= Ax_p + B_u u + B_w w, \\ y &= Cx_p + D_u u + D_w w, \end{aligned} \tag{2.36}$$

where x_p gives the states of the plant, u is the control inputs and w is the exogenous (disturbance) inputs. The general state-feedback integral control scheme for the system (2.36) is given in Figure 2.15, where the feedback of the system is defined by the integral of the error, $e = r - y$.

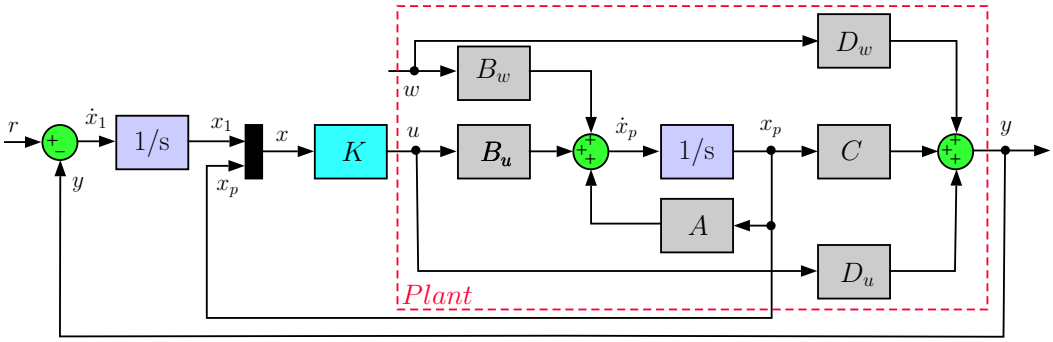

Figure 2.15: State-feedback integral control scheme

We can obtain a specific solution to integral control by enhancing the state vector with the desired dynamics. We add the extra state x_1 which satisfies the following differential relation

$$\dot{x}_1 := r - y = r - (Cx_p + D_u u + D_w w) \quad (= e), \tag{2.37}$$

where

$$x_1 = \int_0^T e\, dt.$$

The augmented plant in Figure 2.16 can be obtained by combining (2.36) with (2.37)

such that

$$\begin{aligned}
\dot{x} &= \begin{bmatrix} 0 & -C \\ 0 & A \end{bmatrix} \begin{bmatrix} x_1 \\ x_p \end{bmatrix} + \begin{bmatrix} -D_u \\ B_u \end{bmatrix} u + \begin{bmatrix} -D_w \\ B_w \end{bmatrix} w + \begin{bmatrix} 1 \\ 0 \end{bmatrix} r \\
&= A_{aug}\, x + B_{u,aug}\, u + B_{w,aug}\, w + W\, r, \\
y &= \begin{bmatrix} 0 & C \end{bmatrix} x + D_u\, u + D_w\, w \\
&= C_{aug}\, x + D_{u,aug}\, u + D_{w,aug}\, w. \qquad (2.38)
\end{aligned}$$

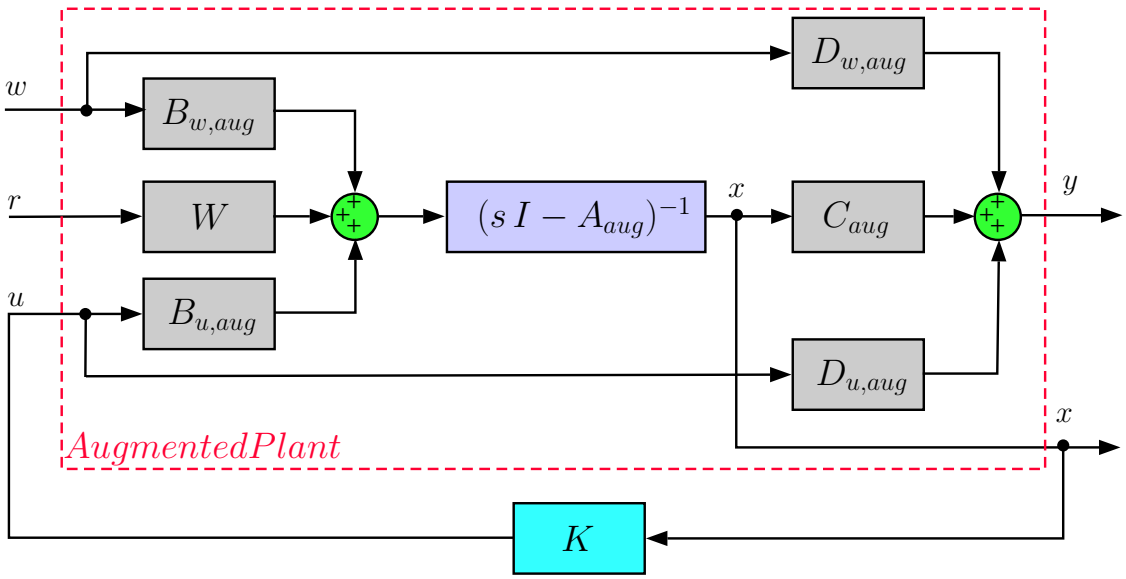

Figure 2.16: Augmented representation of the state-feedback integral control

In (2.32), S was defined in the LQR index term and can be written as $S = z'z$, where z is a regulated (weighted) output such that

$$z = \left[\begin{array}{c|c} Q^{1/2} & 0 \\ \hline 0 & R^{1/2} \end{array}\right] \begin{bmatrix} x \\ u \end{bmatrix}. \qquad (2.39)$$

Here, the term N in (2.32) is disregarded. Combining the output of the system, y, with the regulated output in (2.39) gives the new augmented plant outputs as

$$z_{aug} = \begin{bmatrix} z \\ y \end{bmatrix} = \left[\begin{array}{c|c|c} Q^{1/2} & 0 & 0 \\ \hline 0 & R^{1/2} & 0 \\ \hline C_{aug} & D_{u,aug} & D_{w,aug} \end{array}\right] \begin{bmatrix} x \\ u \\ w \end{bmatrix}. \tag{2.40}$$

Finally, the weighted version of the state-feedback integral control in Figure 2.17 is obtained. The plant outputs in (2.40) will use the following sections to find a switched controller via stability analysis approaches.

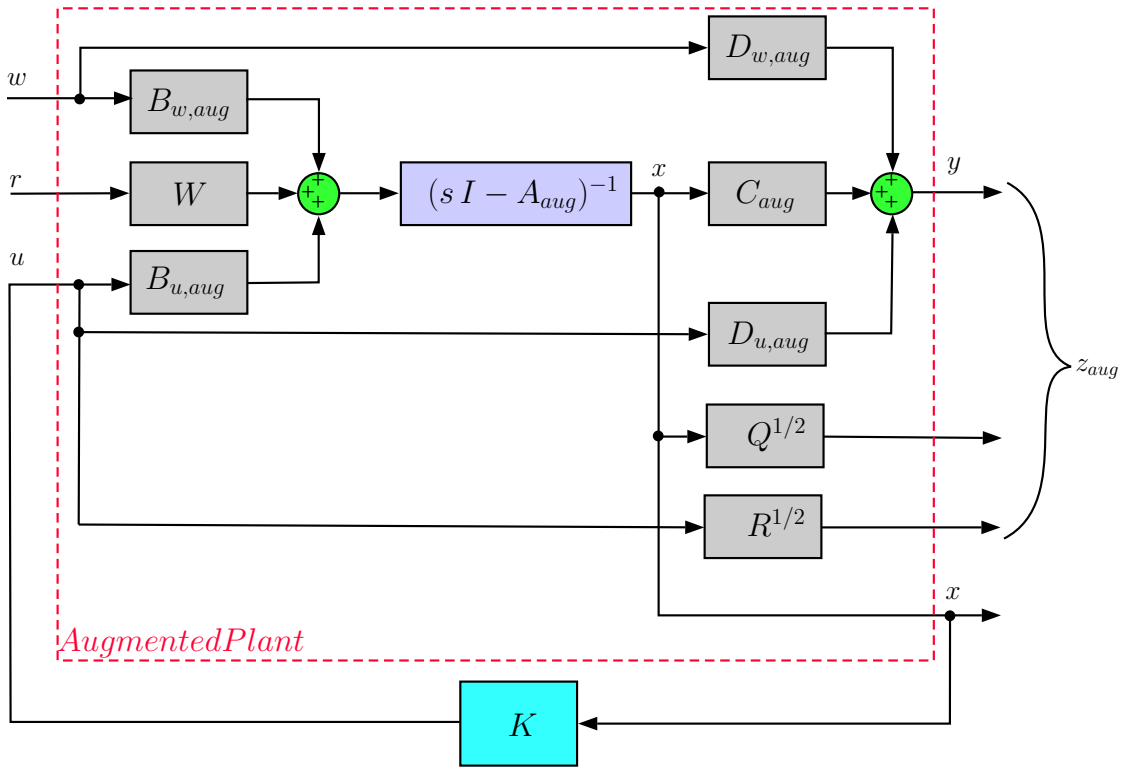

Figure 2.17: State-feedback integral control scheme with LQR weight

2.5 Summary

In this chapter, the basic concepts and methods for stability analysis have been presented. The indirect and direct Lyapunov stability analysis methods are given. These methods are illustrated using various examples. Additionally, stability analysis for switch-

ed systems have been introduced depending on arbitrary and constrained switching signals. Basic approaches to find switched system stability have been given. The minimum dwell time theory and state-dependent switching theory in Section 2.3.2 will be extended in the following two chapters for switched systems that have polytopic parameter uncertainty. In addition, $\mathcal{H}_2-$optimal control and LQR methods have been presented. These methods will be used and extended in the following chapters. At the end of the chapter, state-feedback integral control strategy is given.

CHAPTER 3

Minimum Dwell Time Stability Analysis for Polytopic Systems

3.1 Introduction

Theorem 2.3.2 (Section 2.3.2) provides the least conservative minimum dwell time estimation given in terms of quadratic Lyapunov functions. However, because the first LMI (2.7) depends on $e^{A_i T}$, which is not convex in A_i, Theorem 2.3.2 cannot be generalized to handle uncertain polytopic systems in a simple manner. To tackle this issue, another dwell time technique will be used. The technique assumes linearly time-varying Lyapunov functions. This assumption produces less conservative results when compared to time-invariant Lyapunov functions. Also, parameter dependent, time-varying Lyapunov functions will be introduced later for further relaxed conditions. The dwell time analyses will be then extended to $\mathcal{L}_2$ and $\mathcal{H}_2$ performance.

The rest of this chapter is structured as follows: Section 3.2 introduces the description of linear polytopic systems with uncertain parameters. In particular, minimum dwell time

theory is given in this section. Based on the minimum dwell time approach, the general description and the requirements of the stability analysis and $\mathcal{L}_2$-gain methodologies are introduced in Section 3.3 and the subsequent sections are built on this section. The stability analysis method and $\mathcal{L}_2$ performance gain are derived using parameter independent Lyapunov functions and parameter dependent Lyapunov functions in Sections 3.4 and 3.5, respectively. In Section 3.6, the state-feedback controller design approaches are examined with the methods described in Sections 3.4 and 3.5. An example is given at the end of each section.

3.2 System description

Consider the switched linear system:

$$\begin{aligned} \dot{x}(t) &= A_{\sigma(t)}x(t) + B_{u,\sigma(t)}u(t) + B_{w,\sigma(t)}w(t), \quad x(0) = 0, \\ z(t) &= C_{\sigma(t)}x(t) + D_{u,\sigma(t)}u(t) + D_{w,\sigma(t)}w(t), \end{aligned} \tag{3.1}$$

where the state is $x(t) \in \mathbb{R}^n$, the control signal is $u(t) \in \mathbb{R}^k$, an exogenous disturbance is $w(t) \in \mathbb{R}^l$ and the objective vector is $z(t) \in \mathbb{R}^m$. For each $t \geq 0$, the switching rule $\sigma(t)$ is such that $A_{\sigma(t)} \in \{A_1, \ldots, A_M\}$, $B_{u,\sigma(t)} \in \{B_{u,_1}, \ldots, B_{u,_M}\}$, $B_{w,\sigma(t)} \in \{B_{w,1}, \ldots, B_{w,_M}\}$, $C_{\sigma(t)} \in \{C_1, \ldots, C_M\}$, $D_{u,\sigma(t)} \in \{D_{u,_1}, \ldots, D_{u,_M}\}$ and $D_{w,\sigma(t)} \in \{D_{w,_1}, \ldots, D_{w,_M}\}$. It is considered that all system matrices are uncertain and reside within the following polytope:

$$\Omega = \bigcup_{i=1,\ldots,M} \Omega_i, \quad \Omega_i = \sum_{j=1}^{N} \eta_j \Omega_i^{(j)}, \quad \sum_{j=1}^{N} \eta_j = 1, \quad \eta_j \geq 0, \tag{3.2}$$

where $\Omega_i = \left[\begin{array}{c|cc} A_i & B_{u,i} & B_{w,i} \\ \hline C_i & D_{u,i} & D_{w,i} \end{array}\right]$, $\Omega_i^{(j)} = \left[\begin{array}{c|cc} A_i^{(j)} & B_{u,i}^{(j)} & B_{w,i}^{(j)} \\ \hline C_i^{(j)} & D_{u,i}^{(j)} & D_{w,i}^{(j)} \end{array}\right]$, i is the index of the subpolytopes, M denotes number of subpolytopes, j is the index of the subpolytope vertices and N denotes the number of subpolytope vertices. For instance, a polytopic system with overlapping subpolytopes is given in Figure 3.1, where each coloured rectangular

represents a different subpolytope and each vertex is marked with dots. This polytopic system has 6 subpolytopes, $M = 6$, and each subpolytope has 4 vertices, $N = 4$. Here, the number of subpolytopes vertices are selected to be the same for the simplicity but could be different for each subpolytope.

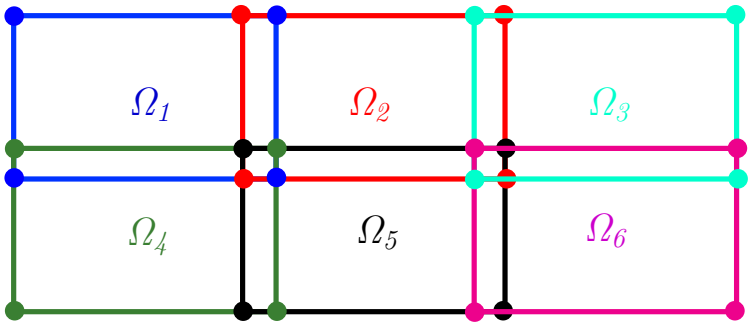

Figure 3.1: A polytopic system with overlapping subpolytopes

Note that, each subpolytope needs to be overlapping in the dwell time approach and it is assumed that the switched system matrices are convex combination of the related subpolytope vertices (Pogromsky et al., 1998). A constraint of a minimum dwell time during the switching between subsystems arises due to the overlap between the subpolytopes. During the minimum dwell time, it is assumed that the rates of change of the parameters are bounded.

Definition* 3.2.1*: From Definition 2.3.1, the minimum dwell time between two switching instants is divided into H equal sampling time intervals. It is then defined as $t_{k,h} = t_k + h\frac{T}{H}$ for $h = 0, \ldots, H$ if the initial subsystem and switching instant are given by $i(0) = \sigma(0)$ and $t_1, t_2, \ldots$, respectively. This definition with the dwell time constraint stands for $t_{k,H} \leq t_{k+1,0} = t_{k+1}$, which is explained geometrically in Figure 3.2. We will use this definition to define the time-varying matrices, P_i, in the following sections.

3.3 Stability Analysis and $\mathcal{L}_2$-gain

In this section, the general stability analysis and $\mathcal{L}_2$ performance gain methods are introduced in the perspective of the time-varying Lyapunov matrices. It also includes a

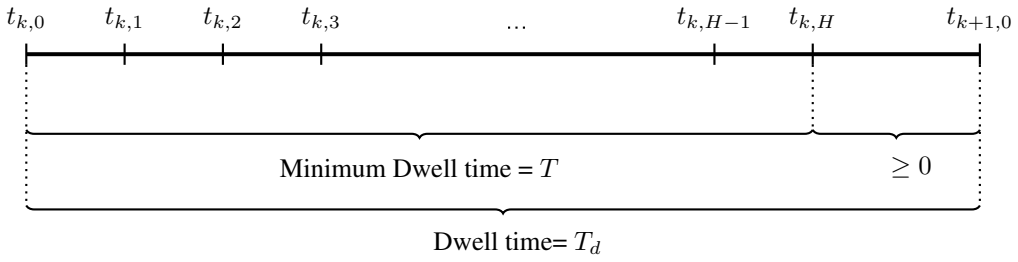

Figure 3.2: Dividing the minimum dwell time into H equal parts

brief description and the requirements of the stability analysis and $\mathcal{L}_2$-gain methodologies. The results of this section cannot used directly to find stability and $\mathcal{L}_2$-gain of the switched systems therefore the following sections are also built on this section.

3.3.1 Stability Analysis

The positive definite matrices P_i used in stability analysis are assumed to vary linearly with time during the minimum dwell time. Hence, the Lyapunov function $V(t)$ with time-varying matrices, $P_i(t)$, is given such that

$$V(t) = x'(t)P_i(t)x(t), \qquad i = 1, \ldots, M \tag{3.3}$$

needs to satisfy the following conditions:

Condition* 3.1** (Positive-Definiteness):*** $V(x) > 0$ for all $x \in \mathbb{R}^n$ and $x \neq 0$. Positive values of the Lyapunov function in (3.3) can be achieved by the existence of symmetric positive definite matrices $P_i(t) > 0,\ i = 1, \ldots, M$.

Condition* 3.2** (Decreasing in time):*** $\dot{V}(x) < 0$ for all $x \in \mathbb{R}^n$ and $x \neq 0$. Negative values of the derivative of the Lyapunov function in (3.3) along the subsystem's trajectories is

$$\dot{V}(x) = x'(\dot{P}_i(t) + A_i^{(j)'}P_i(t) + P_i(t)A_i^{(j)})x < 0, \quad \forall i,\ \forall j. \tag{3.4}$$

Here, $\dot{P}_i(t)$ are taken into account due to the time-varying matrices, $P_i(t)$. From (Boyarski and Shaked, 2009), linearly time-varying , $P_i(t)$, for all $t \in [t_{k,h} \quad t_{k,h+1}],\ h = 0, \ldots, H-1$ is a convex combination of the unknown constant matrices, $P_{i,h}$ and $P_{i,h+1}$, such that

$$
\begin{aligned}
P_i(t) &= r_1(t)P_{i,h} + r_2(t)P_{i,h+1}, \quad 0 \le r_1(t) \le 1, \\
0 \le r_2(t) \le 1, \quad r_1(t) + r_2(t) &= 1, \quad r_2(t) \triangleq \frac{t - t_{k,h}}{t_{k,h+1} - t_{k,h}},
\end{aligned} \tag{3.5}
$$

where the convex coordinates of $P_i(t)$ are defined as $r_1(t)$ and $r_2(t)$. Indeed, r_1 is varied from 1 at $t_{k,h}$ to 0 at $t_{k,h+1}$ and r_2 is changed from 0 at $t_{k,h}$ to 1 at $t_{k,h+1}$. Note that, from the convex definition of (3.5), a positive definite $P_i(t)$ for $t_{k,h} \le t \le t_{k,h+1}$ exists if, and only if, the positive definite matrices $P_{i,h}$ and $P_{i,h+1}$ exist. The derivative of $P_i(t)$ is a constant matrix from the description of (3.5) such that

$$
\dot{P}_i(t) = \frac{P_{i,h+1} - P_{i,h}}{t_{k,h+1} - t_{k,h}}. \tag{3.6}
$$

Thus, satisfaction of (3.4) is equivalent to

$$
\begin{aligned}
&\frac{P_{i,h+1} - P_{i,h}}{t_{k,h+1} - t_{k,h}} + A_i^{(j)\prime} P_{i,h} + P_{i,h} A_i^{(j)} < 0, \\
&\frac{P_{i,h+1} - P_{i,h}}{t_{k,h+1} - t_{k,h}} + A_i^{(j)\prime} P_{i,h+1} + P_{i,h+1} A_i^{(j)} < 0, \\
&P_{i,h+1} > 0, \quad P_{i,h} > 0,
\end{aligned} \tag{3.7}
$$

If (3.7) has a solution, the stability of the system (3.1) with an uncertainty (3.2) is proven.

3.3.2 $\mathcal{L}_2$ performance gain

Besides a sufficient condition for the asymptotic stability, the following performance criteria for a scalar γ is sought for the system (3.1) (Allerhand and Shaked, 2010).

$$
J = \int_0^\infty (z'z - \gamma^2 w'w) dt \le 0, \qquad \forall w \in \mathcal{L}_2 \tag{3.8}
$$

Here, γ is the $\mathcal{L}_2$-gain between disturbance inputs, w and desired outputs, z, of the system (3.1). We can define a new criteria with $V(t)$:

$$
\tilde{J} = \lim_{t \to \infty} \{V(t) + \int_0^t (z'z - \gamma^2 w'w) ds\}. \tag{3.9}
$$

It can be seen that $J \leq \tilde{J}$ when $V(t) \geq 0 \, \forall \, t$. Assuming that $V(t)$ can be differentiated over all t, apart from the switching instants, and $x(0) = 0$, then

$$\lim_{t \to \infty} V(t) = \sum_{k=0}^{\infty} \int_{t_k}^{t_{k+1}} \dot{V}(t) dt + \sum_{k=1}^{\infty} (V(t_k) - V(t_k^-)) \tag{3.10}$$

where $t_0 = 0$. The Lyapunov function, $V(t)$ needs to be non-increasing at the switching instants; thereby making this condition is stronger than the normal dwell time conditions. If $V(t)$ satisfies this necessary condition, the following result can be obtained

$$V(t_k) - V(t_k^-) \leq 0 \quad \forall s > 0 \tag{3.11}$$

which then means

$$\lim_{t \to \infty} V(t) \leq \sum_{k=0}^{\infty} \int_{t_k}^{t_{k+1}} \dot{V}(t) dt. \tag{3.12}$$

Substituting (3.12) into (3.9) yields:

$$\begin{aligned} \bar{J} &= \sum_{k=0}^{\infty} \int_{t_k}^{t_{k+1}} \dot{V}(t) dt + \int_0^{\infty} (z'z - \gamma^2 w'w) ds, \\ &= \sum_{k=0}^{\infty} \int_{t_k}^{t_{k+1}} (\dot{V}(t) + z'z - \gamma^2 w'w) ds. \end{aligned} \tag{3.13}$$

Consequently, from (3.8) to (3.13), $J \leq \tilde{J} \leq \bar{J}$ is obtained. If the above Lyapunov function provides $\bar{J} \leq 0$ and the non-increasing condition in (3.11) is held during the switching instants, then the performance criteria in (3.8) are proven. More precisely, the $\mathcal{L}_2$-gain of the system (3.1) will be equal to or less than a prescribed scalar $\gamma > 0$. From (3.13), the following condition needs to be satisfied

$$\dot{V}(t) + z'z - \gamma^2 w'w < 0. \tag{3.14}$$

Substituting (3.4) into (3.14) and applying standard derivation of the Bounded Real Lemma (BRL) for linear systems (Boyd et al., 1994), the following inequality is obtained

$$\begin{bmatrix} \dot{P}_i(t) + P_i(t)A_i^{(j)} + A_i^{(j)'}P_i(t) & P_i(t)B_{w,i}^{(j)} & C_i^{(j)'} \\ * & -\gamma^2 I & D_{w,i}^{(j)'} \\ * & * & -I \end{bmatrix} < 0. \tag{3.15}$$

Note that the first diagonal block of the above inequality comes from (3.4). The second row and column come from $w'w$ and the third row and column come from $z'z$. This inequality is defined for $\mathcal{L}_2$ performance gain between disturbance inputs, w, and desired outputs, z. If the $\mathcal{L}_2$-gain between control inputs, u, and desired outputs, z, is sought, the disturbance inputs in (3.8) will be replaced with the control inputs, and the disturbance matrices B_w and D_w in (3.15) become the input matrices B_u and D_u.

Substituting (3.6) into (3.15), the inequality becomes

$$\begin{bmatrix} \frac{P_{i,h+1}-P_{i,h}}{t_{k,h+1}-t_{k,h}} + A_i^{(j)'}P_{i,h} + P_{i,h}A_i^{(j)} & P_{i,h}B_{w,i}^{(j)} & C_i^{(j)'} \\ * & -\gamma^2 I & D_{w,i}^{(j)'} \\ * & * & -I \end{bmatrix} < 0,$$

$$\begin{bmatrix} \frac{P_{i,h+1}-P_{i,h}}{t_{k,h+1}-t_{k,h}} + A_i^{(j)'}P_{i,h+1} + P_{i,h+1}A_i^{(j)} & P_{i,h+1}B_{w,i}^{(j)} & C_i^{(j)'} \\ * & -\gamma^2 I & D_{w,i}^{(j)'} \\ * & * & -I \end{bmatrix} < 0, \tag{3.16}$$

$$P_{i,h+1} > 0, \quad P_{i,h} > 0,$$

In this section, general theories are presented for the time-varying Lyapunov matrices P_i but these cannot be directly used for the stability and $\mathcal{L}_2$ performance gain analysis of the system (3.1) with parameter uncertainty (3.2). In Section 3.4, the Lyapunov matrices in these theories are assumed to vary only with time, but this assumption may cause conservative results for the dwell time. Hence, in Section 3.5, the Lyapunov matrices varying both with time and cell partition parameters are also used in these theories.

3.4 Parameter Independent Lyapunov Function

In this thesis, the term *parameter independent Lyapunov function* is used to refer to a Lyapunov function that only depends on time and not the uncertain parameters of the system matrices. More precisely, the same Lyapunov function is applied to all the points in the uncertain polytopes, Ω_i in (3.2). In this section, the stability analysis method and $\mathcal{L}_2$ performance gain given in Section 3.3 are introduced using a parameter independent Lyapunov function.

A time-varying and parameter independent Lyapunov function, $V(t)$, is defined as

$$V(t) = x'(t)P_{\sigma(t)}(t)x(t), \tag{3.17}$$

where $P_{\sigma(t)}(t) \in \{P_1(t), \ldots, P_M(t)\}$ according to $\sigma(t)$, defined as:

$$P_i(t) = \begin{cases} P_{i_0,H} & t \in [0, t_1), \\ P_{i,h} + (P_{i,h+1} - P_{i,h}) \dfrac{(t - t_{k,h})}{\frac{T}{H}} & t \in [t_{k,h}, t_{k,h+1}), \\ P_{i,H} & t \in [t_{k,H}, t_{k+1,0}). \end{cases} \tag{3.18}$$

where $h = 0, \ldots, H-1$, the number of the switching is defined as $k = 1, 2, \ldots$ and H is a given positive integer. The change of the Lyapunov matrix $P_i(t)$ is presented in Figure 3.3. Here, the matrix $P_i(t)$ is constant and equal to $P_{i_0,H}$ before the first switching instant. During the minimum dwell time, the matrix $P_i(t)$ changes linearly from $P_{i,h}$ to $P_{i,h+1}$ and time intervals are assumed as $t \in [t_{k,h}, t_{k,h+1})$. After the minimum dwell time, and before the following switching instant, the matrix $P_i(t)$ is constant and equal to $P_{i,H}$. Note that a large H provides a less conservative result at the expense of computational complexity (Allerhand and Shaked, 2011).

►►► Stability Analysis using Parameter Independent Lyapunov Function

The parameter independent Lyapunov function (3.17) is here used to analyse the stability of the system (3.1) with the parameter uncertainty (3.2). According to the conditions of Section 3.3.1, the following theorem is given for the stability analysis:

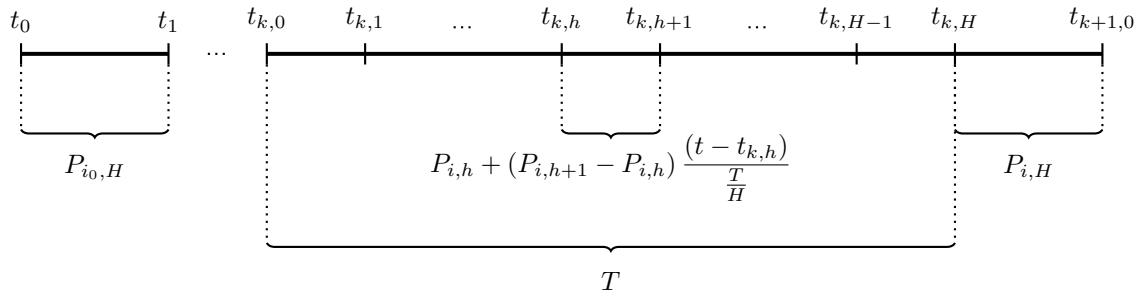

Figure 3.3: A graph presenting the Lyapunov matrix, $P_i(t)$

***Theorem* 3.4.1** (Allerhand and Shaked (2011))*:* For a given $T > 0$, if there exist a set of positive definite matrices $P_{i,h} > 0,\ i = 1, \ldots, M,\ h = 0, \ldots, H$ that satisfy the following LMIs for all $i = 1, \ldots, M$ and $j = 1, \ldots, N$:

$$\begin{aligned} \frac{P_{i,h+1} - P_{i,h}}{T/H} + P_{i,h}A_i^{(j)} + A_i^{(j)'}P_{i,h} < 0, \\ \frac{P_{i,h+1} - P_{i,h}}{T/H} + P_{i,h+1}A_i^{(j)} + A_i^{(j)'}P_{i,h+1} < 0, \end{aligned} \tag{3.19a}$$

where $h = 0, \ldots, H-1$

$$P_{i,H}A_i^{(j)} + A_i^{(j)'}P_{i,H} < 0, \tag{3.19b}$$

$$P_{i,H} - P_{s,0} \geq 0, \qquad \forall s \in \{1, \ldots, M\} \text{ and } s \neq i \tag{3.19c}$$

then the system (3.1) with the uncertainty (3.2) is globally asymptotically stable for any switching rule with a dwell time that is greater than the minimum dwell time, T.

Note that, before the first switching, the decreasing of the Lyapunov function is ensured by the condition (3.19b). During the minimum dwell time, the conditions in (3.19a) which come from the LMIs in (3.7), ensure that the Lyapunov function is decreasing. Then, the condition in (3.19b) guarantees that $V(t)$ is decreasing, after the minimum dwell time and before the next switching. During the switching instants, the Lyapunov function is ensured to be non-increasing by the condition in (3.19c). Figure 3.4 illustrates the change of the Lyapunov function as guaranteed by Theorem 3.4.1.

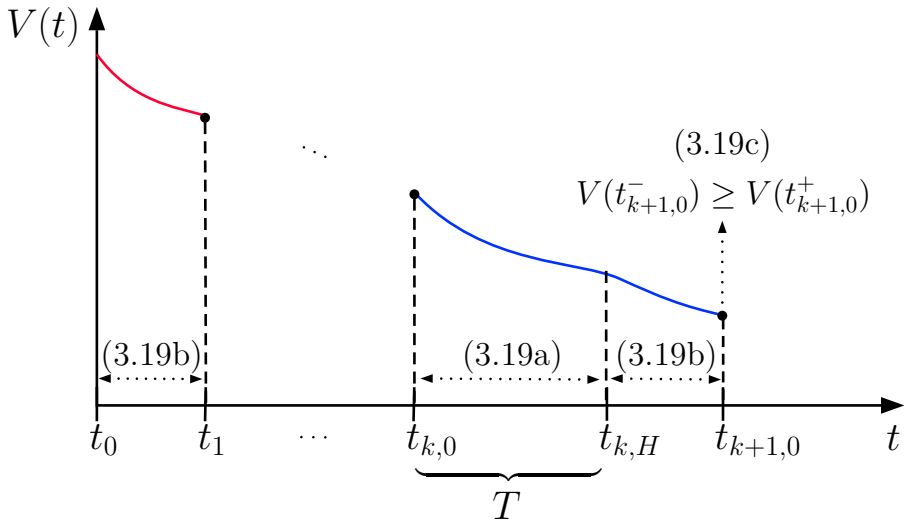

Figure 3.4: Illustration of the change of Lyapunov function

Remark: It is assumed that the parameters of the system (3.1) reside within the polytope, and the system matrices are convex combinations of the polytope vertices. Hence, the theorem proves the stability of the system, despite being defined on the vertices of the cells. The system matrices, A_i, are to be convex combinations of the vertices as

$$A_i = \sum_{j=1}^{N} \eta_j A_i^{(j)}, \quad \sum_{j=1}^{N} \eta_j = 1, \quad \eta_j \geq 0$$

then Condition 3.2 can be written as the above system matrices such that

$$\sum_{j=1}^{N} \eta_j x' \left(\dot{P}_i + A_i^{(j)'} P_i + P_i A_i^{(j)} \right) x < 0 \tag{3.20}$$

When we compare the inequalities in (3.4) and (3.20), it can be seen that if the solution can be found by using Theorem 3.4.1, it will also verify the inequalities in (3.20). In other words, if Theorem 3.4.1 gives a sufficient result for the vertices of the cells, it will also prove the stability of all the system dynamics within the cells.

Example* 3.1*: Consider the switched linear system $\dot{x} = A_i x$ and the system matrices reside within the following polytope:

$$A_i = \sum_{j=1}^{N} \eta_j A_i^{(j)}, \quad \sum_{j=1}^{N} \eta_j = 1, \quad \eta_j \geq 0$$

Here, the system matrices are a convex combination of the following matrices

$$A_1^{(1)} = \begin{bmatrix} -2 & 6 \\ 1 & -7 \end{bmatrix}, \qquad A_1^{(2)} = \begin{bmatrix} -3.2 & 3.6 \\ -2.6 & -2.2 \end{bmatrix},$$

$$A_2^{(1)} = \begin{bmatrix} -4 & 2 \\ -5 & 1 \end{bmatrix}, \qquad A_2^{(2)} = \begin{bmatrix} -2.8 & 4.4 \\ -1.4 & -3.8 \end{bmatrix}.$$

The given system is then solved by using Theorem 3.4.1 with $H = 1$ and the minimum dwell time is found as $T = 0.643\,s$. Using the definition in (3.18), the time-varying $P_i(t)$ can be found based on the following set of matrices, which come from solutions of the inequalities

$$P_{1,0} = \begin{bmatrix} 4.5404 & 0.3008 \\ 0.3008 & 4.8754 \end{bmatrix} \qquad P_{1,1} = \begin{bmatrix} 8.6059 & -3.9557 \\ -3.9557 & 16.7169 \end{bmatrix},$$

$$P_{2,0} = \begin{bmatrix} 8.6050 & -3.9002 \\ -3.9002 & 7.2385 \end{bmatrix} \qquad P_{2,1} = \begin{bmatrix} 11.5653 & -3.4353 \\ -3.4353 & 6.8631 \end{bmatrix}.$$

In this example, the solver finds 12 variables by solving 18 different LMIs in $0.5614\,s$. These variables come from the component of the matrices $P_{i,h},\ i = 1, \ldots, M,\ h = 0, \ldots, H$. The minimum dwell time results are given in Table 3.1 for different values of H. Table 3.1 shows that the number of variables and inequalities increases with an increasing H, whereas the minimum dwell time decreases. The solver time increases rapidly with the number of LMIs and the number of variables.

Remark: In Theorem 3.4.1, $P_{i,h},\ i = 1, \ldots, M,\ h = 0, \ldots, H$ are the variable matrices. The number of LMI variables the solver needs to find are $M(H+1)\Upsilon$. Therefore, the solver deals with $M(M+2NH+H+N)$ different inequalities to find these variables. M is the number of subpolytopes, N is the number of subpolytope vertices, H is a prescribed integer and Υ is the number of components in the symmetric positive definite matrices $P_{i,h}$. Υ can be calculated as $n(n+1)/2$, where n is the size of the $A_i^{(j)}$ matrices.

H	1	2	5	10	100
T(s)	0.643	0.470	0.156	0.133	0.119
Solving Time (s)	0.5614	0.7482	1.1294	1.8504	15.9403
Num. of LMIs	18	28	58	108	1008
Num. of Variable	12	18	36	66	606

Table 3.1: The results of the Example 3.1 for various H

►►► $\mathcal{L}_2$-gain using Parameter Independent Lyapunov Function

The parameter independent Lyapunov function (3.17) is here used to satisfy both stability and performance criteria of the system (3.1) with the parameter uncertainty (3.2). According to the $\mathcal{L}_2$-gain definition in Section 3.3.2, the following theorem is given for the $\mathcal{L}_2$ performance gain:

***Theorem* 3.4.2** (Allerhand and Shaked (2013))**:** For a given $T > 0$, if there exist a set of positive definite matrices $P_{i,h} > 0,\ i = 1, \ldots, M,\ h = 0, \ldots, H$ that satisfy the following LMIs for all $i = 1, \ldots, M$ and $j = 1, \ldots, N$:

$$\begin{bmatrix} \frac{(P_{i,h+1} - P_{i,h})}{T/H} + P_{i,h}A_i^{(j)} + A_i^{(j)\prime}P_{i,h} & P_{i,h}B_{w,i}^{(j)} & C_i^{(j)\prime} \\ * & -\gamma^2 I & D_{w,i}^{(j)\prime} \\ * & * & -I \end{bmatrix} < 0, \tag{3.21a}$$

$$\begin{bmatrix} \frac{(P_{i,h+1} - P_{i,h})}{T/H} + P_{i,h+1}A_i^{(j)} + A_i^{(j)\prime}P_{i,h+1} & P_{i,h+1}B_{w,i}^{(j)} & C_i^{(j)\prime} \\ * & -\gamma^2 I & D_{w,i}^{(j)\prime} \\ * & * & -I \end{bmatrix} < 0,$$

where $h = 0, \ldots, H-1$

$$\begin{bmatrix} P_{i,H}A_i^{(j)} + A_i^{(j)'}P_{i,H} & P_{i,H}B_{w,i}^{(j)} & C_i^{(j)'} \\ * & -\gamma^2 I & D_{w,i}^{(j)'} \\ * & * & -I \end{bmatrix} < 0 \tag{3.21b}$$

$$P_{i,H} - P_{s,0} \geq 0, \qquad \forall s \in \{1, \ldots, M\} \text{ and } s \neq i \tag{3.21c}$$

then the $\mathcal{L}_2$-gain of the system (3.1) with the uncertainty (3.2) is smaller than a positive scalar γ for any switching rule with a dwell time that is greater than the minimum dwell time, T. Here, H is a given integer, $i = 1, \ldots, M$ and $j = 1, \ldots, N$.

The LMIs in Theorem 3.4.2 can be investigated in four categories which are: before first switching; during the minimum dwell time; before the switching instants and during the switching instants. Firstly, before the first switching, $P_i(t)$ is constant and the Lyapunov function, $V(t)$, is proven to be decreasing by the LMI (3.21b) whilst the system stays within the same subsystem. The LMIs (3.21a) then guarantee that $V(t)$ is strictly decreasing during the minimum dwell time, which comes from the LMI (3.16). For any $t \in [t_{k,H}, t_{k+1,0})$, the LMI (3.21b) proves that the Lyapunov function is strictly decreasing. During the switching instants, the Lyapunov function is proved to be non-increasing by the LMI (3.21c). According to Lasalle's invariance principle (Hespanha, 2004a), the asymptotic stability is proven for the system due to having different switching points.

***Example* 3.2:** Consider the switched linear system (3.1) with the polytopic system parameters (3.2), which are given such that

$$A_1^{(1)} = \begin{bmatrix} -2 & 6 \\ 1 & -7 \end{bmatrix}, \quad B_{w,1}^{(1)} = \begin{bmatrix} -2 \\ 5 \end{bmatrix}, \quad C_1^{(1)} = \begin{bmatrix} 3 & 1 \end{bmatrix}, \quad D_{w,1}^{(1)} = -0.8,$$

$$A_1^{(2)} = \begin{bmatrix} -3.2 & 3.6 \\ -2.6 & -2.2 \end{bmatrix}, \quad B_{w,1}^{(2)} = \begin{bmatrix} -0.2 \\ 2.27 \end{bmatrix}, \quad C_1^{(2)} = \begin{bmatrix} 4.2 & 1.6 \end{bmatrix}, \quad D_{w,1}^{(2)} = -0.08,$$

$$A_2^{(1)} = \begin{bmatrix} -4 & 2 \\ -5 & 1 \end{bmatrix}, \quad B_{w,2}^{(1)} = \begin{bmatrix} 1 \\ 0.45 \end{bmatrix}, \quad C_2^{(1)} = \begin{bmatrix} 5 & 2 \end{bmatrix}, \quad D_{w,2}^{(1)} = 0.4,$$

$$A_2^{(2)} = \begin{bmatrix} -2.8 & 4.4 \\ -1.4 & -3.8 \end{bmatrix}, \quad B_{w,2}^{(2)} = \begin{bmatrix} -0.8 \\ 3.18 \end{bmatrix}, \quad C_2^{(2)} = \begin{bmatrix} 3.8 & 1.4 \end{bmatrix}, \quad D_{w,2}^{(2)} = -0.32.$$

The given system is solved by using Theorem 3.4.2 with $H = 1$ and the minimum dwell time is found as $T = 0.643\,s$. In this example, 13 variables are found by solving 19 different LMIs in $1.2163\,s$. These variables come from the component of the matrices $P_{i,h},\ i = 1, \ldots, M$, $h = 0, \ldots, H$ and $\mathcal{L}_2$-gain, γ. The minimum dwell time results for different values of H are given in Table 3.2, and the $\mathcal{L}_2$-gain results are shown in Table 3.3 for various dwell times T_d and scalar H. Table 3.2 shows that when H is increased, the minimum dwell time is decreased; however, solving time, the number of LMIs and the number of variables are increased. In addition, Table 3.3 indicates that $\mathcal{L}_2$-gain is decreased when the dwell time, T_d and/or H increase.

H	1	2	5	10	100
T(s)	0.643	0.470	0.156	0.133	0.119
Solving Time (s)	1.2163	1.2822	1.8668	2.9336	23.8612
Num. of LMIs	19	29	59	109	1009
Num. of Variable	13	19	37	67	607

Table 3.2: The minimum dwell time, the number of LMIs and the number of variables for various H

Remark: In Theorem 3.4.2, $P_{i,h},\ i = 1, \ldots, M,\ h = 0, \ldots, H$ and γ are the variables. The number of variables that the LMI solver needs to find are $M(H+1)\Upsilon + 1$. Therefore, the solver deals with $M(M + 2NH + H + N) + 1$ different inequalities to find these vari-

$H \setminus T_d$	1 s	2 s	3 s	4 s	5 s
1	19.3743	11.3665	10.8417	10.6842	10.5972
2	15.3455	11.2082	10.6327	10.4629	10.4040
5	13.1286	10.7246	10.4287	10.3401	10.3086
10	11.7962	10.4859	10.3200	10.2838	10.2745
100	9.9269	9.6834	9.6042	9.5198	9.4908

Table 3.3: $\mathcal{L}_2$-gain, γ results of the Example 3.2 for various H and T_d

ables. The differences between Theorem 3.4.1 and 3.4.2 are that Theorem 3.4.2 has one more variable than Theorem 3.4.1 and, also, that the size of the inequalities in Theorem 3.4.2 are larger than those of Theorem 3.4.1.

3.5 Parameter Dependent Lyapunov function

The parameter independent Lyapunov function (3.17) uses the same Lyapunov matrix (3.18) for all vertices of the subsystems. Hence, it is more conservative with regards to the stability conditions. We can deal with this conservatism issue by using the *parameter (vertex) dependent Lyapunov function*. The Lyapunov matrix of this function depends on both time and vertices of the subsystem in the cell. Before proceeding, it is helpful to give following Lemmas for the stability and $\mathcal{L}_2$ performance gain.

Lemma* 3.5.1** (Finsler (1937)):*** Let $x \in \mathbb{R}^n$, $A \in \mathbb{S}^n$ and $B \in \mathbb{R}^{m\times n}$ such that $rank(B) < n$. The following statements are equivalent:

(i) $x'Qx < 0, \quad \forall Bx = 0, \quad x \neq 0,$

(ii) $\bar{B}'Q\bar{B} < 0$ where $B\bar{B} = 0,$

(iii) $Q - \rho B'B < 0$ for some scalar ρ,

(iv) $Q + XB + B'X' < 0$ for some matrix X.

***Lemma* 3.5.2:** Consider the linear time invariant system, $\dot{x} = Ax(t)$ is asymptotically stable and then the following descriptions are equivalent:

(i) $P > 0, \qquad PA + A'P < 0,$

(ii) $P > 0, \quad \begin{bmatrix} SA + A'S' & P - S + A'G' \\ * & -G' - G \end{bmatrix} < 0$

where the matrices S and G, with suitable dimensions, are Lagrange multipliers. Note that these multipliers represent extra degrees of freedom and the constraint containing the multipliers is less conservative than the constraint with the Lyapunov matrix (de Oliveira and Skelton, 2001; Geromel et al., 1999).

Proof: If the second inequality in (ii) is multiplied from the left hand side by $Y = [I \; A']$ and Y' from right hand side, then the inequalities (i) are obtained. Moreover, if S and G in (ii) are chosen to be P and ζP, respectively, then the inequalities (i) are obtained when $\zeta \to 0$.

In other way, we can choose the matrices in Lemma 3.5.1 as

$$\begin{pmatrix} x(t) \\ \dot{x}(t) \end{pmatrix} \to x, \begin{bmatrix} 0 & P \\ P & 0 \end{bmatrix} \to Q, \begin{bmatrix} A' \\ -I \end{bmatrix} \to B', \begin{bmatrix} S \\ G \end{bmatrix} \to X, \begin{bmatrix} I \\ A \end{bmatrix} \to \bar{B}, \quad (3.22)$$

then Lemma 3.5.2 is obtained from (ii) and (iv) in Lemma 3.5.1.

***Lemma* 3.5.3:** Consider the linear time invariant system,

$$\dot{x} = Ax(t) + B_w w(t),$$
$$z = Cx(t) + D_w w(t),$$

is asymptotically stable and then the following descriptions are equivalent to find the L_2-gain:

(i) $P > 0, \quad \begin{bmatrix} PA + A'P & PB_w & C' \\ * & -\gamma^2 I & D_w' \\ * & * & -I \end{bmatrix} < 0.,$

$$\text{(ii)} \quad P > 0, \quad \begin{bmatrix} SA + A'S' & SB_w & C' & P - S + A'G' \\ * & -\gamma^2 I & D_w' & B_w'G' \\ * & * & -I & 0 \\ * & * & * & -G - G' \end{bmatrix} < 0.$$

where the matrices S and G, with suitable dimensions, are Lagrange multipliers.

Proof: If the inequality in (ii) is multiplied from the left hand side by Y' and Y from right hand side, then the inequality of (i) is obtained, where

$$Y = \begin{bmatrix} I & 0 & 0 \\ 0 & I & 0 \\ 0 & 0 & I \\ A & B_w & 0 \end{bmatrix}.$$

Moreover, if S and G in (ii) are chosen to be P and ζP, respectively, then the inequality in (i) is obtained when $\zeta \to 0$.

A time-varying and parameter dependent Lyapunov function, $V(t)$, are chosen such that

$$V(t) = x'(t)P_{\sigma(t)}x(t), \quad P_{\sigma(t)} = \sum_{j=1}^{N} \eta_j P_{\sigma(t)}^{(j)}, \quad \sum_{j=1}^{N} \eta_j = 1, \quad \eta_j \geq 0, \tag{3.23}$$

where $P_{\sigma(t)}^{(j)}(t) \in \{P_1^{(j)}(t), \ldots, P_M^{(j)}(t)\}$ according to $\sigma(t)$, defined as:

$$P_i^{(j)}(t) = \begin{cases} P_{i_0,H}^{(j)} & t \in [0, t_1), \\ P_{i,h}^{(j)} + (P_{i,h+1}^{(j)} - P_{i,h}^{(j)}) \dfrac{(t - t_{k,h})}{\frac{T}{H}} & t \in [t_{k,h}, t_{k,h+1}), \\ P_{i,H}^{(j)} & t \in [t_{k,H}, t_{k+1,0}). \end{cases} \tag{3.24}$$

where $h = 0, \ldots, H-1$, $j = 1, \ldots, N$, the number of the switching is defined by $k = 1, 2, \ldots$ and H is a given positive integer.

Note that the change of the Lyapunov matrix $P_i^{(j)}(t)$ with respect to time is similar to the change of the Lyapunov matrix $P_i(t)$ in Figure 3.3. The only difference between them is that Lyapunov matrix in (3.23) depend on the subpolytope vertices (Allerhand and Shaked, 2011).

►►► Stability Analysis using Parameter Dependent Lyapunov function

The parameter dependent Lyapunov function (3.23) is here used to analyse the stability of the system (3.1) with the parameter uncertainty (3.2). If Lemma 3.5.2 is applied to the conditions in Section 3.3.1, then the following Theorem is obtained for the stability analysis:

Theorem* 3.5.4** (Allerhand and Shaked (2011)):*** For a given $T > 0$, if there exist the set of matrices $S_{i,h},\ G_{i,h}$ and positive definite matrices $P_{i,h}^{(j)} > 0,\ i = 1,\dots,M,\ h = 0,\dots,H,\ j = 1,\dots,N$ that satisfy the following LMIs for all $i = 1,\dots,M$ and $j = 1,\dots,N$:

$$\begin{bmatrix} \dfrac{P_{i,h+1}^{(j)} - P_{i,h}^{(j)}}{T/H} + S_{i,h}A_i^{(j)} + A_i^{(j)'}S_{i,h}' & P_{i,h}^{(j)} - S_{i,h} + A_i^{(j)'}G_{i,h}' \\ * & -G_{i,h}' - G_{i,h} \end{bmatrix} < 0,$$

$$\begin{bmatrix} \dfrac{P_{i,h+1}^{(j)} - P_{i,h}^{(j)}}{T/H} + S_{i,h+1}A_i^{(j)} + A_i^{(j)'}S_{i,h+1}' & P_{i,h+1}^{(j)} - S_{i,h+1} + A_i^{(j)'}G_{i,h+1}' \\ * & -G_{i,h+1}' - G_{i,h+1} \end{bmatrix} < 0,$$

where $h = 0,\dots,H-1$

$$\begin{bmatrix} S_{i,H}A_i^{(j)} + A_i^{(j)'}S_{i,H}' & P_{i,H}^{(j)} - S_{i,H} + A_i^{(j)'}G_{i,H}' \\ * & -G_{i,H}' - G_{i,H} \end{bmatrix} < 0,$$

$$P_{i,H}^{(j)} - P_{s,0}^{(j)} \geq 0, \qquad \forall s \in \{1,\dots,M\} \text{ and } s \neq i,$$

then the system (3.1) with an uncertainty (3.2) is globally asymptotically stable for any switching rule with a dwell time that is greater than the minimum dwell time, T.

Example* 3.3*: Consider the same system given in Example 3.1. The stability of the system is provided using Theorem 3.5.4 with $H = 1$, and the minimum dwell time is found as $T = 0.482\,s$. The solver finds 56 variables by solving 24 different LMIs in $0.7525\,s$. These variables come from the components of the matrices $S_{i,h},\ G_{i,h}$ and $P_{i,h}^{(j)},\ \ i = 1,\dots,M,\ h = 0,\dots,H,\ j = 1,\dots,N$.

The minimum dwell time results are given in Table 3.4 for different values of H. Table 3.4 shows that the number of inequalities and variables increases, and the minimum dwell time decreases, with an increasing H. The solver time increases with the number of LMIs and the number of variables.

H	1	2	5	10	100
T(s)	0.482	0.293	0.105	0.089	0.083
Solving Time (s)	0.7525	0.9634	1.8052	3.3563	29.9927
Num. of LMIs	24	36	72	132	1212
Num. of Variable	56	84	168	308	2828

Table 3.4: The minimum dwell time, the number of LMIs and the number of variables for various H

Remark: In Theorem 3.5.4, $S_{i,h},\ G_{i,h}$ and $P_{i,h}^{(j)},\ \ i = 1,\ldots,M,\ h = 0,\ldots,H,\ j = 1,\ldots,N$ are the variables. The number of variables [the LMI solver needs to find] can be calculated using $M(H+1)(\Upsilon_S + \Upsilon_G + N\Upsilon_P)$, which is given in Table 3.5. Therefore, the solver deals with $MN(M+3H+1)$ different inequalities to find these variables.

Variable Name	Number of Variable
$P_{i,h}^{(j)}$	$M(H+1)N\Upsilon_P$
$S_{i,h}$	$M(H+1)\Upsilon_S$
$G_{i,h}$	$M(H+1)\Upsilon_G$
Total	$M(H+1)(\Upsilon_S + \Upsilon_G + N\Upsilon_P)$

Table 3.5: Number of variables (Theorem 3.5.4)

►►► $\mathcal{L}_2$-gain using Parameter Dependent Lyapunov function

The parameter independent Lyapunov function (3.23) is here used to satisfy both stability and performance criteria of the system (3.1) with the parameter uncertainty (3.2).

If Lemma 3.5.3 is applied to the $\mathcal{L}_2$-gain definition in Section 3.3.2, then the following Theorem is obtained for the $\mathcal{L}_2$ performance gain:

***Theorem* 3.5.5** (Allerhand and Shaked (2013))*:* For a given $T > 0$, if there exist the set of matrices $S_{i,h},\ G_{i,h}$ and positive definite matrices $P_{i,h}^{(j)} > 0,\ i = 1,\dots,M,\ h = 0,\dots,H,\ j = 1,\dots,N$ that satisfy the following LMIs for all $i = 1,\dots,M$ and $j = 1,\dots,N$:

$$\begin{bmatrix} \begin{pmatrix} \frac{(P_{i,h+1}^{(j)} - P_{i,h}^{(j)})}{T/H} + \\ S_{i,h}A_i^{(j)} + A_i^{(j)'}S_{i,h}' \end{pmatrix} & S_{i,h}B_{w,i}^{(j)} & C_i^{(j)'} & P_{i,h}^{(j)} - S_{i,h} + A_i^{(j)'}G_{i,h}' \\ * & -\gamma^2 I & D_{w,i}^{(j)'} & B_{w,i}^{(j)'}G_{i,h}' \\ * & * & -I & 0 \\ * & * & * & -G_{i,h}' - G_{i,h} \end{bmatrix} < 0,$$

$$\begin{bmatrix} \begin{pmatrix} \frac{(P_{i,h+1}^{(j)} - P_{i,h}^{(j)})}{T/H} + \\ S_{i,h+1}A_i^{(j)} + A_i^{(j)'}S_{i,h+1}' \end{pmatrix} & S_{i,h+1}B_{w,i}^{(j)} & C_i^{(j)'} & \begin{pmatrix} P_{i,h+1}^{(j)} - S_{i,h+1} \\ +A_i^{(j)'}G_{i,h+1}' \end{pmatrix} \\ * & -\gamma^2 I & D_{w,i}^{(j)'} & B_{w,i}^{(j)'}G_{i,h+1}' \\ * & * & -I & 0 \\ * & * & * & -G_{i,h+1}' - G_{i,h+1} \end{bmatrix} < 0,$$

where $h = 0,\dots,H-1$,

$$\begin{bmatrix} S_{i,H}A_i^{(j)} + A_i^{(j)'}S_{i,H}' & S_{i,H}B_{w,i}^{(j)} & C_i^{(j)'} & P_{i,H}^{(j)} - S_{i,H} + A_i^{(j)'}G_{i,H}' \\ * & -\gamma^2 I & D_{w,i}^{(j)'} & B_{w,i}^{(j)'}G_{i,H}' \\ * & * & -I & 0 \\ * & * & * & -G_{i,H}' - G_{i,H} \end{bmatrix} < 0,$$

$$P_{i,H}^{(j)} - P_{s,0}^{(j)} \geq 0, \qquad \forall s \in \{1,\dots,M\} \text{ and } s \neq i,$$

then the $\mathcal{L}_2$-gain of the system (3.1) with the uncertainty (3.2) is smaller than a positive scalar γ for any switching rule with a dwell time that is greater than the minimum dwell time, T.

***Example* 3.4:** Consider the same system as in Example 3.2. The stability of the system is provided using Theorem 3.5.5 with $H = 1$ and the minimum dwell time is found as $T = 0.482\,s$. The solver finds 57 variables by solving 25 different LMIs in $1.0438\,s$. These variables come from the components of the matrices $S_{i,h},\ G_{i,h},\ P_{i,h}^{(j)},\ i = 1,\ldots,M,\ h = 0,\ldots,H,\ j = 1,\ldots,N$ and $\mathcal{L}_2$-gain, γ.

The minimum dwell time results are given in Table 3.6 for various values of H. This table shows that the minimum dwell time decreases with increasing H. At the same time, solving time, the number of LMIs and the number of variables increase.

H	1	2	5	10	100
T(s)	0.482	0.293	0.105	0.089	0.083
Solving Time (s)	1.0438	1.3222	2.4739	5.1647	47.2486
Num. of LMIs	25	37	73	133	1213
Num. of Variable	57	85	169	309	2829

Table 3.6: The minimum dwell time, the number of LMIs and the number of variables for various H

The $\mathcal{L}_2$-gain results are shown in Table 3.7 according to different dwell times, T_d and scalar H. The table shows that $\mathcal{L}_2$ performance gain is decreasing whilst H and/or T_d are increasing. In addition to this, minimum dwell times and $\mathcal{L}_2$-gains are found to be lower compared to the result of Theorem 3.4.2 given in Tables 3.2 and 3.3.

Remark: In Theorem 3.5.5, $S_{i,h},\ G_{i,h},\ P_{i,h}^{(j)},\ i = 1,\ldots,M,\ h = 0,\ldots,H,\ j = 1,\ldots,N$ and γ are the variables. The number of variables [the LMI solver needs to find] can be calculated using $M(H+1)(\Upsilon_S+\Upsilon_G+N\Upsilon_P)+1$, which is given in Table 3.8. Therefore, the solver deals with $MN(M+3H+1)+1$ different inequalities to find these variables.

$H \setminus T_d$	1 s	2 s	3 s	4 s	5 s
1	8.3032	6.9905	6.6839	6.5482	6.4731
2	7.8320	6.6037	6.3945	6.3329	6.3065
5	7.3400	6.3678	6.2871	6.2707	6.2656
10	7.1713	6.3059	6.2688	6.2634	6.2622
100	6.9567	6.2703	6.2628	6.2618	6.2617

Table 3.7: The $\mathcal{L}_2$-gain, γ results of the Example 3.4 for various H and T_d

Variable Name	Number of Variable
$P_{i,h}^{(j)}$	$M(H+1)N\Upsilon_P$
$S_{i,h}$	$M(H+1)\Upsilon_S$
$G_{i,h}$	$M(H+1)\Upsilon_G$
γ	1
Total	$M(H+1)(\Upsilon_S+\Upsilon_G+N\Upsilon_P)+1$

Table 3.8: Number of variables (Theorem 3.5.5)

3.6 State-feedback Controller Design

In this section, two control design approaches are presented based on the parameter independent and dependent Lyapunov functions. The first one guarantees and minimises an $\mathcal{L}_2$ performance criterion (given in (3.8)) whilst the second one minimises the sensitivity of the system output to a zero mean white noise input w.

3.6.1 First Approach

Here, a stabilising state-feedback controller is designed by using the minimum dwell time theories which are based on parameter independent and dependent Lyapunov functions given in Sections 3.4 and 3.5, respectively. The state-feedback controller, $K_{\sigma(t)}(t)$, is sought to satisfy the performance criterion in (3.8) and stabilizes the system (3.1) with

$u(t) = K_{\sigma(t)}(t)x(t)$. We have

$$\begin{aligned} \dot{x} &= \left(A_{\sigma(t)} + B_{u,\sigma(t)}K_{\sigma(t)}(t)\right)x(t) + B_{w,\sigma(t)}w(t), \quad x(0) = 0, \\ z &= \left(C_{\sigma(t)} + D_{u,\sigma(t)}K_{\sigma(t)}(t)\right)x(t) + D_{w,\sigma(t)}w(t), \end{aligned} \tag{3.28}$$

with the polytopic uncertainties

$$\Omega = \bigcup_{i=1,\ldots,M} \Omega_i, \quad \Omega_i = \sum_{j=1}^{N} \eta_j \Omega_i^{(j)}, \quad \sum_{j=1}^{N} \eta_j = 1, \quad \eta_j \geq 0, \tag{3.29}$$

where $\Omega_i = \left[\begin{array}{c:c} A_i + B_{u,i}K_i & B_{w,i} \\ \hdashline C_i + D_{u,i}K_i & D_{w,i} \end{array}\right]$, $\Omega_i^{(j)} = \left[\begin{array}{c:c} A_i^{(j)} + B_{u,i}^{(j)}K_i & B_{w,i}^{(j)} \\ \hdashline C_i^{(j)} + D_{u,i}^{(j)}K_i & D_{w,i}^{(j)} \end{array}\right]$.

Using (3.15) with system matrices in (3.28), the state-feedback controller gains cannot be directly found because of coupling between the variables $P_i(t)$ and K_i. Hence, if the inequality in (3.15) is multiplied by

$$\begin{bmatrix} P_i(t)^{-1} & 0 & 0 \\ 0 & I & 0 \\ 0 & 0 & I \end{bmatrix}$$

from the left and right hand side, and $Q_i(t) = P_i(t)^{-1}$ is substituted, then the following inequality is found

$$\begin{bmatrix} -\dot{Q}_i(t) + A_i^{(j)}Q_i(t) + Q_i(t)A_i^{(j)\prime} & B_{w,i}^{(j)} & Q_i(t)C_i^{(j)\prime} \\ * & -\gamma^2 I & D_{w,i}^{(j)\prime} \\ * & * & -I \end{bmatrix} < 0. \tag{3.30}$$

The state-feedback rule, $u(t) = K_i(t)x(t)$, is applied to the inequality in (3.30) and thus

$$\begin{bmatrix} \begin{pmatrix} -\dot{Q}_i(t) + A_i^{(j)}Q_i(t) + Q_i(t)A_i^{(j)\prime} \\ +B_{u,i}^{(j)}K_iQ_i + Q_iK_i'B_{u,i}^{(j)\prime} \end{pmatrix} & B_{w,i}^{(j)} & \begin{pmatrix} Q_i(t)C_i^{(j)\prime} + \\ Q_iK_i'D_{u,i}^{(j)\prime} \end{pmatrix} \\ * & -\gamma^2 I & D_{w,i}^{(j)\prime} \\ * & * & -I \end{bmatrix} < 0.$$

To remove the coupling between the variables, the change of variable method is applied to $Y_i = K_i Q_i$ such that

$$\begin{bmatrix} \begin{pmatrix} -\dot{Q}_i(t) + A_i^{(j)} Q_i(t) + Q_i(t) A_i^{(j)'} \\ + B_{u,i}^{(j)} Y_i + Y_i' B_{u,i}^{(j)'} \end{pmatrix} & B_{w,i}^{(j)} & \begin{pmatrix} Q_i(t) C_i^{(j)'} + \\ Y_i' D_{u,i}^{(j)'} \end{pmatrix} \\ * & -\gamma^2 I & D_{w,i}^{(j)'} \\ * & * & -I \end{bmatrix} < 0. \quad (3.31)$$

►►► Controller Design using Parameter Independent Lyapunov Function

To calculate the state-feedback controller with a parameter independent Lyapunov matrices $Q_i(t)$ is defined as:

$$Q_i(t) = \begin{cases} Q_{i_0,H} & t \in [0, t_1), \\ Q_{i,h} + (Q_{i,h+1} - Q_{i,h}) \dfrac{(t - t_{k,h})}{\frac{T}{H}} & t \in [t_{k,h}, t_{k,h+1}), \\ Q_{i,H} & t \in [t_{k,H}, t_{k+1,0}). \end{cases} \quad (3.32)$$

where $h = 0, 1, \ldots, H-1$, the switching index is defined as $k \in \mathbb{N}$ and H is a given positive integer. $Q_i(t)$ changes similar to the matrix $P_i(t)$ in Figure 3.3.

Using (3.31) and (3.32), the following state-feedback controller design theorem is formulated for the system (3.28) with an uncertainty (3.29):

Theorem* 3.6.1** (Allerhand and Shaked (2010)):*** For a given $T > 0$, if the set of matrices $Y_{i,h}$ of compatible size and the collection of positive definite matrices $Q_{i,h} > 0,\ i = 1, \ldots, M,\ h = 0, \ldots, H$ satisfy the following LMIs for all $i = 1, \ldots, M$ and

$j = 1, \ldots, N$:

$$\begin{bmatrix} \begin{pmatrix} \frac{H(Q_{i,h} - Q_{i,h+1})}{T} + A_i^{(j)} Q_{i,h} + \\ Q_{i,h} A_i^{(j)\prime} + B_{u,i}^{(j)} Y_{i,h} + Y_{i,h}' B_{u,i}^{(j)\prime} \end{pmatrix} & B_{w,i}^{(j)} & Q_{i,h} C_i^{(j)\prime} + Y_{i,h}' D_{u,i}^{(j)\prime} \\ * & -\gamma^2 I & D_{w,i}^{(j)\prime} \\ * & * & -I \end{bmatrix} < 0,$$

$$\begin{bmatrix} \begin{pmatrix} \frac{H(Q_{i,h} - Q_{i,h+1})}{T} + A_i^{(j)} Q_{i,h+1} + \\ Q_{i,h+1} A_i^{(j)\prime} + B_{u,i}^{(j)} Y_{i,h+1} + Y_{i,h+1}' B_{u,i}^{(j)\prime} \end{pmatrix} & B_{w,i}^{(j)} & \begin{pmatrix} Q_{i,h+1} C_i^{(j)\prime} \\ + Y_{i,h+1}' D_{u,i}^{(j)\prime} \end{pmatrix} \\ * & -\gamma^2 I & D_{w,i}^{(j)\prime} \\ * & * & -I \end{bmatrix} < 0,$$

where $h = 0, \ldots, H-1$

$$\begin{bmatrix} \begin{pmatrix} A_i^{(j)} Q_{i,H} + Q_{i,H} A_i^{(j)\prime} \\ + B_{u,i}^{(j)} Y_{i,H} + Y_{i,H}' B_{u,i}^{(j)\prime} \end{pmatrix} & B_{w,i}^{(j)} & Q_{i,H} C_i^{(j)\prime} + Y_{i,H}' D_{u,i}^{(j)\prime} \\ * & -\gamma^2 I & D_{w,i}^{(j)\prime} \\ * & * & -I \end{bmatrix} < 0,$$

$$Q_{i,H} - Q_{s,0} \leq 0, \qquad \forall s \in \{1, \ldots, M\} \text{ and } s \neq i$$

then the $\mathcal{L}_2$-gain of the system (3.28) with an uncertainty (3.29) is smaller than a positive scalar γ for any switching rule with a dwell time that is greater than the minimum dwell time, T.

Then, the state-feedback gain matrix can be calculated such that

$$K_i(t) = \begin{cases} Y_{i_0,H} Q_{i_0,H}^{-1} & t \in [0, t_1), \\ \bar{Y}_{i,h} \bar{Q}_{i,h}^{-1} & t \in [t_{k,h}, t_{k,h+1}), \\ Y_{i,H} Q_{i,H}^{-1} & t \in [t_{k,H}, t_{k+1,0}). \end{cases} \tag{3.35}$$

where $\bar{Y}_{i,h} = Y_{i,h} + (Y_{i,h+1} - Y_{i,h}) \dfrac{(t - t_{k,r})}{T/H}$ and $\bar{Q}_{i,h} = Q_{i,h} + (Q_{i,h+1} - Q_{i,h}) \dfrac{(t - t_{k,r})}{T/H}$. Note that this theorem allows us to compute the state-feedback gain which is time-varying

during the dwell time. A time-varying controller can help to eliminate the transient effects of switching which arise after each switch.

***Example* 3.5:** Consider the same system in Example 3.2 with the following system parameters:

$$B_{u,1}^{(1)} = \begin{bmatrix} 0 \\ 1 \end{bmatrix}, \quad B_{u,1}^{(2)} = \begin{bmatrix} -0.6 \\ 1 \end{bmatrix}, \quad B_{u,2}^{(1)} = \begin{bmatrix} -1 \\ 1 \end{bmatrix}, \quad B_{u,2}^{(2)} = \begin{bmatrix} -0.4 \\ 1 \end{bmatrix},$$
$$D_{u,1}^{(1)} = 0, \qquad D_{u,1}^{(2)} = 2.4, \qquad D_{u,2}^{(1)} = 4, \qquad D_{u,2}^{(2)} = 1.6.$$

It is desired to design the time-varying controllers by using Theorem 3.6.1. This theorem solves 29 inequalities for $H = 2$ and $T = 0.3\,s$. The performance gain is then found as $\gamma = 3.2748$ with 31 variables. The time-varying controllers can be calculated by using equation (3.35) with the following matrices

$$Y_{1,0} = [-0.5677, \ -0.0419], \qquad Y_{2,0} = [-0.2573, \ -0.2810],$$
$$Y_{1,1} = [-0.3980, \ -0.2004], \qquad Y_{2,1} = [-0.2853, \ -0.2689],$$
$$Y_{1,2} = [-0.1428, \ -0.2746], \qquad Y_{2,2} = [-0.2532, \ -0.2276],$$

$$Q_{1,0} = \begin{bmatrix} 0.1646 & -0.0393 \\ -0.0393 & 0.3093 \end{bmatrix}, \qquad Q_{2,0} = \begin{bmatrix} 0.1667 & 0.0309 \\ 0.0309 & 0.2371 \end{bmatrix},$$
$$Q_{1,1} = \begin{bmatrix} 0.1491 & -0.0195 \\ -0.0195 & 0.2110 \end{bmatrix}, \qquad Q_{2,1} = \begin{bmatrix} 0.1378 & 0.0206 \\ 0.0206 & 0.2427 \end{bmatrix},$$
$$Q_{1,2} = \begin{bmatrix} 0.1367 & -0.0183 \\ -0.0183 & 0.1563 \end{bmatrix}, \qquad Q_{2,2} = \begin{bmatrix} 0.1188 & 0.0161 \\ 0.0161 & 0.2422 \end{bmatrix}.$$

Remark: In Theorem 3.6.1, $Y_{i,h},\ Q_{i,h},\ i = 1,\ldots,M,\ h = 0,\ldots,H$ and γ are the variables. The number of variables [the LMI solver needs to find] can be calculated using $M(H+1)(\Upsilon_Y + \Upsilon_Q) + 1$. Therefore, the solver deals with $M(M + N + 2NH + H) + 1$ different inequalities to find these variables. Solving Theorem 3.6.1 is more complex than Theorem 3.4.1 and 3.4.2 due to the number of variables and the size of the inequalities. However, Theorem 3.6.1 provides the controller design as well as ensuring stability and minimising $\mathcal{L}_2-$gain.

Theorem 3.6.1 allows us to compute only the time-varying state-feedback gain but since this type of controller is not preferred in most of the cases, a controller design method with a parameter dependent Lyapunov function will be presented.

►►► Controller Design using Parameter Dependent Lyapunov Function

To calculate the state-feedback controller with a parameter dependent Lyapunov function, the same method in Lemma 3.5.3 is applied to the inequality in (3.30)

$$\begin{bmatrix} \begin{pmatrix} -\dot{Q}_i(t) + A_i^{(j)} S_i(t) \\ +S_i'(t) A_i^{(j)\prime} \end{pmatrix} & B_{w,i}^{(j)} & S_i'(t) C_i^{(j)\prime} & \begin{pmatrix} Q_i(t) - S_i'(t) \\ +A_i^{(j)} G_i(t) \end{pmatrix} \\ * & -\gamma^2 I & D_{w,i}^{(j)\prime} & 0 \\ * & * & -I & C_i^{(j)} G_i(t) \\ * & * & * & -G_i'(t) - G_i(t) \end{bmatrix} < 0. \quad (3.36)$$

To verify the above inequality, if the inequality in (3.30) is multiplied from the left hand side by Y_T' and Y_T from right hand side, then the inequality (3.36) is obtained, where:

$$Y_T = \begin{bmatrix} I & 0 & 0 \\ 0 & I & 0 \\ 0 & 0 & I \\ A_i^{(j)\prime} & 0 & C_i^{(j)\prime} \end{bmatrix}$$

In addition, if S_i and G_i in (3.36) are chosen to be Q_i and ζQ_i, respectively, then the inequality in (3.30) is obtained when $\zeta \to 0$.

The state-feedback rule, $u(t) = K_i(t)x(t)$ is applied to the inequality (3.36), G is defined as $G = \beta S$ and the change of variable method is applied to $Y_i = K_i Q_i$ to remove the coupling between the variables. Then, the time-varying and parameter dependent positive definite matrix Q_i is chosen such that

$$Q_i(t) = \sum_{j=1}^{N} \eta_j Q_i^{(j)}(t), \quad \sum_{j=1}^{N} \eta_j = 1, \quad \eta_j \geq 0, \quad (3.37)$$

where $Q_i^{(j)}(t) \in \{Q_1^{(j)}(t), \ldots, Q_M^{(j)}(t)\}$ defined as:

$$Q_i^{(j)}(t) = \begin{cases} Q_{i_0,H}^{(j)} & t \in [0, t_1), \\ Q_{i,h}^{(j)} + (Q_{i,h+1}^{(j)} - Q_{i,h}^{(j)}) \dfrac{(t - t_{k,h})}{\frac{T}{H}} & t \in [t_{k,h}, t_{k,h+1}), \\ Q_{i,H}^{(j)} & t \in [t_{k,H}, t_{k+1,0}). \end{cases} \tag{3.38}$$

where $h = 0, \ldots, H-1$, $j = 1, \ldots, N$, the number of the switching is defined by $k = 1, 2, \ldots$ and H is a given positive integer. The change of the positive definite matrix $Q_i^{(j)}(t)$ with respect to time is similar to the change of the matrix $Q_i(t)$ in (3.32) .

Then, the state-feedback control design with parameter dependent Lyapunov function can be written as follows:

Theorem* 3.6.2** (Allerhand and Shaked (2013)):*** For given scalars β and $T > 0$, if the set of matrices $S_{i,h}$ and $Y_{i,h}$ of compatible size and the collection of positive definite matrices $Q_{i,h}^{(j)} > 0,\ i = 1, \ldots, M,\ h = 0, \ldots, H,\ j = 1, \ldots, N$ satisfy the following LMIs for all $i = 1, \ldots, M$ and $j = 1, \ldots, N$:

$$\begin{bmatrix} \Gamma & B_{w,i}^{(j)} & S_{i,h}' C_i^{(j)\prime} + Y_{i,h}' D_{u,i}^{(j)\prime} & Q_{i,h}^{(j)} - S_{i,h}' + \beta A_i^{(j)} S_{i,h} + \beta B_{u,i}^{(j)} Y_{i,h} \\ * & -\gamma^2 I & D_{w,i}^{(j)\prime} & 0 \\ * & * & -I & \beta C_i^{(j)} S_{i,h} + \beta D_{u,i}^{(j)} Y_{i,h} \\ * & * & * & -\beta S_{i,h}' - \beta S_{i,h} \end{bmatrix} < 0,$$

$$\begin{bmatrix} \Theta & B_{w,i}^{(j)} & S_{i,h+1}' C_i^{(j)\prime} + Y_{i,h+1}' D_{u,i}^{(j)\prime} & \begin{pmatrix} Q_{i,h+1}^{(j)} - S_{i,h+1}' + \\ \beta (A_i^{(j)} S_{i,h+1} + B_{u,i}^{(j)} Y_{i,h+1}) \end{pmatrix} \\ * & -\gamma^2 I & D_{w,i}^{(j)\prime} & 0 \\ * & * & -I & \beta C_i^{(j)} S_{i,h+1} + \beta D_{u,i}^{(j)} Y_{i,h+1} \\ * & * & * & -\beta S_{i,h+1}' - \beta S_{i,h+1} \end{bmatrix} < 0,$$

where $h = 0, \ldots, H-1$

$$\begin{bmatrix} \psi & B_{w,i}^{(j)} & S_{i,H}' C_i^{(j)'} + Y_{i,H}' D_{u,i}^{(j)'} & Q_{i,H}^{(j)} - S_{i,H}' + \beta(A_i^{(j)} S_{i,H} + B_{u,i}^{(j)} Y_{i,H}) \\ * & -\gamma^2 I & D_{w,i}^{(j)'} & 0 \\ * & * & -I & \beta C_i^{(j)} S_{i,H} + \beta D_{u,i}^{(j)} Y_{i,H} \\ * & * & * & -\beta S_{i,H}' - \beta S_{i,H} \end{bmatrix} < 0,$$

$$Q_{i,H}^{(j)} - Q_{s,0}^{(j)} \leq 0. \qquad \forall s \in \{1, \ldots, M\} \text{ and } s \neq i$$

Here:

$$\Gamma = \frac{H(Q_{i,h}^{(j)} - Q_{i,h+1}^{(j)})}{T} + A_i^{(j)} S_{i,h} + S_{i,h}' A_i^{(j)'} + B_{u,i}^{(j)} Y_{i,h} + Y_{i,h}' B_{u,i}^{(j)'},$$

$$\Theta = \frac{H(Q_{i,h}^{(j)} - Q_{i,h+1}^{(j)})}{T} + A_i^{(j)} S_{i,h+1} + S_{i,h+1}' A_i^{(j)'} + B_{u,i}^{(j)} Y_{i,h+1} + Y_{i,h+1}' B_{u,i}^{(j)'},$$

$$\psi = A_i^{(j)} S_{i,H} + S_{i,H}' A_i^{(j)'} + B_{u,i}^{(j)} Y_{i,H} + Y_{i,H}' B_{u,i}^{(j)'},$$

then the $\mathcal{L}_2$-gain of the system (3.28) with an uncertainty (3.29) is smaller than a positive scalar γ for any switching rule with a dwell time that is greater than the minimum dwell time, T.

Then, the state-feedback gain matrix can be defined such that

$$K_i(t) = \begin{cases} Y_{i_0,H} S_{i_0,H}^{-1} & t \in [0, t_1), \\ \bar{Y}_{i,h} \bar{S}_{i,h}^{-1} & t \in [t_{k,h}, t_{k,h+1}), \\ Y_{i,H} S_{i,H}^{-1} & t \in [t_{k,H}, t_{k+1,0}). \end{cases} \tag{3.41}$$

where $\bar{Y}_{i,h} = Y_{i,h} + (Y_{i,h+1} - Y_{i,h}) \dfrac{(t - t_{k,r})}{T/H}$ and $\bar{S}_{i,h} = S_{i,h} + (S_{i,h+1} - S_{i,h}) \dfrac{(t - t_{k,h})}{T/H}$.

Remark: If $Y_{i,h}$ and $S_{i,h}$ are assumed to be independent of h, then a constant controller gain for each subpolytope can be found. The state-feedback gain then becomes $K_i = Y_i S_i^{-1}$.

***Example* 3.6:** Consider the same system given in Example 3.5. It is desired to design the state-feedback control with a parameter dependent Lyapunov function. The prescribed scalars H and β are chosen as 2 and 0.04, respectively. Theorem 3.6.2 is then solved with a dwell time of $T = 0.3\,s$. The performance gain is found $\gamma = 2.8037$ by solving 37 LMIs with 73 variables. The solutions of the variables are such that

$$Y_{1,0} = [-0.8032, -0.3527], \qquad Y_{2,0} = [-0.3054, -0.4094],$$

$$Y_{1,1} = [-0.1947, -0.7947], \qquad Y_{2,1} = [-0.1712, -0.3122],$$

$$Y_{1,2} = [\ \ 0.0249, -0.7195], \qquad Y_{2,2} = [-0.1100, -0.3012],$$

$$S_{1,0} = \begin{bmatrix} 0.2308 & -0.0582 \\ -0.0966 & 0.3877 \end{bmatrix}, \qquad S_{2,0} = \begin{bmatrix} 0.2545 & 0.1145 \\ -0.0150 & 0.3112 \end{bmatrix},$$

$$S_{1,1} = \begin{bmatrix} 0.2041 & 0.0011 \\ -0.1451 & 0.3730 \end{bmatrix}, \qquad S_{2,1} = \begin{bmatrix} 0.1804 & 0.0681 \\ -0.0413 & 0.3252 \end{bmatrix},$$

$$S_{1,2} = \begin{bmatrix} 0.1812 & -0.0122 \\ -0.1194 & 0.2946 \end{bmatrix}, \qquad S_{2,2} = \begin{bmatrix} 0.1321 & 0.0620 \\ -0.0687 & 0.3491 \end{bmatrix}.$$

The time-varying state-feedback controller is given by (3.41) with the above matrices. If it is assumed that $Y_{i,h}$ and $S_{i,h}$ are independent of h, the constant controller gains are found such that

$$K_1 = [-3.2638,\ -1.7833], \qquad K_2 = [-0.8926,\ -0.7194],$$

where the performance gain is calculated as $\gamma = 3.0499$ by solving 37 LMIs with 49 variables. Note that, during the constant controller design, the solver deals with the same number of inequalities but the number of variables is decreased from 73 to 49. γ is increased from 2.8037 to 3.0499 due to the restriction of having time invariants $Y_{i,h}$ and $S_{i,h}$.

Remark: To solve Theorem 3.6.2, the variable matrices $S_{i,h},\ Y_{i,h},\ Q_{i,h}^{(j)},\ \ i = 1, \ldots, M,$ $h = 0, \ldots, H,\ j = 1, \ldots, N$ and γ need to be found. The total number of variables the LMI solver needs to find is $M(H+1)(\Upsilon_S + \Upsilon_Y + N\Upsilon_Q) + 1$, which is given in Table 3.9. Therefore, the solver deals with $MN(M+3H+1)+1$ different inequalities to find these variables. If the constant state-feedback gains are sought, the total number of variables the LMI solver need to find is $M(\Upsilon_S + \Upsilon_Y + (H+1)N\Upsilon_Q) + 1$.

Variable Name	Number of Variable	Number of Variable (constant)
$Q_{i,h}^{(j)}$	$M(H+1)N\Upsilon_Q$	$M(H+1)N\Upsilon_Q$
$S_{i,h}$	$M(H+1)\Upsilon_S$	$M\Upsilon_S$
$Y_{i,h}$	$M(H+1)\Upsilon_Y$	$M\Upsilon_Y$
γ	1	1
Total	$M(H+1)(\Upsilon_S + \Upsilon_Y + N\Upsilon_Q) + 1$	$M(\Upsilon_S + \Upsilon_Y + (H+1)N\Upsilon_Q) + 1$

Table 3.9: Number of variables (Theorem 3.6.2)

3.6.2 Second Approach

As a more convenient method, we present a state-feedback controller design approach that deals with the effects of the white noise input on the switched system with polytopic parameter uncertainties. This approach combines the $\mathcal{H}_2-$optimal control in Section 2.4.1 and the minimum dwell time methods mentioned in the previous sections. In addition, it allows us to design the state-feedback $\mathcal{H}_2-$optimal controller for the switched system with polytopic parameter uncertainties. The difference with regards to the first approach is the $\mathcal{H}_2$ optimization technique minimises sensitivity of the system output to a zero mean white noise input w.

The $\mathcal{H}_2-$optimal control in Theorem 2.4.2 can be formulated for the switched system in the following lemma.

***Lemma* 3.6.3:** Consider a switched system with state-feedback, $u = K_i x$

$$\begin{aligned} \dot{x} &= A_i x + B_{u,i} u + B_{w,i} w, \\ z &= C_i x + D_{u,i} u, \end{aligned} \tag{3.42}$$

the $\mathcal{H}_2$-optimal state-feedback control in Theorem 2.4.2 can be extended for the switched system.

If there exist the collection of symmetric matrices $Q_i > 0$ and Z and the set of matrices Y_i, then $\mathcal{H}_2$-gain of the system (3.42) with state-feedback, $u = K_i x$ is less than υ, if the following conditions hold:

$$\begin{aligned} Tr(Z) &< \upsilon^2, \\ \begin{bmatrix} Z & B'_{w,i} \\ * & Q_i(t) \end{bmatrix} &> 0, \\ \begin{bmatrix} \begin{pmatrix} -\dot{Q}_i(t) + A_i Q_i(t) + Q_i(t) A_i' \\ +B_{u,i} Y_i(t) + Y_i(t)' B_{u,i}' \end{pmatrix} & Q_i(t) C_i' + Y_i(t)' D_{u,i}' \\ * & -I \end{bmatrix} &< 0, \end{aligned} \tag{3.43}$$

then the closed-loop system is quadratically stable and the $\mathcal{H}_2$-gain from w to z is less than or equal to $\upsilon = \sqrt{Tr(Z)}$.

Proof: Inequality (3.43) is an application of inequality (2.23) introduced earlier.

Remark: Minimising $Tr(Z)$ gives the best upper bound. Then, the state-feedback controller is $K_i = Y_i Q_i^{-1}$.

►►► Controller Design using Parameter Independent Lyapunov Function

***Theorem* 3.6.4:** For a given $T > 0$, if the set of matrices $Y_{i,h}$ of compatible size and the collection of symmetric matrices Z and $Q_{i,h} > 0,\ i = 1, \ldots, M,\ h = 0, \ldots, H$ satisfy

the following LMIs for all $i = 1, \ldots, M$ and $j = 1, \ldots, N$:

$$\begin{bmatrix} Z & B_{w,i}^{(j)'} \\ * & Q_{i,h} \end{bmatrix} > 0, \qquad \forall h \in \{0, \ldots, H\},$$

$$\begin{bmatrix} \begin{pmatrix} \frac{H(Q_{i,h} - Q_{i,h+1})}{T} + A_i^{(j)} Q_{i,h} + \\ Q_{i,h} A_i^{(j)'} + B_{u,i}^{(j)} Y_{i,h} + Y_{i,h}' B_{u,i}^{(j)'} \end{pmatrix} & Q_{i,h} C_i^{(j)'} + Y_{i,h}' D_{u,i}^{(j)'} \\ * & -I \end{bmatrix} < 0,$$

$$\begin{bmatrix} \begin{pmatrix} \frac{H(Q_{i,h} - Q_{i,h+1})}{T} + A_i^{(j)} Q_{i,h+1} + \\ Q_{i,h+1} A_i^{(j)'} + B_{u,i}^{(j)} Y_{i,h+1} + Y_{i,h+1}' B_{u,i}^{(j)'} \end{pmatrix} & Q_{i,h+1} C_i^{(j)'} + Y_{i,h+1}' D_{u,i}^{(j)'} \\ * & -I \end{bmatrix} < 0,$$

where $h = 0, \ldots, H-1$

$$\begin{bmatrix} A_i^{(j)} Q_{i,H} + Q_{i,H} A_i^{(j)'} + B_{u,i}^{(j)} Y_{i,H} + Y_{i,H}' B_{u,i}^{(j)'} & Q_{i,H} C_i^{(j)'} + Y_{i,H}' D_{u,i}^{(j)'} \\ * & -I \end{bmatrix} < 0,$$

$$Q_{i,H} - Q_{s,0} \leq 0, \qquad \forall s \in \{1, \ldots, M\} \text{ and } s \neq i$$

then there exists a state-feedback regulator $K_{\sigma(t)}(t) \in \{K_1(t), \ldots, K_M(t)\}$ according to $\sigma(t)$, defined as:

$$K_i(t) = \begin{cases} Y_{i_0,H} Q_{i_0,H}^{-1} & t \in [0, t_1), \\ \bar{Y}_{i,h} \bar{Q}_{i,h}^{-1} & t \in [t_{k,h}, t_{k,h+1}), \\ Y_{i,H} Q_{i,H}^{-1} & t \in [t_{k,H}, t_{k+1,0}). \end{cases} \tag{3.45}$$

where $\bar{Y}_{i,h} = Y_{i,h} + (Y_{i,h+1} - Y_{i,h}) \frac{(t - t_{k,h})}{T/H}$ and $\bar{Q}_{i,h} = Q_{i,h} + (Q_{i,h+1} - Q_{i,h}) \frac{(t - t_{k,h})}{T/H}$, such that the closed-loop system (system (3.28) with (3.45) and an uncertainty (3.29)) is quadratically stable for any switching rule with a dwell time that is greater than the minimum dwell time, T and such that the $\mathcal{H}_2$-gain from w to z is less than or equal to $\upsilon = \sqrt{Tr(Z)}$.

Proof: If Q_i in the inequality (3.43) is chosen as in (3.32), then Theorem 3.6.4 for the state-feedback $\mathcal{H}_2-$optimal controller design is formulated for the system (3.28) with an uncertainty (3.29).

Remark: Minimising $Tr(Z)$ gives the best upper bound. Note that this theorem provides a state-feedback gain which is time varying during the dwell time.

Example* 3.7*: Consider the system in Example 3.5. It is desired to design the time-varying controllers by using Theorem 3.6.4. This theorem solves 48 inequalities for $H = 2$ and $T = 0.3\,s$. The $\mathcal{H}_2-$optimal gain is then found as $v = 10.6$ with 31 variables. The time-varying controllers can be calculated by using equation (3.49) with the following matrices

$$
\begin{aligned}
Y_{1,0} &= [-0.9986, \quad 0.0941], & Y_{2,0} &= [-0.3513, \ -0.3330],\\
Y_{1,1} &= [-0.7475, \ -0.2775], & Y_{2,1} &= [-0.4054, \ -0.3521],\\
Y_{1,2} &= [-0.6305, \ -0.4931], & Y_{2,2} &= [-0.3837, \ -0.3193],
\end{aligned}
$$

$$
\begin{aligned}
Q_{1,0} &= \begin{bmatrix} 0.3281 & -0.1757 \\ -0.1757 & 0.6512 \end{bmatrix}, & Q_{2,0} &= \begin{bmatrix} 0.2366 & 0.0295 \\ 0.0295 & 0.3203 \end{bmatrix},\\
Q_{1,1} &= \begin{bmatrix} 0.2565 & -0.0712 \\ -0.0712 & 0.4288 \end{bmatrix}, & Q_{2,1} &= \begin{bmatrix} 0.1945 & 0.0271 \\ 0.0271 & 0.3747 \end{bmatrix},\\
Q_{1,2} &= \begin{bmatrix} 0.2168 & -0.0045 \\ -0.0045 & 0.2618 \end{bmatrix}, & Q_{2,2} &= \begin{bmatrix} 0.1740 & 0.0272 \\ 0.0272 & 0.3841 \end{bmatrix}.
\end{aligned}
$$

►►► Controller Design using Parameter Dependent Lyapunov Function

To calculate the state-feedback $\mathcal{H}_2$-optimal controller with a parameter dependent Lyapunov function, the same method in Lemma 3.5.2 is applied to the third inequality in (3.43),

$$
\begin{bmatrix} -\dot{Q}_i(t) + A_{cl}S_i(t) + S_i'(t)A_{cl}' & S_i'(t)C_{cl}' & Q_i(t) - S_i'(t) + A_{cl}G_i(t) \\ * & -I & C_{cl}G_i(t) \\ * & * & -G_i'(t) - G_i(t) \end{bmatrix} < 0. \quad (3.46)
$$

where the closed-loop system matrices are $A_{cl} = A_i + B_iK_i$ and $C_{cl} = C_i + D_iK_i$.

To verify the above inequality, if the second inequality in (3.43) is multiplied from the left hand side by Y_T' and Y_T from right hand side, then the inequality (3.46) is obtained,

where:

$$Y_T = \begin{bmatrix} I & 0 \\ 0 & I \\ A'_{cl} & C'_{cl} \end{bmatrix}$$

In addition, if S_i and G_i in (3.43) are chosen to be Q_i and ζQ_i, respectively, then the inequality in (3.46) is obtained when $\zeta \to 0$.

If the time-varying and parameter dependent positive definite matrix Q_i is chosen as in (3.37), then the following state-feedback $\mathcal{H}_2-$optimal controller design theorem is formulated for the system (3.28) with an uncertainty (3.29):

***Theorem* 3.6.5:** For given scalars $\beta > 0$ and $T > 0$, if the set of matrices $S_{i,h}$ and $Y_{i,h}$ are of compatible size and the collection of symmetric matrices Z and $Q_{i,h}^{(j)} > 0,\ i = 1,\dots,M,\ h = 0,\dots,H,\ j = 1,\dots,N$ satisfy the following LMIs for all $i = 1,\dots,M$ and $j = 1,\dots,N$:

$$\begin{bmatrix} Z & B_{w,i}^{(j)'} \\ * & Q_{i,h}^{(j)} \end{bmatrix} > 0, \qquad \forall h \in \{0,\dots,H\},$$

$$\begin{bmatrix} \Gamma & S'_{i,h}C_i^{(j)'} + Y'_{i,h}D_{u,i}^{(j)'} & Q_{i,h}^{(j)} - S'_{i,h} + \beta A_i^{(j)} S_{i,h} + \beta B_{u,i}^{(j)} Y_{i,h} \\ * & -I & \beta C_i^{(j)} S_{i,h} + \beta D_{u,i}^{(j)} Y_{i,h} \\ * & * & -\beta S'_{i,h} - \beta S_{i,h} \end{bmatrix} < 0,$$

$$\begin{bmatrix} \Theta & S'_{i,h+1}C_i^{(j)'} + Y'_{i,h+1}D_{u,i}^{(j)'} & Q_{i,h+1}^{(j)} - S'_{i,h+1} + \beta A_i^{(j)} S_{i,h+1} + \beta B_{u,i}^{(j)} Y_{i,h+1} \\ * & -I & \beta C_i^{(j)} S_{i,h+1} + \beta D_{u,i}^{(j)} Y_{i,h+1} \\ * & * & -\beta S'_{i,h+1} - \beta S_{i,h+1} \end{bmatrix} < 0,$$

where $h = 0,\dots,H-1$

$$\begin{bmatrix} \psi & S'_{i,H}C_i^{(j)'} + Y'_{i,H}D_{u,i}^{(j)'} & Q_{i,H}^{(j)} - S'_{i,H} + \beta A_i^{(j)} S_{i,H} + \beta B_{u,i}^{(j)} Y_{i,H} \\ * & -I & \beta C_i^{(j)} S_{i,H} + \beta D_{u,i}^{(j)} Y_{i,H} \\ * & * & -\beta S'_{i,H} - \beta S_{i,H} \end{bmatrix} < 0,$$

$$Q_{i,H}^{(j)} - Q_{s,0}^{(j)} \leq 0. \qquad \forall s \in \{1,\dots,M\} \text{ and } s \neq i$$

Here:

$$\Gamma = \frac{H(Q_{i,h}^{(j)} - Q_{i,h+1}^{(j)})}{T} + A_i^{(j)} S_{i,h} + S_{i,h}' A_i^{(j)'} + B_{u,i}^{(j)} Y_{i,h} + Y_{i,h}' B_{u,i}^{(j)'},$$

$$\Theta = \frac{H(Q_{i,h}^{(j)} - Q_{i,h+1}^{(j)})}{T} + A_i^{(j)} S_{i,h+1} + S_{i,h+1}' A_i^{(j)'} + B_{u,i}^{(j)} Y_{i,h+1} + Y_{i,h+1}' B_{u,i}^{(j)'},$$

$$\psi = A_i^{(j)} S_{i,H} + S_{i,H}' A_i^{(j)'} + B_{u,i}^{(j)} Y_{i,H} + Y_{i,H}' B_{u,i}^{(j)'},$$

then there exists a state-feedback regulator $K_{\sigma(t)}(t) \in \{K_1(t), \ldots, K_M(t)\}$ according to $\sigma(t)$, defined as:

$$K_i(t) = \begin{cases} Y_{i_0,H} Q_{i_0,H}^{-1} & t \in [0, t_1), \\ \bar{Y}_{i,h} \bar{Q}_{i,h}^{-1} & t \in [t_{k,h}, t_{k,h+1}), \\ Y_{i,H} Q_{i,H}^{-1} & t \in [t_{k,H}, t_{k+1,0}). \end{cases} \tag{3.49}$$

where $\bar{Y}_{i,h} = Y_{i,h} + (Y_{i,h+1} - Y_{i,h})\frac{(t-t_{k,h})}{T/H}$ and $\bar{Q}_{i,h} = Q_{i,h} + (Q_{i,h+1} - Q_{i,h})\frac{(t-t_{k,h})}{T/H}$, such that the closed-loop system (system (3.28) with (3.45) and an uncertainty (3.29)) is quadratically stable for any switching rule with a dwell time that is greater than the minimum dwell time, T and such that the $\mathcal{H}_2$-gain from w to z is less than or equal to $\upsilon = \sqrt{Tr(Z)}$.

Proof: Theorem can be derived in a straightforward manner, based on the inequalities in (3.43) and (3.46) with Q_i in (3.37). Here, G_i is defined as $G_i = \beta S_i$ and the change of variable method is applied to $Y_i = K_i Q_i$ to remove the coupling between the variables.

Remark: Minimising $Tr(Z)$ gives the best upper bound. Note that this theorem provides a state-feedback gain which is time varying during the dwell time. If $Y_{i,h}$ and $S_{i,h}$ are assumed to be independent of h, then a constant controller gain for each subpolytope can be found. The state-feedback gain then becomes $K_i = Y_i S_i^{-1}$.

***Example* 3.8:** Consider the system in Example 3.5. It is desired to design the state-feedback control with a parameter dependent Lyapunov function. The prescribed scalars H and β are chosen as 2 and 0.04, respectively. Theorem 3.6.5 is then solved with a dwell

time of $T = 0.3\,s$. The performance gain is found $\upsilon = 3.5846$ by solving 56 LMIs with 73 variables. The solutions of the variables are such that

$$Y_{1,0} = [-1.8543,\ 0.7628], \qquad Y_{2,0} = [-1.3169,\ -0.7610],$$

$$Y_{1,1} = [-1.9911,\ 0.4591], \qquad Y_{2,1} = [-1.9286,\ -1.4932],$$

$$Y_{1,2} = [-2.9443,\ 1.4831], \qquad Y_{2,2} = [-2.4215,\ -1.5396],$$

$$Q_{1,0} = \begin{bmatrix} 0.8200 & -0.8211 \\ -0.5930 & 1.4315 \end{bmatrix}, \qquad Q_{2,0} = \begin{bmatrix} 0.9448 & -0.0041 \\ -0.0503 & 1.3353 \end{bmatrix},$$

$$Q_{1,1} = \begin{bmatrix} 1.2490 & -0.8314 \\ -1.4656 & 2.5131 \end{bmatrix}, \qquad Q_{2,1} = \begin{bmatrix} 1.2452 & 0.1314 \\ -0.1423 & 2.5938 \end{bmatrix},$$

$$Q_{1,2} = \begin{bmatrix} 1.3674 & -0.6839 \\ -1.9020 & 3.0668 \end{bmatrix}, \qquad Q_{2,2} = \begin{bmatrix} 1.2912 & 0.7505 \\ -0.4435 & 3.3752 \end{bmatrix}.$$

The time-varying state-feedback controller is given by (3.49) with the above matrices. If it is assumed that $Y_{i,h}$ and $S_{i,h}$ are independent of h, the constant controller gains are found such that

$$K_1 = [-3.1224,\ -1.1763], \qquad K_2 = [-1.5038,\ -0.6759],$$

where the performance gain is calculated as $\upsilon = 4.8909$ by solving 56 LMIs with 49 variables. Note that, during the constant controller design, the solver deals with the same number of inequalities but the number of variables is decreased from 73 to 49. υ is increased from 3.5846 to 4.8909 due to the restriction of having time invariants $Y_{i,h}$ and $S_{i,h}$.

3.7 Summary

Stability analyses of switched systems with polytopic parameter uncertainty have been presented in this chapter. The minimum dwell time stability theories based on parameter independent / dependent Lyapunov functions were adopted from (Allerhand and Shaked, 2011) and (Allerhand and Shaked, 2013). Considering these theories, $\mathcal{L}_2$-gain and $\mathcal{H}_2$-optimal gain approaches have been used to design a state-feedback switched controller. The LMIs in the mentioned theorems have been formulated using the modelling and optimization toolbox, YALMIP, in MATLAB (Lofberg, 2004). An illustrative example has been solved at the end of each section. The results of these examples showed that whilst the parameter dependent Lyapunov function solves more LMIs, it nevertheless provides a smaller minimum dwell time for the switched systems.

CHAPTER 4

Piecewise Quadratic Stability Analysis

4.1 Introduction

Basic concepts of switched system stability analysis have been introduced in Chapter 2, and stability analysis dependant on slow switching signals has been further extended to the minimum dwell time analysis with parameter independent / dependent LF in Chapter 3. In addition to these methodologies, the extended version of the state-dependent switching analysis for piecewise linear systems will be introduced in this chapter.

Piecewise linear (PWL) systems are a class of non-linear system. PWL systems have different types, such as being PWL in the input variable, u, PWL in the time, t, and PWL in the system state, x. In this chapter, we will focus on the most common case, which is PWL in the system state. More specifically, we will introduce two approaches for stability analysis of general PWL systems, which are common, and piecewise, quadratic stabilities. In addition, these approaches are extended to the $\mathcal{L}_2$-gain analysis and state-feedback controller design.

The rest of this chapter is structured as follows: the PWL system is described in Sec-

tion 4.2. Section 4.3 examines the quadratic stability analysis for PWL systems. The quadratic approach in Chapter 2 is extended with the $S-$procedure method. Additionally, in Section 4.4, the piecewise quadratic stability analysis technique is discussed. $\mathcal{L}_2$ performance criteria are applied to the common and piecewise quadratic stability analysis methods in Section 4.5. In Section 4.6, the state-feedback controller design technique is discussed in terms of imposing upper and lower bounds on the optimal cost. Finally, the chapter is concluded with Section 4.7.

4.2 System Description

In PWL systems, the state space is divided into a set of regions, $\mathbb{X}_i$. The standard form of PWL systems can be described as

$$\left.\begin{aligned} \dot{x}(t) &= A_i\, x(t) + B_i\, u(t) + a_i \\ y(t) &= C_i\, x(t) + D_i\, u(t) + c_i \end{aligned}\right\} \qquad x(t) \in \mathbb{X}_i \text{ and } \quad a_i \in \mathbb{R}^n \tag{4.1}$$

where $\mathbb{X}_i \subseteq \mathbb{R}^n$ for $i \in \mathcal{I}$ is a partition of the state space into a number of regions. $\mathcal{I}$ denotes the index set of regions (Hedlund and Johansson, 1999). In this section, we will use the following notations for PWL systems:

$$\bar{A}_i = \begin{bmatrix} A_i & a_i \\ 0 & 0 \end{bmatrix},\ \bar{B}_i = \begin{bmatrix} B_i \\ 0 \end{bmatrix},\ \bar{C}_i = \begin{bmatrix} C_i & c_i \end{bmatrix},\ \bar{x}(t) = \begin{bmatrix} x(t) \\ 1 \end{bmatrix},$$

and the system in (4.1) then becomes an augmented representation

$$\left.\begin{aligned} \dot{\bar{x}}(t) &= \bar{A}_i\, \bar{x}(t) + \bar{B}_i\, u(t) \\ y(t) &= \bar{C}_i\, \bar{x}(t) + D_i\, u(t) \end{aligned}\right\} \quad x(t) \in \mathbb{X}_i, \tag{4.2}$$

The equilibrium point of the system (4.2) is assumed to be located at $x_e = 0$. The index set $\mathcal{I}$ is divided into $\mathcal{I}_0$ and $\mathcal{I}_1$ such that if any given region contains the origin, it is then shown as the index set $\mathcal{I}_0 \subset \mathcal{I}$. In these regions, the vectors a_i and c_i are assumed to be zero. On the other hand, if a region does not contain the origin, it will be shown as the index set $\mathcal{I}_1 = \mathcal{I} \setminus \mathcal{I}_0$. It is also assumed that the regions, $\mathbb{X}_i$, are closed polyhedral cells

with a pairwise disjointed interior. The intersection of a set of closed half-spaces define these regions, $\mathbb{X}_i$. The set of closed half-spaces for each region, called *cell-identifiers*, are given such that

$$\mathbb{X}_i = \{G_i\, x + g_i \geq 0\} = \left\{ \left[\begin{array}{cc} G_i & g_i \end{array} \right] \bar{x} \geq 0 \right\} = \{\bar{G}_i\, \bar{x} \geq 0\}. \tag{4.3}$$

4.3 Quadratic Stability for PWL Systems

In this section, the relaxed conditions for the common quadratic Lyapunov approach in (2.3) will be defined based on state-dependent switching. To search for global stability of the switched system in (4.2), a quadratic Lyapunov function according to two types of index sets is defined as

$$V(x) = \left\{ \begin{array}{lll} x'Px & x \in \mathbb{X}_i & i \in I_0 \\ \bar{x}'\bar{P}\bar{x} & x \in \mathbb{X}_i & i \in I_1 \end{array} \right. \tag{4.4}$$

where

$$\bar{P} = \left[\begin{array}{cc} P & 0_{n\times 1} \\ 0_{1\times n} & 0_{1\times 1} \end{array} \right]$$

then the common quadratic Lyapunov function is required to satisfy the following conditions:

***Condition* 4.1** (Positive-Definiteness)*:* $V(x) > 0$ for all $x \in \mathbb{X}_i$ and $x \neq 0$. The positive-definiteness of the common quadratic Lyapunov function along the subsystem's trajectories can be shown such that

$$V(x) = \left\{ \begin{array}{lll} x'Px > 0 & x \in \mathbb{X}_i & i \in I_0 \\ \bar{x}'\bar{P}\bar{x} > 0 & x \in \mathbb{X}_i & i \in I_1 \end{array} \right. \tag{4.5}$$

***Condition* 4.2** (Decreasing in time)*:* $\dot{V}(x) < 0$ for all $x \in \mathbb{X}_i$ and $x \neq 0$. The negative-definiteness of the derivative of the common quadratic Lyapunov function along the subsystem's trajectories can be given such that

$$\dot{V}(x) = \left\{ \begin{array}{lll} x'(A_i'P + PA_i)x < 0 & x \in \mathbb{X}_i & i \in I_0 \\ \bar{x}'(\bar{A}_i'\bar{P} + \bar{P}\bar{A}_i)\bar{x} < 0 & x \in \mathbb{X}_i & i \in I_1 \end{array} \right. \tag{4.6}$$

The inequalities in (4.6) are defined globally. The common quadratic Lyapunov function algorithm can only be solved when the switched systems are asymptotically stable under arbitrary switching signals, as shown in Section 2.3. For this reason, these conditions can be unnecessarily restricted for the piecewise affine systems' analysis. Using the $S-$procedure in these conditions can be helpful for stability analysis (Boyd et al., 1994). So, we can consider the positive semi-definite matrices R_i and $\bar{R}_i$ that assure the following inequalities

$$x' R_i x \geqslant 0, \quad \bar{x}' \bar{R}_i \bar{x} \geqslant 0, \ \text{ for } x \in \mathbb{X}_i \tag{4.7}$$

and apply in (4.6) to get the following non-restrictive conditions for stability

$$\begin{aligned} x'(A_i' P + P A_i + R_i)x < 0 \quad x \in \mathbb{X}_i \quad i \in I_0 \\ \bar{x}'(\bar{A}_i' \bar{P} + \bar{P} \bar{A}_i + \bar{R}_i)\bar{x} < 0 \quad x \in \mathbb{X}_i \quad i \in I_1 \end{aligned} \tag{4.8}$$

Here, if the positive definite matrix, P, satisfies these inequalities when $x \in \mathbb{X}_i$, it clearly provides the inequalities in (4.5) and (4.6). Moreover, it is easier to solve (4.8) than the Lyapunov inequalities in (4.6) when $x \notin \mathbb{X}_i$. More precisely, the inequalities in (4.7) will be negative when $x \notin \mathbb{X}_i$, so the inequalities in (4.8) are defined as relaxed conditions for the common quadratic Lyapunov function.

The matrices which are used for in the $S-$procedure can be constructed from the system definition as follows

$$\begin{aligned} x' R_i x \quad &:= x' E_i' M_i E_i x \geqslant 0, \qquad && x \in \mathbb{X}_i, \quad i \in I_0 \\ \bar{x}' \bar{R}_i \bar{x} \quad &:= \bar{x}' \bar{E}_i' M_i \bar{E}_i \bar{x} \geqslant 0, \qquad && x \in \mathbb{X}_i, \quad i \in I_1 \end{aligned}$$

where the symmetric matrices, M_i, have non-negative entries. The boundaries of cell $\mathbb{X}_i$ are defined with $\bar{E}_i = [E_i \quad e_i]$, which is called the *cell bounding matrix* because it defines cell boundaries and satisfies

$$\bar{E}_i \, \bar{x} \geq 0.$$

Computation methods of the *cell-bounding-matrices* will be given at the end of this section. According to the above conditions, the following theorem will be defined for quadratic stability analysis:

Theorem* 4.3.1*: If the symmetric matrices, M_i, which have non-negative entries, and the symmetric positive definite matrix, $P > 0$, exist and satisfy the following LMIs

$$\begin{aligned} A_i'P + PA_i + E_i'M_iE_i < 0, \qquad & x \in \mathbb{X}_i, \quad i \in I_0 \\ \bar{A}_i'\bar{P} + \bar{P}\bar{A}_i + \bar{E}_i'M_i\bar{E}_i < 0, \qquad & x \in \mathbb{X}_i, \quad i \in I_1 \end{aligned} \tag{4.9}$$

then the origin is globally exponentially stable for a given switched system in (4.2). Note that the vectors, a_i and e_i, are assumed to be equal zero when $i \in \mathcal{I}_0$. The non-negativity of the matrices, M_i, comes from the $S-$procedure properties; M_i do not need to be full matrices, (Johansson and Rantzer, 1998).

Non-negativity of the symmetric matrices, M_i:

$S-$procedure deals with the non-negativity of a quadratic function (or quadratic form) under quadratic inequalities. It is used in control theory and robust optimisation as one of its most fundamental tools. Also, numerous mathematical fields are related to $S-$procedure, such as quadratic functions, convex analysis and numerical range (Derinkuyu and Pınar, 2006).

We look for the constraint that the non-negativity of one quadratic form indicates non-negativity of another. More precisely, we want to find when it is true that for all x, $x'E_1x \geqslant 0 \Longrightarrow x'E_0x \geqslant 0$, where $E_0 = E_0',\ E_1 = E_1' \in R^{n\times n}$. We will achieve this constraint with a simple condition: if there exists $\varepsilon \geqslant 0, \varepsilon \in R$, with $E_0 \geqslant \varepsilon E_1$, then we ensure that $x'E_0x \geqslant 0$ if, and only if, $x'E_1x \geqslant 0$ and we have $x'E_0x \geqslant x'E_1x \geqslant 0$. The $S-$procedure condition can be generalized for multiple quadratic forms such that

$$x'E_1x \geqslant 0, \ldots, x'E_mx \geqslant 0 \Longrightarrow x'E_0x \geqslant 0 \tag{4.10}$$

where $E_0 = E_0', \ldots, E_m = E_m' \in R^{n\times n}$ and quadratic forms of the variable $x \in R^n$. If there exists $\varepsilon_1 \geqslant 0, \ldots, \varepsilon_m \geqslant 0$ with $E_0 \geqslant \varepsilon_1E_1 + \ldots + \varepsilon_mE_m$ (clearly, $E_0 - \sum_{i=1}^{m} \varepsilon_iE_i \geqslant 0$) then the property of (4.10) surely holds. The constants ε_i are called multipliers. For the $S-$procedure, for strict inequalities, quadratic forms and examples, see (Boyd et al., 1994).

From the above definitions, we will define the inequalities in (4.9) such that

$$A_i'P + PA_i + E_i'M_iE_i = A_i'P + PA_i + \sum_{jk} m_{jk}e_{ik}'e_{ij} < 0, \qquad x \in \mathbb{X}_i, \quad i \in I_0$$
$$\bar{A}_i'\bar{P} + \bar{P}\bar{A}_i + \bar{E}_i'M_i\bar{E}_i = \bar{A}_i'\bar{P} + \bar{P}\bar{A}_i + \sum_{jk} m_{jk}\bar{e}_{ik}'\bar{e}_{ij} < 0, \qquad x \in \mathbb{X}_i, \quad i \in I_1$$

where e_{ij} implies the j^{th} row of E_i and e_{ik}' implies the k^{th} column of E_i'. This indicates that the only sufficient condition of the $S-$procedure comes from the non-negative entries of the symmetric matrices M_i.

Example* 4.1*: Consider a switched linear system $\dot{x}(t) = A_ix(t)$ with the state matrices

$$A_1 = A_3 = \begin{bmatrix} -0.1 & 1 \\ -2 & -0.5 \end{bmatrix}, \qquad A_2 = A_4 = \begin{bmatrix} -0.1 & 2 \\ -1 & -0.5 \end{bmatrix}.$$

Using Conditions 4.1 and 4.2, a common quadratic Lyapunov function is not found for this switched system. On the other hand, the trajectories of each of the subsystems, which are given in Figure 4.1, are individually stable.

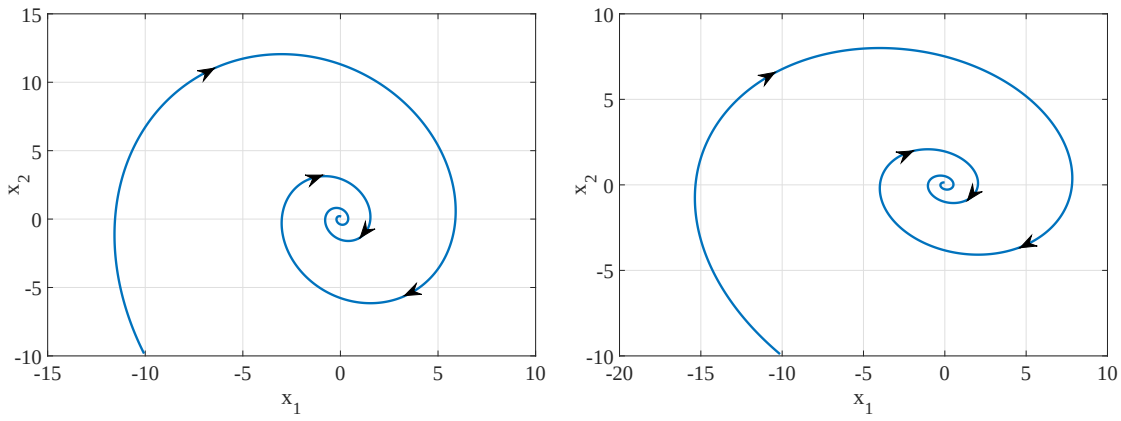

Figure 4.1: Trajectories of each subsystems, left $A_1 = A_3$ and right $A_2 = A_4$

Although a feasible solution is not found, the stability of the switched system is addressed using Theorem 4.3.1. Here, the *cell bounding matrix* of the system is given, such that

$$E_1 = -E_3 = \begin{bmatrix} -1 & 5 \\ -1 & -5 \end{bmatrix}, \qquad E_2 = -E_4 = \begin{bmatrix} 1 & -5 \\ -1 & -5 \end{bmatrix}.$$

and the Lyapunov matrix is found such that

$$P = \begin{bmatrix} 41.7250 & 11.2841 \\ 11.2841 & 70.0420 \end{bmatrix}. \tag{4.11}$$

The given switched system is simulated with initial states $x_0 = [-10 \ -10]'$. Then, the Lyapunov function of the system with a calculated Lyapunov matrix (4.11) changes as in Figure 4.2 (right), which proves the stability under a given switching rule. Here, the dashed lines show the switching instances. In addition, a trajectory of such a switched system is given in Figure 4.2 (left), where the dashed lines indicate the boundaries of the cells.

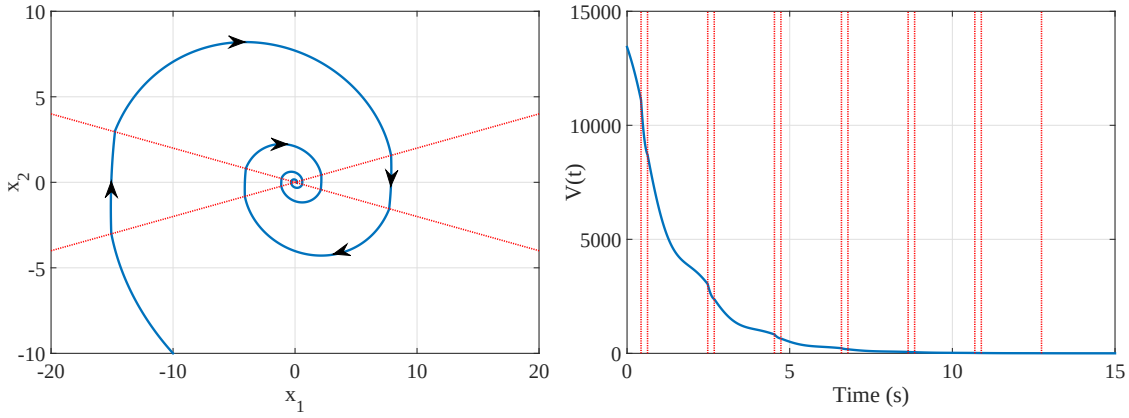

Figure 4.2: Trajectory and Lyapunov function of the switched system

It can be clearly seen that using the $S-$procedure gives relaxed conditions for the quadratic stability analysis. The following section will explain that the quadratic stability analysis with $S-$procedure is still conservative for a piecewise system analysis. Hence, a piecewise Lyapunov-like function will be also given to define piecewise quadratic stability analysis in the following section.

4.3.1 Computing the *cell-bounding-matrices*

The *cell-bounding-matrices*, $\bar{E}_i$ are closely related to the *cell-identifiers*, $\bar{G}_i$ in (4.3). Actually, the only difference between them is the zero-interpolation property which plays a critical role in defining strict LMIs for searching the Lyapunov function. Here, the

cell-identifiers will initially be defined by finding the intersection of a set of closed half-spaces. Then, the computation algorithm will be given for the *cell-bounding-matrices* with the zero-interpolation property using the related *cell-identifiers*.

Hyperplane and Half-space

Hyperplane and half-spaces are geometrically depicted in Figure 4.3. The hyperplanes in R^n are described as being the collection of points

$$Z = \{x \in R^n \mid \quad G(x - x_0) = 0\} \tag{4.12}$$

which is also defined such that

$$Z = \{x \in R^n \mid \quad Gx = g\} \tag{4.13}$$

A hyperplane in R^n splits all of R^n into three independent sets

$$Z_1 = \{x \in R^n \mid \quad Gx > g\}$$
$$Z_2 = \{x \in R^n \mid \quad Gx = g\}$$
$$Z_3 = \{x \in R^n \mid \quad Gx < g\}$$

Open Half-Spaces: Open half-spaces are defined when the above sets are defined as $Z_1 = \{x \in R^n \mid \quad Gx > g\}$ or $Z_3 = \{x \in R^n \mid \quad Gx < g\}$; see Figure 4.3 (right).

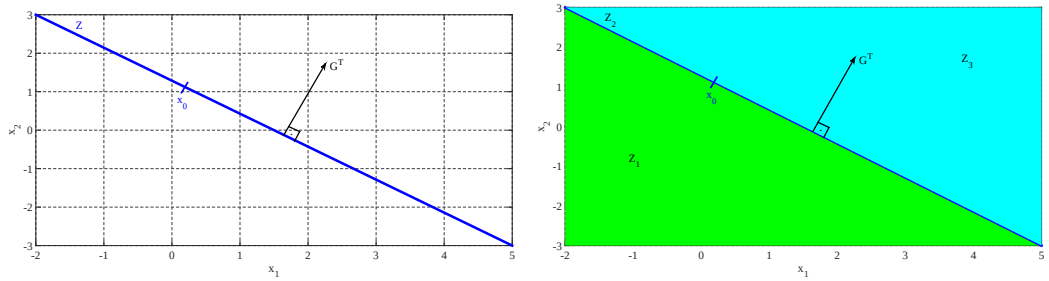

Figure 4.3: Hyperplane (left) and Half-spaces (right)

Closed Half-Spaces: Closed half-spaces are defined when the sets above are defined as $Z_4 = \{x \in R^n \mid \quad Gx \geq g\}$ or $Z_5 = \{x \in R^n \mid \quad Gx \leq g\}$, (Hadley, 1961) . An intersection of the set of defined closed half-spaces defines the *cell-identifiers* in (4.3).

The cell-bounding-matrices from the cell-identifiers : Consider the *cell-identifiers*, $\bar{G}_i$ is defined as above. The relating *cell-bounding-matrices* can be calculated as follows:

⋇ If the cell contains the origin, $i \in I_0$, then E_i can be found by removing all rows of $\bar{G}_i$ whose g_i values are not equal to zero.

⋇ If the cell does not contain the origin, $i \in I_1$ and $\mathbb{X}_i$ is bounded, then E_i is defined to be equal to $\bar{G}_i$ (Hedlund and Johansson, 1999). Otherwise, E_i is found by adding the row $[0_{1\times n} \quad 1]$ to $\bar{G}_i$. The following example will clarify this method.

***Example* 4.2:** Consider the switched system with the state-dependent switching law given in Figure 4.4. Hyperplanes of the given system can be defined as

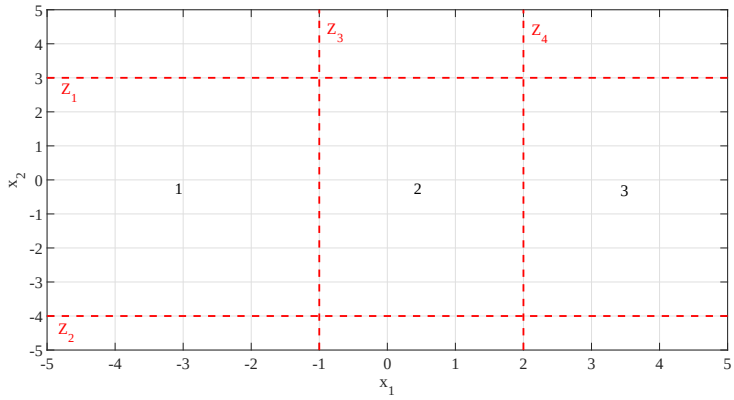

Figure 4.4: State-dependent switching law in Example 4.2

$$Z_1 = [0 \quad 1]\, x = \quad 3, \qquad Z_2 = [0 \quad 1]\, x = -4,$$
$$Z_3 = [1 \quad 0]\, x = -1, \qquad Z_4 = [1 \quad 0]\, x = \quad 2.$$

From the above defined hyperplanes, the *cell-identifiers* can be computed as follows

$$\mathbb{X}_1 = \begin{bmatrix} 0 & -1 & 3 \\ 0 & 1 & 4 \\ -1 & 0 & -1 \end{bmatrix} \bar{x} \geq 0, \qquad \mathbb{X}_2 = \begin{bmatrix} 0 & -1 & 3 \\ 0 & 1 & 4 \\ 1 & 0 & 1 \\ -1 & 0 & 2 \end{bmatrix} \bar{x} \geq 0,$$

$$\mathbb{X}_3 = \begin{bmatrix} 0 & -1 & 3 \\ 0 & 1 & 4 \\ 1 & 0 & -2 \end{bmatrix} \bar{x} \geq 0.$$

Now, a computational method to obtain the *cell-bounding-matrices*, $\bar{E}_i$, as discussed above, will be applied to the *cell-identifiers* individually. Firstly, Cell 2 contains the origin, so for this cell, rows of $\bar{G}_2$ whose g_2 is not equal to zero will be removed. It can clearly be seen that all g_2 are not equal to zero, thus all rows of $\bar{G}_2$ are deleted, and hence the *cell-bounding-matrices* for Cell 2 must also be equal to zero, $\bar{E}_2 = 0$. Moreover, Cells 1 and 3 do not contain the origin and both cells are unbounded, so the row $[0_{1\times n} \quad 1]$ is added to $\bar{G}_1$ and $\bar{G}_3$. Then the related *cell-bounding-matrices* is obtained as follows

$$\bar{E}_1 = \begin{bmatrix} 0 & -1 & 3 \\ 0 & 1 & 4 \\ -1 & 0 & -1 \\ 0 & 0 & 1 \end{bmatrix}, \quad \bar{E}_2 = \begin{bmatrix} 0_{1\times n} & 0 \\ 0_{1\times n} & 0 \\ 0_{1\times n} & 0 \\ 0_{1\times n} & 0 \end{bmatrix}, \quad \bar{E}_3 = \begin{bmatrix} 0 & -1 & 3 \\ 0 & 1 & 4 \\ 1 & 0 & -2 \\ 0 & 0 & 1 \end{bmatrix}.$$

4.4 Piecewise Quadratic Stability

The relaxed conditions of the quadratic stability analysis in Theorem 4.3.1 are still restricted for piecewise affine system analysis. The conservatism of the quadratic stability will be explained with the following example.

Example* 4.3*: Consider the switched linear system $\dot{x}(t) = A_i x(t)$ which contains four cells, $\mathbb{X}_i = (\mathbb{X}_1, \ldots, \mathbb{X}_4)$, shown in Figure 4.5, and having state matrices

$$A_1 = A_3 = \begin{bmatrix} -0.5 & 1 \\ -5 & -0.5 \end{bmatrix}, \qquad A_2 = A_4 = \begin{bmatrix} -0.5 & 5 \\ -1 & -0.5 \end{bmatrix}.$$

From Figure 4.5 (dashed line), the *cell-bounding-matrices* can be calculated as

$$E_1 = -E_3 = \begin{bmatrix} -1 & 2 \\ -1 & -2 \end{bmatrix}, \qquad E_2 = -E_4 = \begin{bmatrix} 1 & -2 \\ -1 & -2 \end{bmatrix}.$$

The eigenvalues of the state matrices are same and lie in the negative half plane, $\lambda_i = -0.5000 \pm 2.2361\, i$. Although real parts of the eigenvalues are negative and the

trajectory of the switched system coverages to zero in Figure 4.5, there is no solution to (4.9).

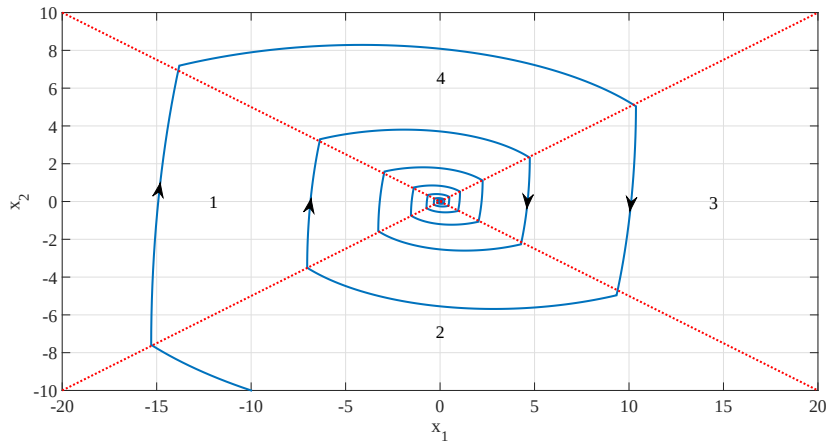

Figure 4.5: Cell boundaries (dashed) and trajectory (solid) in the Example 4.3

As a result of this example, if the dynamics given by A_i are used within cell $\mathbb{X}_i$ and not used outside of it, then the common quadratic Lyapunov function can be restricted unnecessarily for piecewise affine system analysis. Piecewise quadratic Lyapunov functions and piecewise quadratic stability are given to lessen the conservatism of the common quadratic Lyapunov function (Johansson, 2003).

The piecewise quadratic stability analysis defines different Lyapunov matrices to focus on the system matrices within the defined cell $\mathbb{X}_i$. The $S-$procedure, which was mentioned in the previous section, is also used to generate this stability technique. To search the stability of the switched system in (4.2), the continuous piecewise quadratic Lyapunov function, according to two types of index sets, is defined as

$$V(x) = \begin{cases} x'P_i x & x \in \mathbb{X}_i \quad i \in I_0 \\ \bar{x}'\bar{P}_i\bar{x} & x \in \mathbb{X}_i \quad i \in I_1 \end{cases} \tag{4.14}$$

and needs to satisfy the following conditions:

***Condition* 4.3** (Continuity)*:* The piecewise quadratic Lyapunov function needs to be continuous at the boundaries of the hyperplanes, $Z_{ij} = \{x \mid G'_{ij}x + g_{ij} = 0\}$,

$$V_i(x) = V_j(x) \qquad \forall x \in Z_{ij} \tag{4.15}$$

The free parameters of the Lyapunov-like matrices can be collected in the symmetric matrix, T, such that

$$\begin{aligned} P_i &= F_i' T F_i, \qquad P_j = F_j' T F_j, \quad \text{for } i,j \in I_0 \\ \bar{P}_i &= \bar{F}_i' T \bar{F}_i, \qquad \bar{P}_j = \bar{F}_j' T \bar{F}_j, \quad \text{for } i,j \in I_1 \end{aligned} \tag{4.16}$$

Here the *continuity matrix*, $\bar{F}_i = [F_i \quad f_i]$ for cell $\mathbb{X}_i$ satisfies the following equality across the cell boundaries

$$\bar{F}_i\, \bar{x}(t) = \bar{F}_j\, \bar{x}(t), \quad x \in \mathbb{X}_i \cap \mathbb{X}_j, \quad i,j \in \mathcal{I}. \tag{4.17}$$

Remark: The vectors, f_i, are assumed to be equal to zero when $i \in \mathcal{I}_0$. A unique continuity matrix does not exist for any given cell. For example, the following matrix can be used in all cells:

$$\bar{F}_i = [I_{n\times n} \quad 0_{n\times 1}] \quad i \in \mathcal{I}$$

Condition* 4.4** (Positive-Definiteness):*** $V_i(x) > 0$ for all $x \in \mathbb{X}_i$ and $x \neq 0$. The positive-definiteness of the piecewise Lyapunov function along the trajectories of the subsystems can be shown, such that

$$V(x) = \begin{cases} x' P_i x > 0 & x \in \mathbb{X}_i \quad i \in I_0 \\ \bar{x}' \bar{P}_i \bar{x} > 0 & x \in \mathbb{X}_i \quad i \in I_1 \end{cases} \tag{4.18}$$

Substituting (4.16) into (4.18) allows this inequality to be written with the *continuity matrix* and symmetric matrix, T, such that

$$V(x) = \begin{cases} x' F_i' T F_i x > 0 & x \in \mathbb{X}_i \quad i \in I_0 \\ \bar{x}' \bar{F}_i' T \bar{F}_i \bar{x} > 0 & x \in \mathbb{X}_i \quad i \in I_1 \end{cases} \tag{4.19}$$

Condition* 4.5** (Decreasing in time):*** $\dot{V}_i(x) < 0$ for all $x \in \mathbb{X}_i$ and $x \neq 0$. The negative-definiteness of the derivative of the piecewise Lyapunov function along the trajectories of the subsystems can be given such that

$$\dot{V}_i(x) = \begin{cases} x'(A_i' P_i + P_i A_i) x < 0 & x \in \mathbb{X}_i \quad i \in I_0 \\ \bar{x}'(\bar{A}_i' \bar{P}_i + \bar{P}_i \bar{A}_i) \bar{x} < 0 & x \in \mathbb{X}_i \quad i \in I_1 \end{cases} \tag{4.20}$$

Substituting (4.16) into (4.20) allows this inequality to be rewritten with the *continuity matrix* and symmetric matrix, T, such that

$$\dot{V}_i(x) = \begin{cases} x'(A_i'F_i'TF_i + F_i'TF_iA_i)x < 0 & x \in \mathbb{X}_i \quad i \in I_0 \\ \bar{x}'(\bar{A}_i'\bar{F}_i'T\bar{F}_i + \bar{F}_i'T\bar{F}_i\bar{A}_i)\bar{x} < 0 & x \in \mathbb{X}_i \quad i \in I_1 \end{cases} \tag{4.21}$$

If the $S-$procedure method for Condition 4.2 in Section 4.3 is also applied to the inequalities in Conditions 4.4 and 4.5, then the following theorem can be defined for the piecewise quadratic stability analysis.

***Theorem* 4.4.1** (Johansson and Rantzer (1997b))*:* Let T, M_i and N_i be symmetric matrices and also M_i and N_i have non-negative values in order to satisfy the following LMI problem

$$\left.\begin{array}{l} F_i'TF_i - E_i'N_iE_i > 0 \\ A_i'F_i'TF_i + F_i'TF_iA_i + E_i'M_iE_i < 0 \end{array}\right\} \quad i \in \mathcal{I}_0,$$
$$\left.\begin{array}{l} \bar{F}_i'T\bar{F}_i - \bar{E}_i'N_i\bar{E}_i > 0 \\ \bar{A}_i'\bar{F}_i'T\bar{F}_i + \bar{F}_i'T\bar{F}_i\bar{A}_i + \bar{E}_i'M_i\bar{E}_i < 0 \end{array}\right\} \quad i \in \mathcal{I}_1. \tag{4.22}$$

Then $x(t) \in \bigcup_{i\in I} \mathbb{X}_i$ tends to zero exponentially, which means each continuous piecewise trajectory is satisfied in (4.2) for $t \geqslant 0$.

Remark: The stability conditions in (4.22) are linear matrix inequalities with variables T, M_i and N_i. The *cell bounding* and *continuity matrices* can be found using the algorithms or the toolbox given in (Johansson, 1999). This theorem is illustrated with the following example.

Example* 4.4*: Consider the PWL switched system in Example 4.3. Although there is no solution to achieving quadratic stability, a feasible solution can be found by solving Conditions 4.4 and 4.5 without continuity conditions. Here, a modelling and optimisation toolbox, YALMIP, in MATLAB (Lofberg, 2004) is used to solve the related conditions; the Lyapunov function of such a system is shown in Figure 4.6 with regard to the found Lyapunov matrices

$$P_1 = P_3 = \begin{bmatrix} 19.7459 & -0.9171 \\ -0.9171 & 4.3866 \end{bmatrix}, \quad P_2 = P_4 = \begin{bmatrix} 4.3866 & 0.9171 \\ 0.9171 & 19.7459 \end{bmatrix}.$$

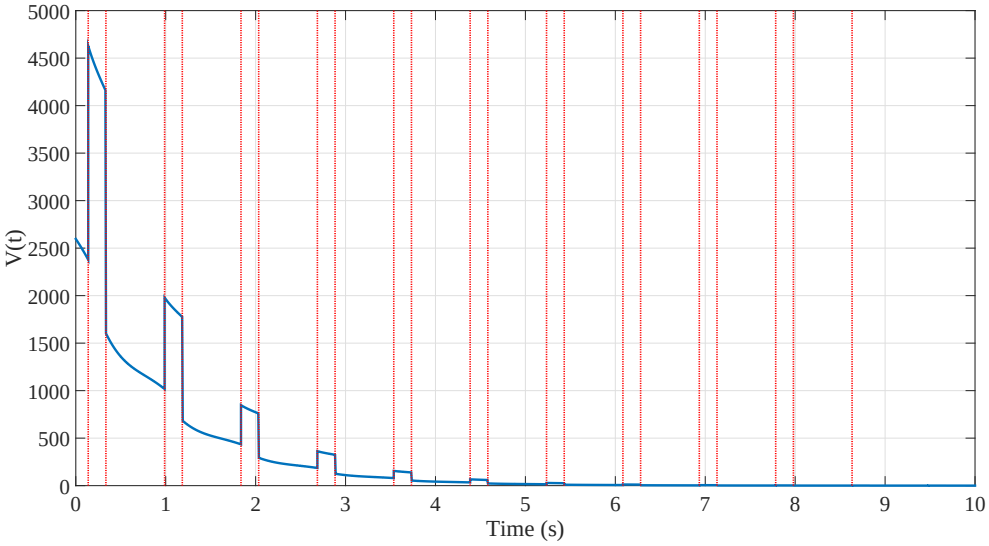

Figure 4.6: Lyapunov function of Example 4.4 (dash lines show switching instances)

The Lyapunov function result in Figure 4.6 shows that discontinuities of the function can occur during the switching instances. The aim of the piecewise quadratic stability is to obtain a continuous piecewise Lyapunov function so Condition 4.3 satisfies the requirement of this aim. In addition to this, Theorem 4.4.1 combines all requirements with $S-$procedure relaxation.

The *continuity matrices*, which is defined as $F_i = [E_i' \quad I_n]'$, and the previously calculated *cell-bounding-matrices* are used to solve Theorem 4.4.1. All cells contain the origin so a_i, e_i and f_i are assumed to be equal to zero. The prescribed inequalities in the above theorem are solved by using a Matlab toolbox (PWLTOOL) in (Hedlund and Johansson, 1999), and the piecewise quadratic Lyapunov function, $V(t) = x(t)'P_i x(t)$, is found with

$$P_1 = P_3 = \begin{bmatrix} 21.3232 & -0.29 \\ -0.29 & 4.2538 \end{bmatrix}, \quad P_2 = P_4 = \begin{bmatrix} 9.8458 & -0.29 \\ -0.29 & 50.1631 \end{bmatrix}.$$

Simulating the given system with initial states $x_0 = [-10 \quad -10]'$, the Lyapunov function of such a system, with the computed Lyapunov matrices, can be found as in Figure 4.7, which proves the stability under a given state-dependent switching rule. Here, the dashed lines show the switching instances.

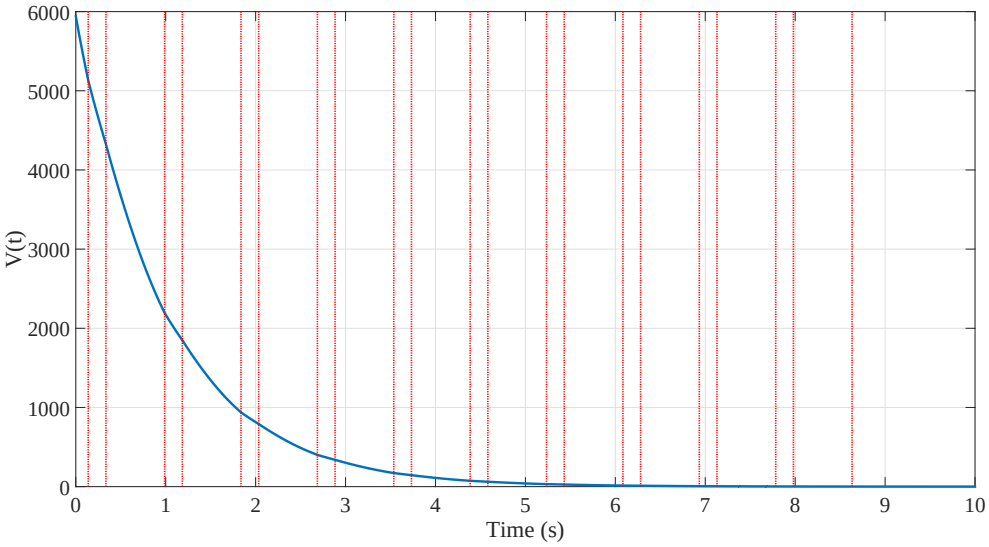

Figure 4.7: Continuous Lyapunov function of Example 4.4

The results of the example clearly prove that the piecewise quadratic stability analysis is less conservative than the quadratic stability analysis. In addition, the continuity of the Lyapunov function is guaranteed by the piecewise quadratic stability approach. The following section will provide $\mathcal{L}_2$ performance gain analysis between disturbance input and output as well as the stability analysis.

4.5 $\mathcal{L}_2$-gain Analysis

The PWL switched system in (4.2) with disturbance input can be described as follows

$$\left.\begin{aligned} \dot{\bar{x}}(t) &= \bar{A}_i\,\bar{x}(t) + \bar{B}_{u,i}\,u(t) + \bar{B}_{w,i}\,w(t) \\ y(t) &= \bar{C}_i\,\bar{x}(t) + D_{u,i}\,u(t) + D_{w,i}\,w(t) \end{aligned}\right\} \quad x(t) \in \mathbb{X}_i, \tag{4.23}$$

where $\bar{B}_{w,i} = [B'_{w,i} \quad 0]'$. In this section, we want to achieve both stability and performance gain between disturbance input and output, thus the system (4.23) needs to satisfy

the following performance criteria:

$$J = \int_0^\infty (z'z - \gamma^2 w'w)dt \leq 0, \qquad \forall w \in \mathcal{L}_2 \tag{4.24}$$

where γ is a positive scalar. Then a new criterion with $V(t)$ is

$$\tilde{J} = \lim_{t\to\infty}\{V(t) + \int_0^t (z'z - \gamma^2 w'w)ds\}. \tag{4.25}$$

It can be seen that $J \leq \tilde{J}$ when $V(t) \geq 0 \,\forall\, t$. Assuming that $V(t)$ is differentiable for all t, apart from the switching instants, and $x(0) = 0$. Hence

$$\lim_{t\to\infty} V(t) = \sum_{s=0}^{\infty} \int_{\tau_s}^{\tau_{s+1}} \dot{V}(t)\, dt + \sum_{s=1}^{\infty} (V(\tau_s) - V(\tau_s^-))$$

where $\tau_0 = 0$. If $V(t)$ satisfies the non-increasing condition at the switching instants, it can be obtained as

$$V(\tau_s) - V(\tau_s^-) \leq 0 \quad \forall s > 0$$

which then satisfies

$$\lim_{t\to\infty} V(t) \leq \sum_{s=0}^{\infty} \int_{\tau_s}^{\tau_{s+1}} \dot{V}(t)dt. \tag{4.26}$$

Substituting (4.26) into (4.25), the following equation can be defined

$$\begin{aligned} \bar{J} &= \sum_{s=0}^{\infty} \int_{\tau_s}^{\tau_{s+1}} \dot{V}(t)dt + \int_0^\infty (z'z - \gamma^2 w'w)ds, \\ &= \sum_{s=0}^{\infty} \int_{\tau_s}^{\tau_{s+1}} (\dot{V}(t) + z'z - \gamma^2 w'w)ds. \end{aligned} \tag{4.27}$$

Consequently, from (4.24) to (4.27), it can be guaranteed that $J \leq \tilde{J} \leq \bar{J}$. If the above Lyapunov function provides $\bar{J} \leq 0$ and non-increasing conditions during the switching instants, then the performance criterion (4.24) is proven. In other words, the $\mathcal{L}_2$-gain of the system (4.23) will be equal to or less than a prescribed scalar $\gamma > 0$. From (4.27), the following condition needs to be satisfied:

$$\dot{V}(t) + z'z - \gamma^2 w'w < 0. \tag{4.28}$$

(4.6) is substituted into (4.28) and then the $S-$procedure and the Bounded Real Lemma (BRL) are used for the linear system (Boyd et al., 1994). The following theorem is given for quadratic stability analysis with $\mathcal{L}_2$-gain.

***Theorem* 4.5.1** ($\mathcal{L}_2$-gain for Common Quadratic Stability)*:* If a symmetric positive definite matrix, $P > 0$, and symmetric matrices, M_i, which have non-negative entries, exist and satisfy the following LMIs

$$\begin{bmatrix} PA_i + A_i'P + E_i'M_iE_i & PB_{w,i} & C_i' \\ * & -\gamma^2 I & D_{w,i}' \\ * & * & -I \end{bmatrix} < 0, \quad i \in \mathcal{I}_0 \tag{4.29}$$

$$\begin{bmatrix} \bar{P}\bar{A}_i + \bar{A}_i'\bar{P} + \bar{E}_i'M_i\bar{E}_i & \bar{P}\bar{B}_{w,i} & \bar{C}_i' \\ * & -\gamma^2 I & D_{w,i}' \\ * & * & -I \end{bmatrix} < 0, \quad i \in \mathcal{I}_1 \tag{4.30}$$

then the $\mathcal{L}_2$-gain of the system (4.23) is less than the positive scalar γ. Note that the first diagonal block of the above inequality comes from $\dot{V}$ in (4.28). The second row and column come from $w'w$ and the third row and column come from $z'z$. Here, γ presents the $\mathcal{L}_2$-gain between disturbance inputs, w, and desired outputs, z of the system (4.23). If the $\mathcal{L}_2$-gain between control inputs, u, and desired outputs, z, are sought, the disturbance inputs in (4.24) can be replaced with the control inputs and the disturbance matrices B_w and D_w in Theorem 4.5.1 turn to the input matrices B_u and D_u.

(4.20) is substituted into (4.28) and then the $S-$procedure and BRL are used for the linear system (Boyd et al., 1994). The following theorem is given for quadratic stability analysis with $\mathcal{L}_2$-gain.

***Theorem* 4.5.2** ($\mathcal{L}_2$-gain for Piecewise Quadratic Stability)*:* If there exists symmetric matrices $T,\ M_i$ and N_i such that M_i and N_i have non-negative values and satisfy the fol-

lowing LMIs problem

$$\left.\begin{array}{l} P_i - E_i' N_i E_i > 0 \\ \\ \left[\begin{array}{ccc} P_i A_i + A_i' P_i + E_i' M_i E_i & P_i B_{w,i} & C_i' \\ * & -\gamma^2 I & D_{w,i}' \\ * & * & -I \end{array}\right] < 0, \end{array}\right\} \; i \in \mathcal{I}_0$$

$$\left.\begin{array}{l} \bar{P}_i - \bar{E}_i' N_i \bar{E}_i > 0 \\ \\ \left[\begin{array}{ccc} \bar{P}_i \bar{A}_i + \bar{A}_i' \bar{P}_i + \bar{E}_i' M_i \bar{E}_i & \bar{P}_i \bar{B}_{w,i} & \bar{C}_i' \\ * & -\gamma^2 I & D_{w,i}' \\ * & * & -I \end{array}\right] < 0, \end{array}\right\} \; i \in \mathcal{I}_1 \tag{4.31}$$

where

$$P_i = F_i' T F_i, \quad \bar{P}_i = \bar{F}_i' T \bar{F}_i$$

then the $\mathcal{L}_2$-gain of the system in (4.23) is less than the positive scalar, γ (Johansson, 2003). Note that the non-negativity of the matrices M_i and N_i are explained in Section 4.3.

***Example* 4.5:** Consider the switched linear system in (4.23) with

$$A_1 = A_3 = \left[\begin{array}{cc} -0.5 & 1 \\ -5 & -0.5 \end{array}\right], \qquad B_{w,1} = B_{w,3} = \left[\begin{array}{c} -0.5 \\ 2 \end{array}\right],$$

$$A_2 = A_4 = \left[\begin{array}{cc} -0.5 & 5 \\ -1 & -0.5 \end{array}\right], \qquad B_{w,2} = B_{w,4} = \left[\begin{array}{c} 0.5 \\ -1 \end{array}\right],$$

$$C_1 = C_3 = \left[\begin{array}{cc} 1 & 0 \end{array}\right], \qquad C_2 = C_4 = \left[\begin{array}{cc} 0 & 1 \end{array}\right],$$

$$D_{w,1} = D_{w,2} = D_{w,3} = D_{w,4} = 0.$$

The state space of the system is divided into four regions, as in Example 4.3, so the same *cell-bounding-matrices* and the same *continuity matrices* are used as in Example

4.4. Then, the $\mathcal{L}_2$ performance gain of the system found as $\gamma = 2.0136$ by using Theorem 4.5.2. The piecewise Lyapunov-like matrices are also found such that

$$P_1 = P_3 = \begin{bmatrix} 1.209 & -0.011 \\ -0.011 & 0.229 \end{bmatrix}, \quad P_2 = P_4 = \begin{bmatrix} 0.589 & -0.011 \\ -0.011 & 2.710 \end{bmatrix}. \tag{4.32}$$

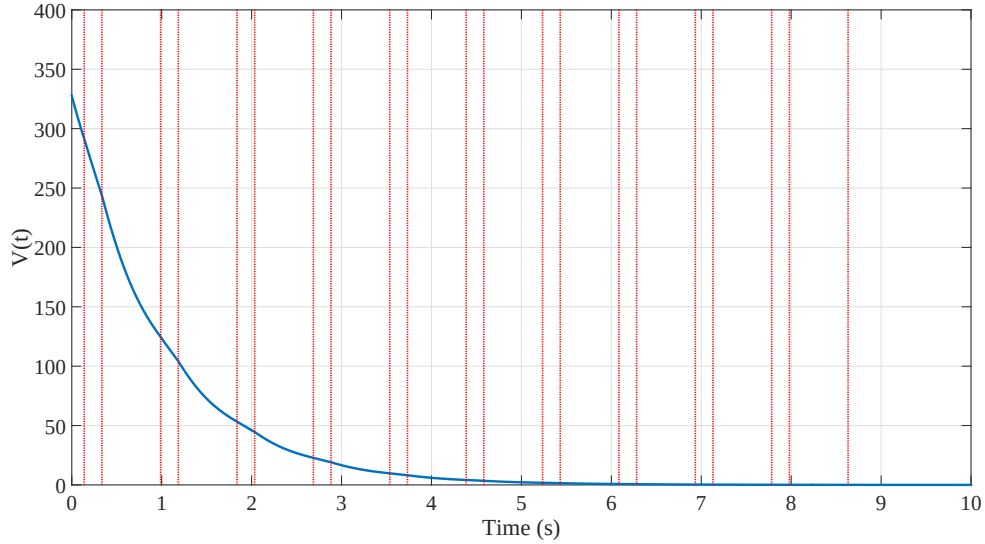

Figure 4.8: Lyapunov energy function of Example 4.5

Then, the value of the Lyapunov (energy) function given in Figure 4.8 can be computed according to the corresponding Lyapunov matrix in (4.32). Because of the performance criteria ($\mathcal{L}_2$-gain), the energy function of the switched system is too low compared to the responses given in Figure 4.7.

4.6 State-feedback Controller Design

We have mentioned the stability analysis and $\mathcal{L}_2$ performance gain approaches for PWL systems in the previous sections. The piecewise quadratic stability methods will be extended to a state-feedback controller design in this section. Although the change

of variables method $Q = P^{-1}$ in Chapter 3 is applied to obtain a convex form of the controller design problem, it is not possible to apply the same method in this section.

In this section, the affect of the upper and lower bounds optimisation methods on cost will be examined, which allow us to design the state-feedback controller. When these methods are combined, performance bounds of the PWL switched system are proven with state-feedback.

The lower and upper bounds on cost (Rantzer and Johansson, 2000)

The general condition of the optimal control problem can be given as

$$\begin{aligned} &\text{minimise} \quad \int_0^\infty \mathsf{L}(x,u)dt \\ &\text{subject to} \quad \begin{cases} \dot{x}(t) = f\Big(x(t),u(t)\Big) \\ x(0) = x_0 \end{cases} \end{aligned} \tag{4.33}$$

The solution to this control problem can be shown to be the Hamilton-Jacobi-Bellman (H-J-B) equation

$$\inf_u \left(\frac{\partial V}{\partial x} f(x,u) + \mathsf{L}(x,u)\right) = 0. \tag{4.34}$$

To find a lower bound on the optimal cost, it can be shown

$$\frac{\partial V}{\partial x}\, f(x,u) + \mathsf{L}(x,u) \geq 0 \quad \forall x,u \tag{4.35}$$

Integrating this inequality and assuming that as time tends infinity, the states tend to zero, $x(\infty) = 0$, then we find

$$V(x_0) - V(0) = -\int_0^\infty \frac{\partial V}{\partial x} f(x,u)\, dt \leq \int_0^\infty \mathsf{L}(x,u)\, dt. \tag{4.36}$$

A lower bound on the optimal cost can be found when every V satisfies (4.35). Correspondingly, the following inequality can be defined to find an upper bound on the optimal cost with a given control law, $u = k(x)$

$$\frac{\partial V}{\partial x}\, f\Big(x,k(x)\Big) + \mathsf{L}\Big(x,k(x)\Big) \leq 0 \quad \forall x \tag{4.37}$$

which proves that

$$\int_0^\infty \mathsf{L}\Big(x, k(x)\Big)\, dt \leq V(x_0) - V(0). \tag{4.38}$$

If any V satisfies (4.37), then the upper bound on the optimal cost has been found. Here, $\mathsf{L}\Big(x, k(x)\Big)$, which is negative, is the decay rate of V, so the Lyapunov function, V, guarantees the stability of the system with a given control law.

If it is considered that L is a piecewise quadratic and f is a PWL, then the system (4.1) changes from a given (or an arbitrary) initial state, $x(0) = x_0$ to $x(\infty) = 0$ according to the control objectives. At the same time, the cost can be given such that

$$J(x_0, u) = \int_0^\infty (\bar{x}'\bar{Q}_i\bar{x} + u'R_iu)dt \quad x \in X_i \tag{4.39}$$

where

$$\bar{Q}_i = \begin{bmatrix} Q & 0 \\ 0 & 0 \end{bmatrix} \quad \text{for } i \in \mathcal{I}_0$$

and Q and R are positive definite matrices. The lower bound on cost for the system (4.1) can be found by using the following theorem:

***Theorem* 4.6.1** (Lower bound on the cost (Rantzer and Johansson, 2000))*:* If there exist the symmetric matrices T and M_i, such that M_i has non-negative entries and they satisfy the following LMIs problem

$$\begin{bmatrix} P_iA_i + A_i'P_i - E_i'M_iE_i + Q_i & P_iB_{u,i} \\ * & R_i \end{bmatrix} > 0, \quad i \in \mathcal{I}_0,$$

$$\begin{bmatrix} \bar{P}_i\bar{A}_i + \bar{A}_i'\bar{P}_i - \bar{E}_i'M_i\bar{E}_i + \bar{Q}_i & \bar{P}_i\bar{B}_{u,i} \\ * & R_i \end{bmatrix} > 0, \quad i \in \mathcal{I}_1$$

where

$$P_i = F_i'TF_i, \quad \bar{P}_i = \bar{F}_i'T\bar{F}_i$$

then every trajectory $x(t) \in \cup_{i\in\mathcal{I}} X_i$ of the system (4.1) satisfies the condition

$$J(x_0, u) \geq \sup_{T,M_i} \bar{x}_0' \bar{P}_{i_0} \bar{x}_0$$

with $x(0) = x_0 \in X_{i_0}$ and $x(\infty)$.

Remark: The minimum value of the cost function (4.39) can be found by using the lower bound theorem, and this method works for any controller. On the other hand, only specific control laws work for the upper bound; for instance, one of the control laws can be defined by minimizing

$$\min_u \left(\frac{\partial V}{\partial x} f(x,u) + \mathsf{L}(x,u). \right) \tag{4.41}$$

Every minimised control law is decided by an optimal controller when V satisfies the H-J-B equation (4.34). On the other hand, if only the inequality (4.35) is satisfied, then one cannot be sure that the control law minimises (4.41), even if it is stabilizing. In the analysis, we can still use this minimization method as an initial point for the control law definition. By comparing to the linear-quadratic optimal control, the expression (4.41) can be minimised by using the following notation

$$\begin{aligned} K_i &= R_i^{-1} B_i' P_i, & \bar{K}_i &= \bar{R}_i^{-1} \bar{B}_i' \bar{P}_i, \\ A_{cl,i} &= A_i - B_i K_i, & \bar{A}_{cl,i} &= \bar{A}_i - \bar{B}_i \bar{K}_i, \\ \mathbf{Q}_i &= Q_i + P_i B_i K_i, & \bar{\mathbf{Q}}_i &= \bar{Q}_i + \bar{P}_i \bar{B}_i \bar{K}_i. \end{aligned} \tag{4.42}$$

The minimised state-feedback control law can be expressed as

$$u = -K_i x - k_i = -\bar{K}_i \quad x \in X_i,\ i \in \mathcal{I}, \quad \text{and } k_i = 0 \quad i \in \mathcal{I}_0 \tag{4.43}$$

The upper bound on cost for the system (4.1) with the stabilizing state-feedback control law can be then found by using the following theorem:

Theorem* 4.6.2** (Upper bound on the cost (Rantzer and Johansson, 2000)):*** If the symmetric matrices T and M_i exist, such that M_i has non-negative entries and they satisfy the following LMIs problem

$$\begin{bmatrix} P_i A_{cl,i} + A_{cl,i}' P_i + E_i' M_i E_i + \mathbf{Q}_i & K_i' \\ * & -R_i^{-1} \end{bmatrix} < 0, \quad i \in \mathcal{I}_0,$$

$$\begin{bmatrix} \bar{P}_i\bar{A}_{cl,i} + \bar{A}'_{cl,i}\bar{P}_i + \bar{E}'_iM_i\bar{E}_i + \bar{Q}_i & \bar{K}'_i \\ * & -R_i^{-1} \end{bmatrix} < 0, \quad i \in \mathcal{I}_1$$

where

$$P_i = F'_iTF_i, \quad \bar{P}_i = \bar{F}'_iT\bar{F}_i$$

then every trajectory $x(t) \in \cup_{i\in\mathcal{I}} X_i$ of the system (4.1) satisfies the condition

$$J(x_0, u) \leq \inf_{T,M_i} \bar{x}'_0\bar{P}_{i_0}\bar{x}_0$$

with $x(0) = x_0 \in X_{i_0}$ and $x(\infty)$.

Remark: Since the K_i and $\bar{K}_i$ are fixed, we can calculate the upper bound of the control performance using semi-definite programming.

***Example* 4.6:** Consider a switched linear system in (4.23) with

$$A_1 = A_3 = \begin{bmatrix} -0.5 & 1 \\ -5 & -0.5 \end{bmatrix}, \quad B_{u,1} = B_{u,3} = \begin{bmatrix} -0.1 \\ 1 \end{bmatrix},$$

$$A_2 = A_4 = \begin{bmatrix} -0.5 & 5 \\ -1 & -0.5 \end{bmatrix}, \quad B_{u,2} = B_{u,4} = \begin{bmatrix} -2 \\ 0.5 \end{bmatrix}.$$

The initial state is given as $x_0 = [-10 \quad -10]'$, and a cost function is defined such that

$$J(x_0, u) = \int_0^\infty (x_1^2(t) + x_2(t)^2 + 0.01u^2(t))dt \quad x \in X_i.$$

Then, an optimal lower bound on the loss function can be found using Theorem 4.6.1,

$$65.512 \leq J(x_0, u).$$

The controller gains can be calculated from the results of a lower bound computation using (4.42),

$$K1 = [-4.7643 \quad -0.5481], \qquad K2 = [-1.5055 \quad -8.7085],$$
$$K3 = [-4.9768 \quad -0.2211], \qquad K4 = [\ 6.3682 \quad -8.8131].$$

Then, an upper bound of the cost function is found using Theorem 4.6.2, with the calculated notation (4.42),

$$J(x_0, u) \leq 102.7755.$$

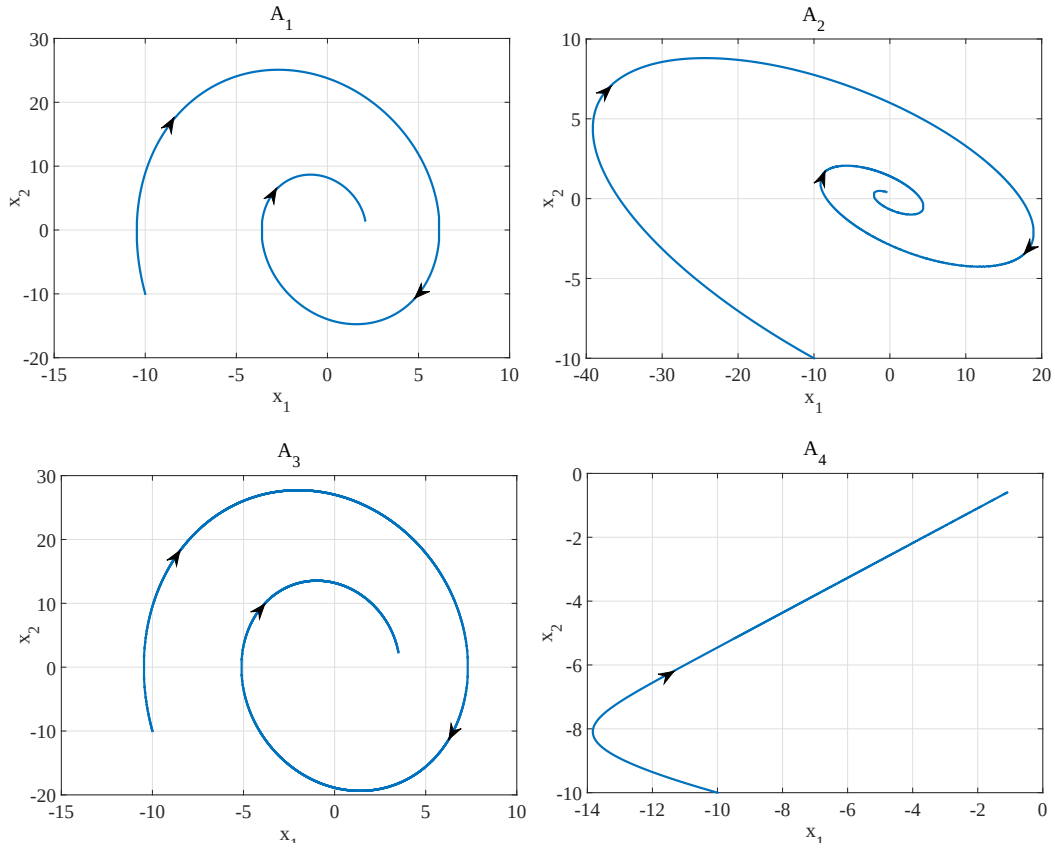

Figure 4.9: Trajectory of the each closed loop subsystems in Example 4.6

According to calculated state-feedback controller gains, Figure 4.9 illustrates the trajectory of each of the closed loop systems. Additionally, the trajectory of the closed loop switched system is given in Figure 4.10. It can be seen that the behaviour of the closed loop switched system trajectory is different from the open loop system trajectory shown in Figure 4.5 because of the effect of state-feedback controllers. Moreover, the trajectories of the closed-loop switched system quickly coverage to zero.

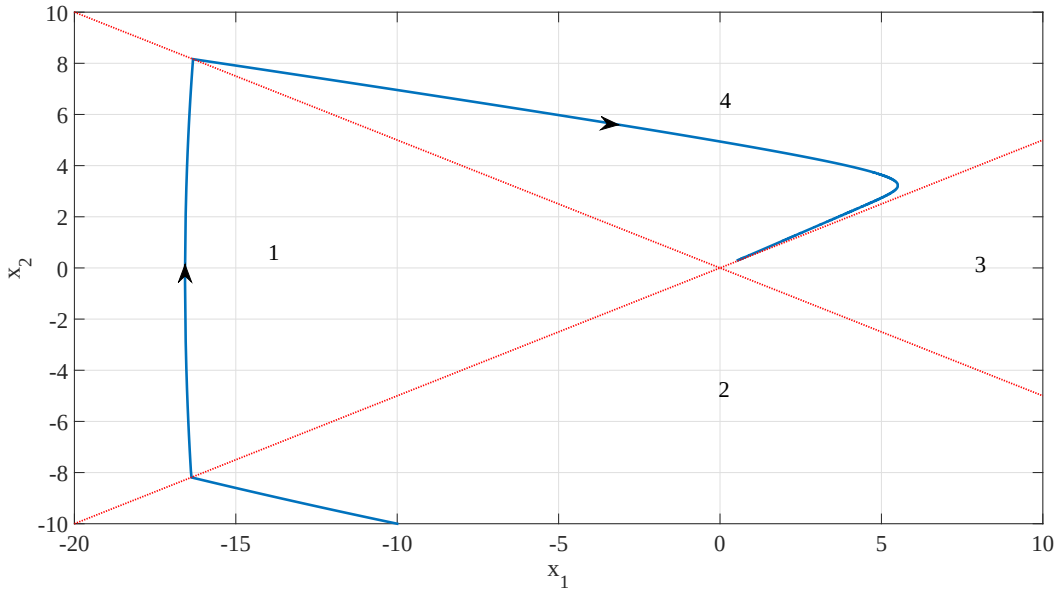

Figure 4.10: Trajectory of the closed loop switched system in Example 4.6

Figure 4.11 shows the Lyapunov function of the switched system according to the Lyapunov matrices, which are calculated in the upper and lower bound theorems. This figure implies that the real value of the Lyapunov function is located between these two values according to the given initial value of the states. It is obvious that the Lyapunov function of the controlled switched system is too low compared to the open loop responses given in Figure 4.7.

4.7 Summary

In this chapter, the state-dependent switching methodology discussed in Chapter 2 is extended to piecewise quadratic stability analysis. The quadratic stability analysis method with state-dependent constraints is introduced. Then, this technique is applied to the piecewise quadratic Lyapunov function and the piecewise quadratic stability analysis method is thus defined. $\mathcal{L}_2$-gain analysis between disturbance inputs and outputs is applied to the defined stability analysis method. In addition to this, the state-feedback controller design approach is given using the upper and lower bound theories.

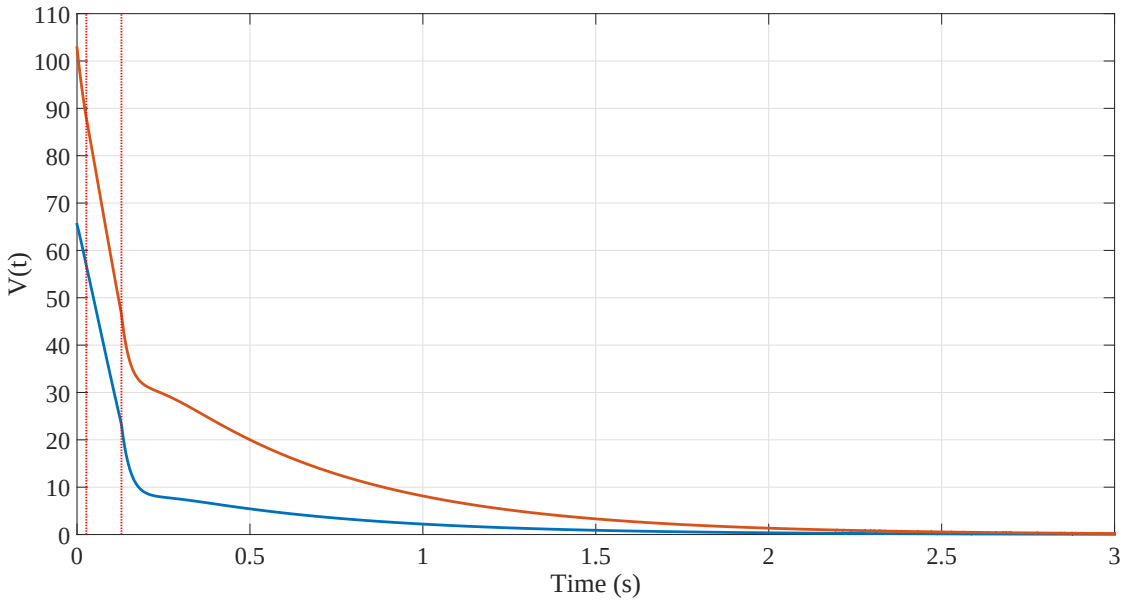

Figure 4.11: Continuous Lyapunov function of Example 4.6

During the stability analysis, the minimum dwell time theory in Chapter 3 only gives a stable result when each of the subsystems is individually stable. Conversely, the piecewise quadratic stability analysis does not require the individual stability of each subsystem; in other words, the piecewise stability analysis might give a stable result even when one or more subsystems are themselves unstable. Hence, the piecewise quadratic stability analysis technique is more attractive than the minimum dwell time stability technique. In the case of controller design, the controller might be designed in both techniques even when the open loop dynamics of some subsystems are not stable. Another difference of between the piecewise stability and minimum dwell time stability analyses is that the minimum dwell time theory assumes that all the subsystems overlap, whereas the piecewise theory assumes the all the cells are disjointed.

In the following chapter, the stability analysis methods in this chapter and Chapter 3 will be used in the ADMIRE fighter aircraft model with state-feedback integral controller. The state-feedback controller design methods will be used for this model.

CHAPTER 5

Controller Design and Stability Analysis for the Fighter Aircraft Model

5.1 Introduction

Stabilizing feedback controller design and achieving desired performance have been playing a more crucial role for the fighter aircraft. New generation aircrafts have wide flight envelopes in terms of aircraft speed and altitude. Due to this reason, it is getting more difficult to achieve a desired tracking performance. In recent years, to achieve this control objective, a number of approaches have been proposed in the context of LPV control design (see, for example, (Papageorgiou et al., 2000; Shin et al., 2002; Sidoryuk et al., 2007)). This approach of LPV control design has some drawbacks as follows: (i) obtaining an LPV model is generally non-trivial and time-consuming, (ii) controller synthesis is computationally demanding and (iii) the LPV controller implementation is more difficult than standard controllers (Turner et al., 2006).

This chapter is motivated by the new approach that the tracking performance over the

wide flight envelopes of modern aircraft can be improved by using a switched feedback controller methodology. However, it is worth noting that switching between controllers can cause transient effect on the closed-loop system response. This problem is treated in this chapter.

The ADMIRE (Aero-Data Model In Research Environment) Benchmark model is used to apply the proposed approach. The application of the ADMIRE model with both switched and constant gain controllers is presented in this chapter. Firstly, the longitudinal dynamics are obtained using a linearised model of ADMIRE. Then, state-feedback integral controllers with constant and switched gain are designed based on the LQR method to compare their respective tracking performances. To guarantee the stability of the switched controlled ADMIRE model, the previously defined stability analysis methods (given in Chapters 3 and 4) are applied. Therefore, the controller design techniques with these stability methods are used to compare the performance of different switched controllers.

The rest of this chapter is structured as follows: Section 5.2 presents the longitudinal control dynamics and linear models of the ADMIRE aircraft model. Then, switched state-feedback controller is designed based on these linear models. According to the stability analysis methods in Chapters 3 and 4, Section 5.3 examines the stability analysis and $\mathcal{L}_2$ performance gain of the ADMIRE aircraft model with the switched state-feedback integral controller designed in Section 5.2.3. Additionally, in Section 5.4, the state-feedback controllers for the ADMIRE aircraft model are also designed using the algorithms in given in Chapters 3 and 4. Section 5.5 reports simulation results for a switched and constant gain state-feedback controlled ADMIRE model, and the benefits and drawbacks of the switched controller are also discussed in this section. In addition, the ADMIRE model is simulated according to the different switched controllers designed in Section 5.4 and calculated in Section 5.2.3. Then, simulation results are compared. Finally, Section 5.6 concludes this chapter.

5.2 The ADMIRE Benchmark Model

5.2.1 Description of ADMIRE

The ADMIRE Model was created by the Aeronautical Research Institute of Sweden in 1997. ADMIRE is a simulation model of a generic and single-seat fighter aircraft with a delta-canard configuration. ADMIRE combines the GAM-data (Generic Aero-data Model) with models of an engine, actuators, dynamics, atmosphere and sensors. The aircraft is equipped with a delta canard configuration, inner and outer elevon deflection and thrust vectoring (Forssell and Nilsson, 2005).

ADMIRE contains twelve states (5.1) defining the dynamics of the aircraft and extra states owing to the existence of actuators, sensors and the Flight Control System (FCS) (Hagström, 2007).

$$x = [V_t,\ \alpha,\ \beta,\ p,\ q,\ r,\ \phi,\ \theta,\ \psi,\ x,\ y,\ z]' \tag{5.1}$$

Left and right canard (δ_{lc}, δ_{rc}), leading edge flaps (δ_{le}), four elevons (δ_{loe}, δ_{lie}, δ_{roe}, δ_{rie}), rudder (δ_r) and throttle setting (t_{ss}) are available control actuators (see Figure 5.1). Air brakes (δ_{ab}), thrust vectoring capability (horizontal δ_{th}, vertical δ_{tv}) and a choice to have the landing gear (δ_{ldg}) up or down are also available in the model (Forssell and Nilsson, 2005). Additionally, ADMIRE is equipped to model atmospheric turbulence/ wind as an external influence/ disturbance. The available disturbance inputs are u_{dist}, v_{dist}, w_{dist} and p_{dist}. Here, the first three inputs are related to body reference wind disturbance, whilst the latter is a rotational effect around the $x-$axis (Hagström, 2007).

In order to provide sufficient handling qualities and stability within the operational envelope (see Figure 5.2), ADMIRE is enlarged with a FCS. The FCS contains a longitudinal and a lateral component. The longitudinal controller provides load factor control for larger Mach numbers (greater than or equal to 0.62) and pitch rate control for low Mach numbers (below 0.58). The corner speed of the Mach number is close to 0.60. A blending function of these two components is performed when the Mach number is between 0.58 and 0.62. The lateral controller enables the pilot to perform initial roll control around

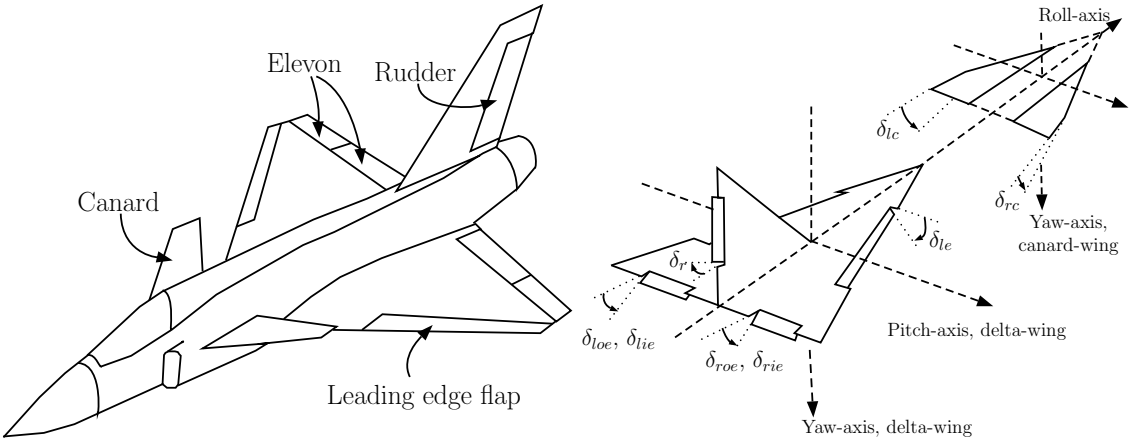

Figure 5.1: ADMIRE Aircraft control surface configuration

the velocity vector of the aircraft and angle of side-slip control (Karlsson, 2007). The flight control system uses sensor models that are integrated into the model, along with a 20 ms delay on the actuator inputs (see Table 5.1). The limit of acceptable deflections and proposals for the angular deflection rate of the control surfaces are given in Table 5.2 (Hagström, 2007). When the aero-data tables of ADMIRE are compared to the original GAM-data, the aero-data tables are expanded in ADMIRE. If Mach number is less than 0.5, the ADMIRE Model can be used to simulate $-30\,^\circ$ to $30\,^\circ$ in side-slip angle (β) and a $-30\,^\circ$ to $90\,^\circ$ angle of attack (α, AoA) (Forssell and Nilsson, 2005).

Modeling Types	**Variables**	**Model**
Air Data Sensors	$V_T,\ \alpha,\ \beta,\ h$	$\frac{1}{1+0.02\,s}$
Inertial Sensors	$p,\ q,\ r,\ n_z$	$\frac{1+0.005346\,s+0.0001903\,s^2}{1+0.03082\,s+0.0004942\,s^2}$
Attitude Sensors	$\theta,\ \phi$	$\frac{1}{1+0.0323\,s+0.00104\,s^2}$
Actuators	$\delta_{lc},\ \delta_{rc},\ \delta_{loe},\ \delta_{roe},\ \delta_{lie},\ \delta_{rie},\ \delta_r$	$\frac{1}{1+0.05\,s}$

Table 5.1: The modelling sensors and actuators (Forssell and Nilsson, 2005)

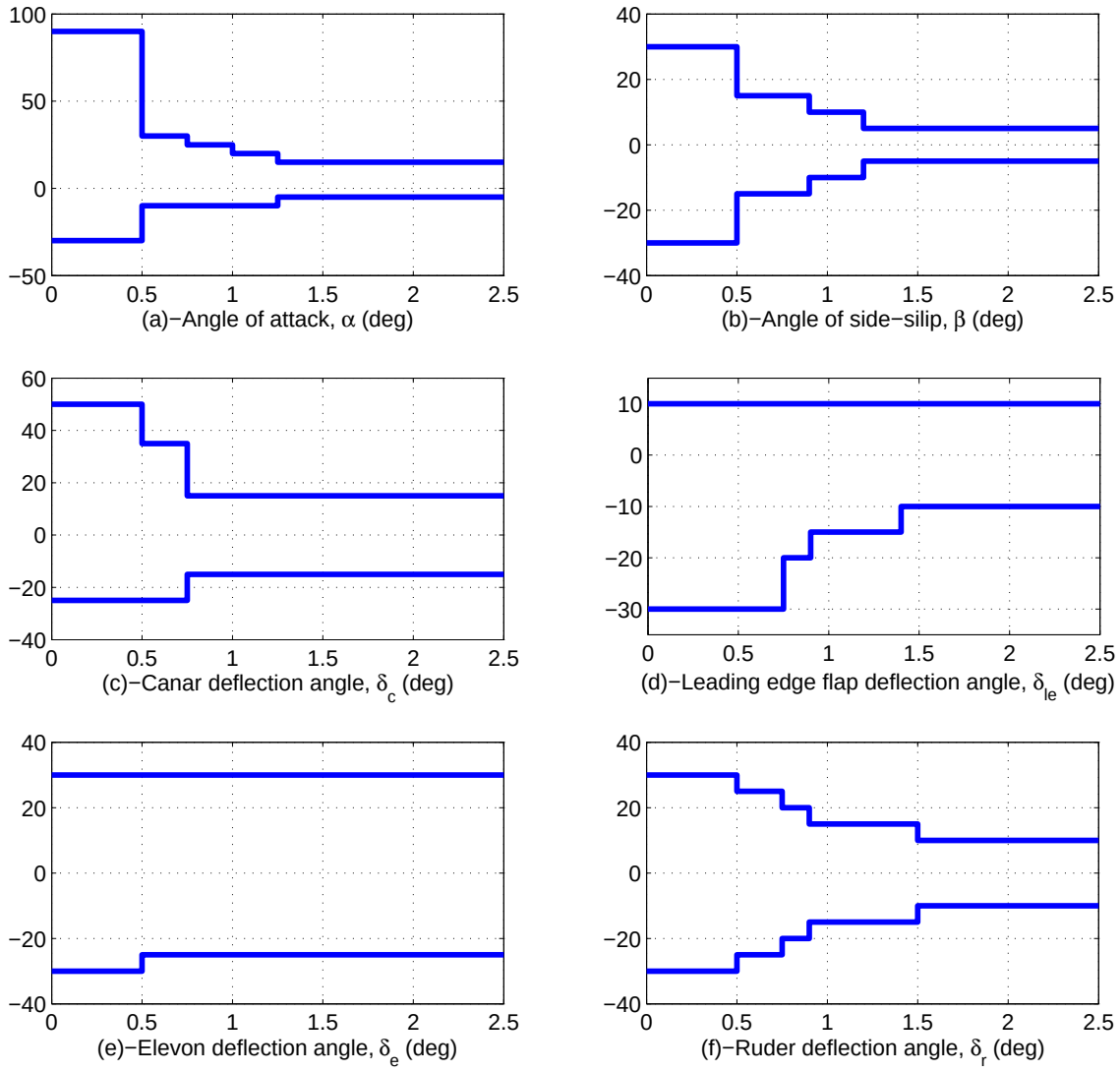

Figure 5.2: Envelope of ADMIRE aero-data model (Hagström, 2007), x axis corresponds to Mach number

Control Surfaces	Min(deg)	Max(deg)	Angular Rate(deg/s)
Elevons	-25	25	± 50
Canard	-55	25	± 50
Ruder	-30	30	± 50
Leading Edge Flap	-10	30	± 50

Table 5.2: Control surface deflection

5.2.2 Linear Models

The ADMIRE model can simulate a wide flight envelope: the altitude changes from $H = 100\,m$ up to $H = 6000\,m$; the Mach number changes from $M = 0.3$ (low subsonic speeds) to $M = 1.4$ (supersonic speeds); see Figure 5.3. Hence, having a wide flight en-

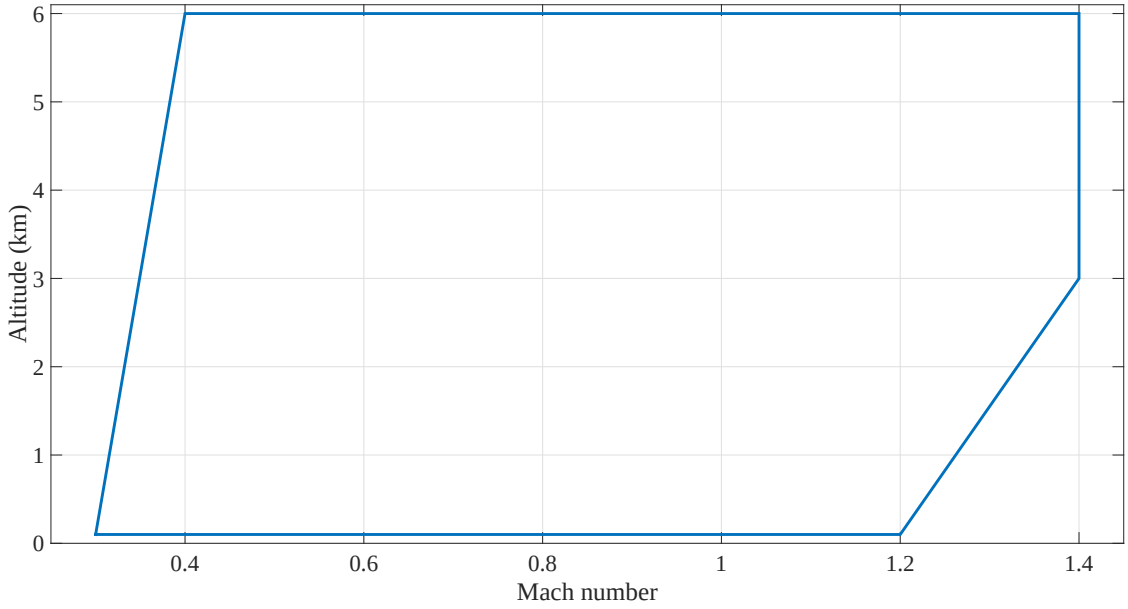

Figure 5.3: Flight Envelope (Hagström, 2007)

velope is the main difficulty of the design problems associated with the ADMIRE model; additionally, the transonic region ($0.9 < M < 1.1$) introduces extra difficulties.

The closed-loop performance fundamentally defines the accuracy of linear model. The linear ADMIRE model is obtained from a linearisation about the trim condition. ADMIRE comes with trimming and linearisation packages which allows for finding linear models. After trimming and linearisation, the state space matrices are found for each equilibrium point such that $A_{bare} = dim(28 \times 28)$, $B_{bare} = dim(28 \times 16)$, $C_{bare} = dim(59 \times 28)$, $D_{bare} = dim(59 \times 16)$. Then, the generic model has 16 inputs (with wind disturbance inputs), 28 states and 59 outputs which are described by

$$\begin{aligned} \dot{x} &= A_{bare}x + B_{bare}u, \\ y &= C_{bare}x + D_{bare}u. \end{aligned} \tag{5.2}$$

The outputs of the model are contained in two parts; a plane part, which includes first 31 outputs, and a sensor part, which includes the last 28 outputs. Attention is restricted to the design of a longitudinal controller for the ADMIRE fighter benchmark model. Hence, the linear longitudinal model has been given such that

$$\begin{aligned} \dot{x}_p &= Ax_p + B_u u + B_w w, \\ y &= Cx_p + D_u u + D_w w, \end{aligned} \tag{5.3}$$

where $x_p = [V_T,\ \alpha,\ q,\ \theta,\ h]'$ is the state vector, $u = [\delta_e,\ t_{ss}]'$ is the control signal, $y := n_z$ is the output to be controlled and $w = [u_{dist},\ w_{dist}]'$ are the wind disturbance inputs along the $x-$ and $z-$axes. δ_e is a symmetric elevon deflection, $\delta_e = \dfrac{(\delta_{loe} + \delta_{lie} + \delta_{roe} + \delta_{rie})}{4}$ and t_{ss} is the throttle stick setting. Here, total velocity, V_T, altitude, h, and pitch angle, θ, states are taken into account to obtain a state-feedback switching rule.

The linear longitudinal model (5.3) is obtained from (5.2) by using the reduction method in (Queinnec et al., 2002). A further details of the longitudinal and lateral directional dynamics are found in (Sidoryuk et al., 2007).

5.2.3 Switched State Feedback Controller Design

In order to design the switched state-feedback controller, the state space matrices of the relevant system need to be found. State space parameters of the linearised system can be obtained from the ADMIRE model (Figure 5.4) for all Mach number values between 0.3 to 1.4 and Altitude values between 100 m to 6000 m. There is no need to find state space parameters for every value of Mach and Altitude, so it is obtained and saved only over a restricted range of state space parameters at Mach $= \{0.3, 0.31, 0.32, \ldots, 1.4\}$ and Altitude $= \{100, 200, 300, \ldots, 6000\, m\}$.

To obtain the state dependent switched system, the flight envelope has been divided into eight cells. The index of the cells are given in Figure 5.5, with the dashed lines showing the boundaries between cells.

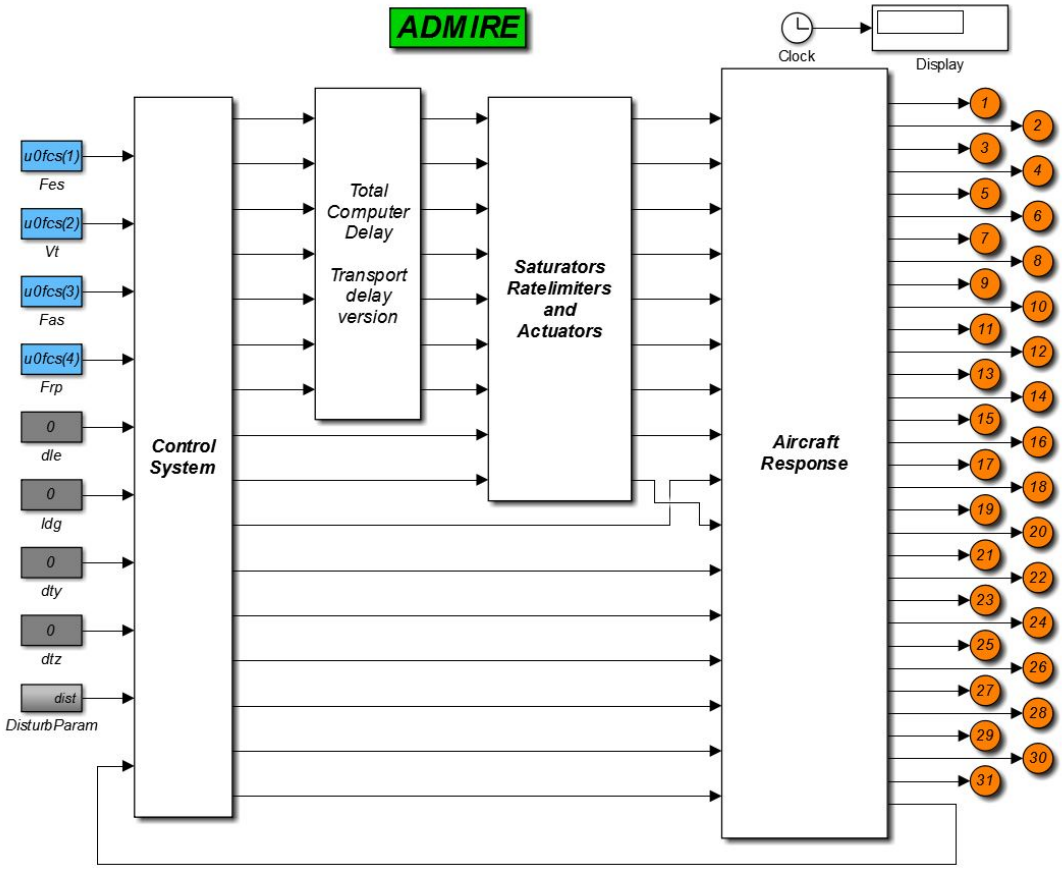

Figure 5.4: ADMIRE Simulink Model

The switched state-feedback integral controller is designed for each cell, and whose data is taken at the center of the cell. The LQR method mentioned above is used to calculate the state-feedback controller gains. The weight matrices Q and R are chosen diagonal with Q, which is of the form $Q = \text{diag}(q_e,\ 0,\ q_\alpha,\ q_q,\ q_\theta,\ 0)$, where the entries set to zero reflect the fact that velocity and altitude are not directly controlled. The selection of the other entries in Q and R follows *Bryson's rule* (Franklin et al., 2010).

The linear model with a state-feedback integral controller is designed as in Figure 5.6. Then, it is simulated with state space parameters which were previously obtained from the ADMIRE model. The state-feedback controller gains are not only designed for the stability of the center of the cell, but each of the controller gains also needs to keep all responses of all operating points in each cell within the template shown in Figure 5.7. The template is generated according to a maximum 20% overshoot, 10% steady-state

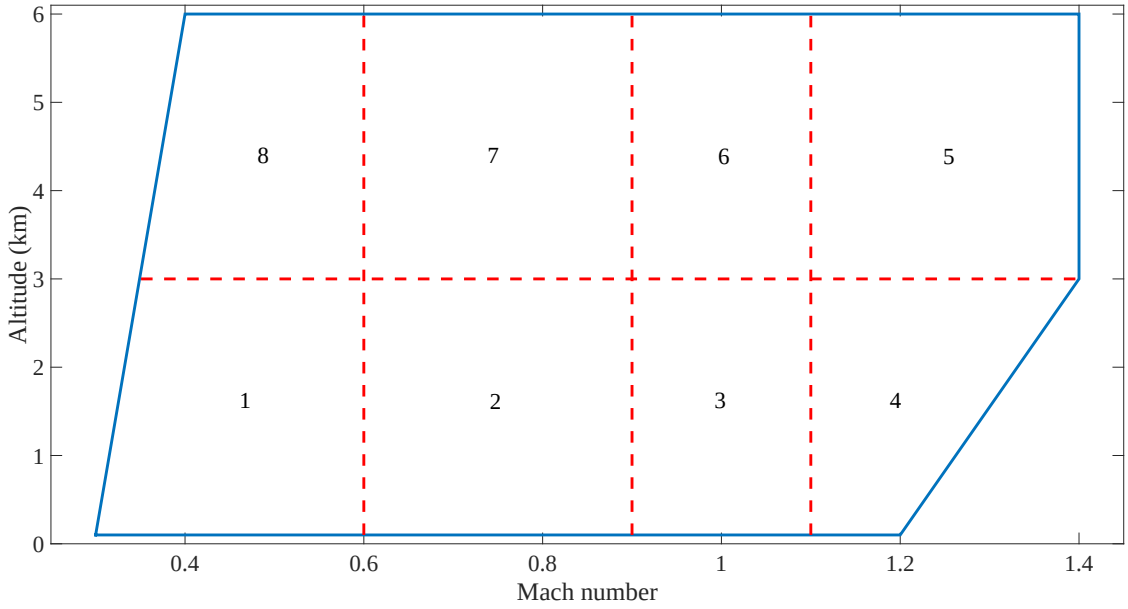

Figure 5.5: The flight envelope with cell partitions

error, $1.2\,s$ rising time and $3.5\,s$ settling time (Karlsson, 2007). Hence, the LQR weight matrices are adjusted to keep responses within the template; responses are given in Figure 5.7.

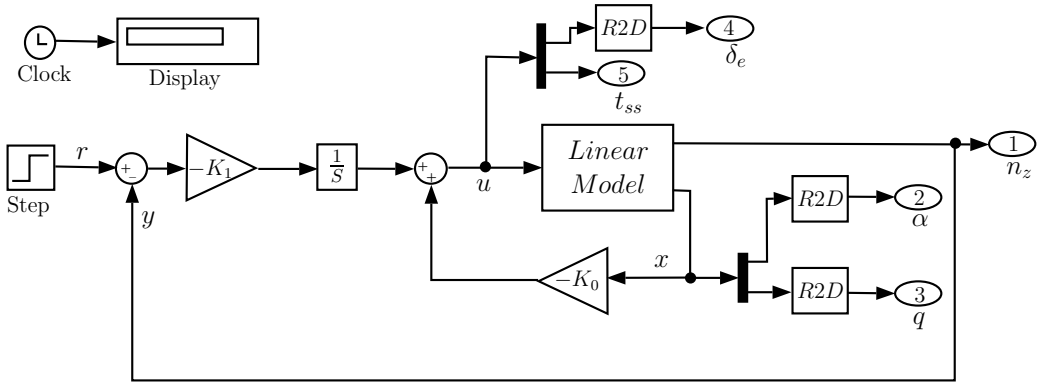

Figure 5.6: Linear Simulink Model

Finally, the designed switched controller gains will be used to analyse the stability of the closed-loop ADMIRE model, and further to simulate the non-linear closed-loop model of ADMIRE in the following sections.

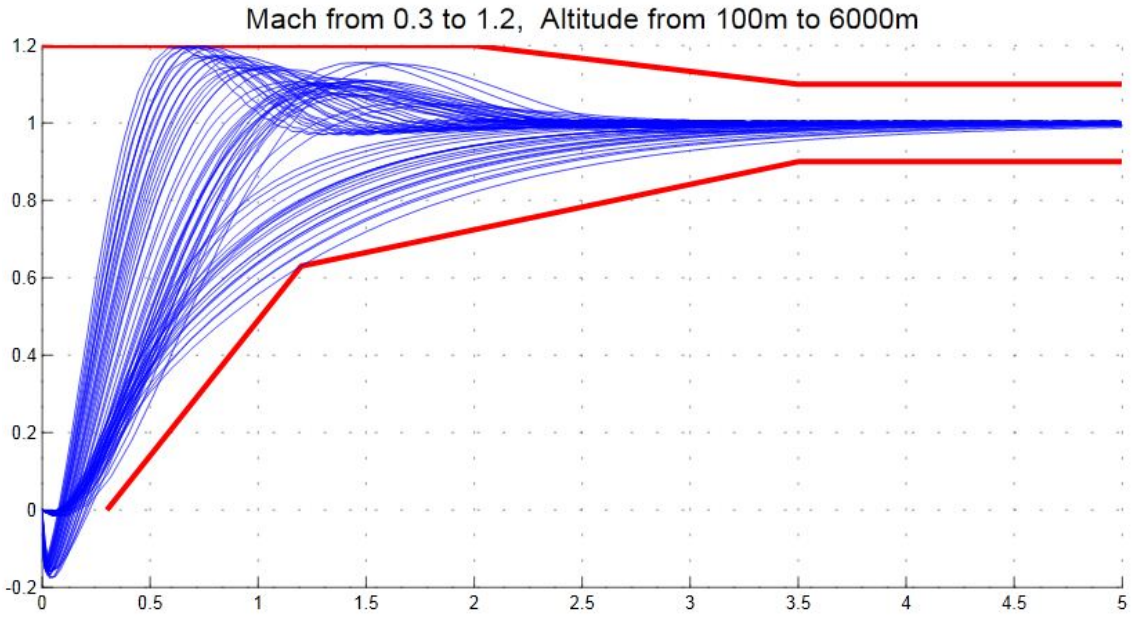

Figure 5.7: n_z responses with state-feedback gain calculated for each value of Mach and Altitude

5.3 Stability and $\mathcal{L}_2$-gain analysis

In this section, we will analyse the stability and $\mathcal{L}_2$ performance gain of the state-feedback integral-controlled ADMIRE aircraft model where controller gains are computed by using the LQR method in Section 5.2.3. The analyses will be performed by using the techniques given in Chapters 3 and 4. This section is divided into two folds according to the stability analysis approaches which are minimum dwell time and piecewise quadratic approaches.

5.3.1 Analysis with Minimum Dwell Time Approach

In this subsection, minimum dwell time approaches in Sections 3.4 and 3.5 are used to analyse the stability and $\mathcal{L}_2$ performance gain of the switched controlled ADMIRE model with LQR gains. In the dwell time approach, the each subsystem needs to be overlapping, hence it is assumed that the flight envelope in Figure 5.8 consists of eight

overlapping cells.

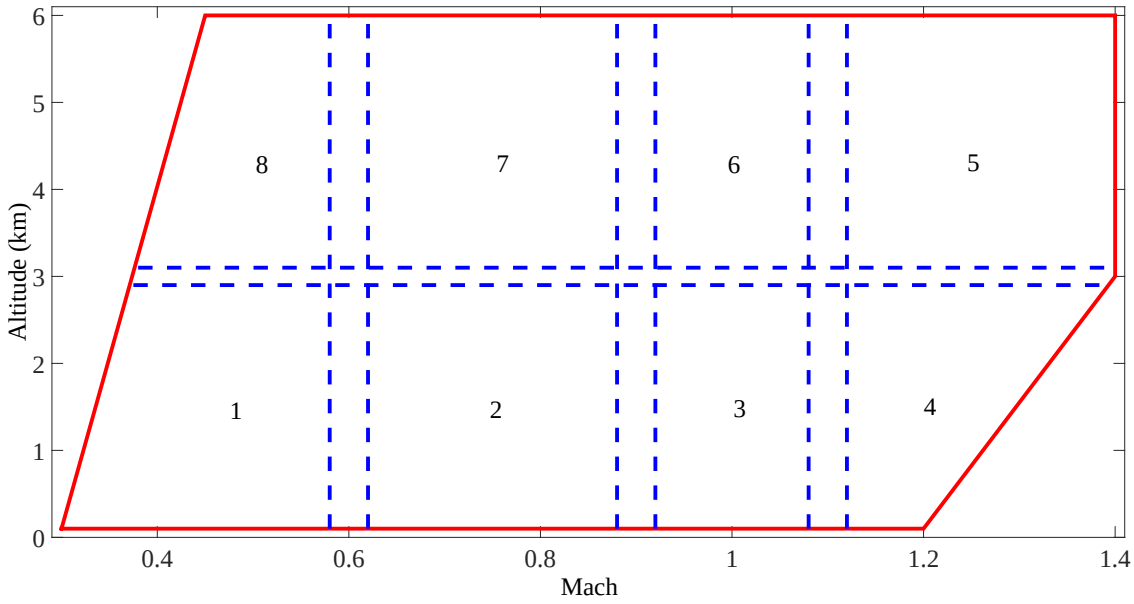

Figure 5.8: The flight envelope with overlapping cell partitions

Before proceeding with the stability and $\mathcal{L}_2$ performance gain analysis of the switched system, it is a strong assumption that each subsystem of the switched system needs to be asymptotically stable (Geromel and Colaneri, 2006). By contrast, the ADMIRE model with state-feedback integral controller is marginally stable for the center of each cell, which is because of the interaction between the integral error of the load factor, n_z, and the pitch angle, θ. Hence, two approaches are presented to deal with this issue. In the first approach, the short period states, α and q are selected to tackle this problem, whilst in the second is to change an output signal from load factor, n_z, to angle of attack, α.

First Approach

For a load factor (normal acceleration) control, we do not need information about some states, such as total velocity, altitude and pitch angle, within the dwell time theory. Thus, these states are removed and asymptotic stability is obtained for each subsystem. For the dwell time analysis, the reduced system can be shown to be

$$\begin{bmatrix} \dot{\alpha} \\ \dot{q} \end{bmatrix} = \begin{bmatrix} Z_\alpha & Z_q \\ M_\alpha & M_q \end{bmatrix} \begin{bmatrix} \alpha \\ q \end{bmatrix} + \begin{bmatrix} Z_{\delta_e} & Z_{t_{ss}} \\ M_{\delta_e} & M_{t_{ss}} \end{bmatrix} \begin{bmatrix} \delta_e \\ t_{ss} \end{bmatrix} + \begin{bmatrix} Z_{u_{dist}} & Z_{w_{dist}} \\ M_{u_{dist}} & M_{w_{dist}} \end{bmatrix} \begin{bmatrix} u_{dist} \\ w_{dist} \end{bmatrix},$$

$$n_z = \begin{bmatrix} n_{z_\alpha} & n_{z_q} \end{bmatrix} \begin{bmatrix} \alpha \\ q \end{bmatrix} + \begin{bmatrix} n_{z_{\delta_e}} & n_{z_{t_{ss}}} \end{bmatrix} \begin{bmatrix} \delta_e \\ t_{ss} \end{bmatrix} + \begin{bmatrix} n_{z_{u_{dist}}} & n_{z_{w_{dist}}} \end{bmatrix} \begin{bmatrix} u_{dist} \\ w_{dist} \end{bmatrix}. \tag{5.4}$$

The augmented system for state-feedback integral controller is obtained according to the system (5.4). The LQR weights are reduced and the LQR gains are recalculated according to the reduced system dynamics and LQR weights. Table 5.3 gives the results of the minimum dwell time theories which are based on the parameter independent Lyapunov function (PILF) and the parameter dependent Lyapunov function (PDLF).

	Stab. PILF	Stab. PDLF	$\mathcal{L}_2$-gain PILF	$\mathcal{L}_2$-gain PDLF
$T(s)$	0.090	0.036	0.090	0.036
Solving Time (s)	3.4498	9.5483	4.6161	11.0014
Num. of LMIs	144	384	145	385
Num. of Var.	96	672	97	673
$\mathcal{L}_2$-gain (γ)	-	-	20.77	13.88

Table 5.3: The minimum dwell time and $\mathcal{L}_2$-gain results for ADMIRE model (for $H = 1$).

The minimum dwell time results for different H's are given in Table 5.4 and $\mathcal{L}_2$-gain results are presented in simple brackets. The minimum dwell time decreases as H increases. The $\mathcal{L}_2$-gain results for both the parameter dependent Lyapunov function method and the parameter independent Lyapunov function method increase as H increases. Because, the theorems are solved for different minimum dwell times. Therefore, the $\mathcal{L}_2$-gains for various H and dwell time, T_d, are also shown in Table 5.5 for both parameter dependent and independent Lyapunov functions. It is obvious that the parameter dependent Lyapunov function approach gives less $\mathcal{L}_2$-gain for the ADMIRE aircraft model. Moreover, Table 5.5 indicates that the $\mathcal{L}_2$-gain is nearly 0.52 when the minimum dwell

H	Stab. PILF	Stab. PDLF	$\mathcal{L}_2$-gain PILF	$\mathcal{L}_2$-gain PDLF
2	0.060	0.027	0.060 (31.57)	0.027 (15.13)
5	0.048	0.023	0.048 (33.23)	0.023 (16.49)
10	0.045	0.021	0.045 (34.17)	0.021 (20.68)

Table 5.4: The minimum dwell time and $\mathcal{L}_2$-gain results (in simple brackets) for the ADMIRE model (for various H).

time is greater than $1\,s$.

$T_d(s) \setminus H$	1	2	5	10
0.1 s	9.2218 (1.8559)	3.0873 (1.3877)	2.1799 (1.1939)	2.0097 (1.1387)
0.2 s	1.4809 (0.9859)	1.1522 (0.8429)	0.9849 (0.7502)	0.9220 (0.7094)
0.5 s	0.8198 (0.6434)	0.7241 (0.5817)	0.6723 (0.5521)	0.6498 (0.5430)
1 s	0.6664 (0.5380)	0.6257 (0.5213)	0.6076 (0.5213)	0.5974 (0.5213)

Table 5.5: The $\mathcal{L}_2$-gain results for various H and T_d (Simple brackets show PDLF).

According to Tables 5.3 and 5.4, the minimum dwell time theories mathematically give the minimum dwell time as equal to or less than $0.09\,s$, but it is physically not possible to move from one cell to another within $0.09\,s$, in the real application. In addition, the $\mathcal{L}_2$-gain results of these theorems are very high, although it is desirable that $\mathcal{L}_2$-gain be equal to or less than 1. This means that the wind disturbance signals are increased if the minimum dwell time is defined as being equal to or less than $0.1\,s$ (see Table 5.5). On the other hand, to obtain wind disturbance attenuation, the minimum dwell time based on PDLF needs to be greater than or equal to $0.2\,s$.

According to restrictions on the real fighter aircraft application, we offered a different method for the minimum dwell time stability analysis of the above-defined closed-loop ADMIRE model. In this case, the switching only occurs between neighbouring cells. For instance, if the trajectory of the system is located in Cell 1 in Figure 5.8, it will only move towards one of the cells $2,\ 7$, and 8 and the switching will occur with one of these cells.

Then, it will move to other neighbouring cells; otherwise, it cannot switch instantly, such as from 1 to 4 in real application. Therefore, the minimum dwell time theory will be applied to the set of neighbouring cells such that

$$S_1 = \{1,\ 2,\ 7,\ 8\}, \qquad S_2 = \{2,\ 3,\ 6,\ 7\}, \qquad S_3 = \{3,\ 4,\ 5,\ 6\}.$$

The common dwell time might be defined by finding the maximum of the minimum dwell times. This expression can be shown to be

$$T_c = \sup\Big\{T_{S_1},\ T_{S_2},\ T_{S_3}\Big\}. \tag{5.5}$$

When the above closed-loop ADMIRE model is performed using this approach then the minimum dwell time is found as per reported in Table 5.6. It can be clearly seen that the minimum dwell time for the neighbour cells is very small, which verifies the stability of the ADMIRE model even during more frequent switching. Moreover, $\mathcal{L}_2$-gain results show that the PDLF method gives a disturbance attenuation for all neighbouring cells.

	Stab. PILF	Stab. PDLF	$\mathcal{L}_2$-gain PILF	$\mathcal{L}_2$-gain PDLF
T_{S_1} and (γ)	4×10^{-8}	2×10^{-8}	4×10^{-8} (3.45)	2×10^{-8} (0.52)
T_{S_2} and (γ)	2×10^{-8}	1×10^{-8}	2×10^{-8} (1.21)	1×10^{-8} (0.54)
T_{S_3} and (γ)	3×10^{-8}	2×10^{-8}	3×10^{-8} (0.66)	2×10^{-8} (0.59)
Num. of LMIs	56	128	57	129
Num. of Var.	48	336	49	337

Table 5.6: The minimum dwell time and $\mathcal{L}_2$-gain results for ADMIRE model (for $H = 1$).

Second Approach

In this approach, we change an output signal of the ADMIRE model from n_z to angle of attack, α, to eliminate interaction between the integral error of n_z and θ. In this case, the ADMIRE model is also assumed to be a polytopic system. A switched state-feedback controller needs to provide asymptotic stability for each of the vertices of each

subpolytope. However, the LQR method in Section 2.4.2 only provides the stability of the given operating point of the system, rather than the requirement above. Hence, the multi-model/ multi-objective state-feedback synthesis function, $msfsyn$, in MATLAB is used to design the state-feedback controller for the polytopic systems which provide the stability of each of the vertices in each subpolytope (for details see Chapter 4 in (Gahinet et al., 1995)).

The minimum dwell time theories are finally applied to the rearranged switched closed-loop system. The results of the minimum dwell time theories for different H's are given in Table 5.7. In this approach, the minimum dwell time is dramatically increased for all stability methods. In addition to this, the results of the neighbouring cells approach previously discussed are presented in Table 5.8 for $H = 1$. In this case, the common dwell time in (5.5) is computed as $T_c = 6.905\,s$ and $T_c = 1.805\,s$ for PILF and PDLF, respectively.

H	Stab. PILF	Stab. PDLF	$\mathcal{L}_2$-gain PILF	$\mathcal{L}_2$-gain PDLF
1	60.56	14	60.56 (2.9945)	14 (0.9242)
2	47.28	11.66	47.28 (1.4732)	11.66 (0.0687)
5	39.08	9.3	39.08 (0.2310)	9.3 (0.0502)
10	34.8	7.79	34.8 (0.2703)	7.79 (0.0298)

Table 5.7: The minimum dwell time and $\mathcal{L}_2$-gain results (in simple brackets) for the ADMIRE model (for various H).

5.3.2 Analysis with Piecewise Quadratic Approach

In this subsection, the common and piecewise quadratic stability analysis methods in Sections 4.3 and 4.4, respectively, are used to investigate the stability of the switched controlled ADMIRE model with LQR gains. The theorems in Section 4.5 are also applied to find $\mathcal{L}_2$ performance gain.

Before analysing the stability and $\mathcal{L}_2$ performance gain, we need to determine certain parameters such as the *cell bounding matrix* and *continuity matrix* of the ADMIRE model.

	Stab. PILF	Stab. PDLF	$\mathcal{L}_2$-gain PILF	$\mathcal{L}_2$-gain PDLF
T_{S_1} and (γ)	0.019	0.105	0.019 (0.0177)	0.105 (0.0068)
T_{S_2} and (γ)	4.480	0.014	4.480 (0.2274)	0.014 (0.0677)
T_{S_3} and (γ)	6.905	1.805	6.905 (0.1710)	1.805 (0.1719)
Num. of LMIs	56	128	57	129
Num. of Var.	168	336	169	337

Table 5.8: The minimum dwell time and $\mathcal{L}_2$-gain results for ADMIRE model (for $H = 1$).

Finding *cell bounding matrices* and *continuity matrices*

The flight envelope of the ADMIRE model is divided into eight disjointed cells as in Figure 5.9 (where the negative sign of the altitude shows the direction). To obtain these

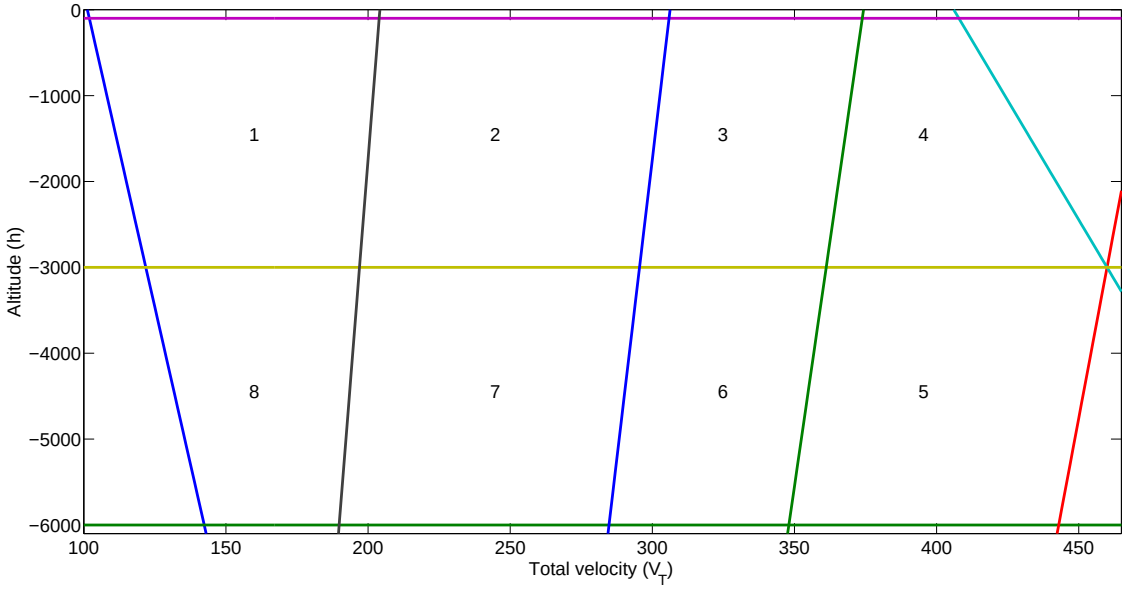

Figure 5.9: Hyperplane partition of the ADMIRE model

cells, we define nine hyperplanes in (5.6) as described in the hyperplane partition method in Section 4.3.1.

$$
\begin{aligned}
&[0, \quad 146, \quad 0, \quad 0, \quad 0, \quad 1, \quad -14785]\, x = 0 \\
&[0, \quad 0, \quad 0, \quad 0, \quad 0, \quad 1, \quad 6000]\, x = 0 \\
&[0, \quad 176.4, \quad 0, \quad 0, \quad 0, \quad -1, \quad -84133]\, x = 0 \\
&[0, \quad 55.6, \quad 0, \quad 0, \quad 0, \quad 1, \quad -22597]\, x = 0 \\
&[0, \quad 0, \quad 0, \quad 0, \quad 0, \quad 1, \quad 100]\, x = 0 \\
&[0, \quad 0, \quad 0, \quad 0, \quad 0, \quad 1, \quad 3000]\, x = 0 \\
&[0, \quad 418.8, \quad 0, \quad 0, \quad 0, \quad -1, \quad -85506]\, x = 0 \\
&[0, \quad 279.2, \quad 0, \quad 0, \quad 0, \quad -1, \quad -85506]\, x = 0 \\
&[0, \quad 228.4, \quad 0, \quad 0, \quad 0, \quad -1, \quad -85506]\, x = 0
\end{aligned}
, \qquad x = \begin{bmatrix} x_1 \\ V_T \\ \alpha \\ q \\ \theta \\ h \\ 1 \end{bmatrix}. \tag{5.6}
$$

These hyperplanes have been used to construct the *cell bounding matrices* and *continuity matrices*. For each cell, the *cell bounding matrices*, $E_i x \geq 0$ are computed as follows:

$$
E_1 = \begin{bmatrix} 0, & 146, & 0_{1\times 3}, & 1, & -14785 \\ 0, & 0, & 0_{1\times 3}, & -1, & -100 \\ 0, & -418.8, & 0_{1\times 3}, & 1, & 85506 \\ 0, & 0, & 0_{1\times 3}, & 1, & 3000 \end{bmatrix}, \quad
E_2 = \begin{bmatrix} 0, & 418.8, & 0_{1\times 3}, & -1, & -85506 \\ 0, & 0, & 0_{1\times 3}, & -1, & -100 \\ 0, & -279.2, & 0_{1\times 3}, & 1, & 85506 \\ 0, & 0, & 0_{1\times 3}, & 1, & 3000 \end{bmatrix},
$$

$$
E_3 = \begin{bmatrix} 0, & 279.2, & 0_{1\times 3}, & -1, & -85506 \\ 0, & 0, & 0_{1\times 3}, & -1, & -100 \\ 0, & -228.4, & 0_{1\times 3}, & 1, & 85506 \\ 0, & 0, & 0_{1\times 3}, & 1, & 3000 \end{bmatrix}, \quad
E_4 = \begin{bmatrix} 0, & 228.4, & 0_{1\times 3}, & -1, & -85506 \\ 0, & 0, & 0_{1\times 3}, & -1, & -100 \\ 0, & -55.6, & 0_{1\times 3}, & -1, & 22597 \\ 0, & 0, & 0_{1\times 3}, & 1, & 3000 \end{bmatrix},
$$

$$
E_5 = \begin{bmatrix} 0, & 228.4, & 0_{1\times 3}, & -1, & -85506 \\ 0, & 0, & 0_{1\times 3}, & -1, & -3000 \\ 0, & -176.4, & 0_{1\times 3}, & 1, & 84133 \\ 0, & 0, & 0_{1\times 3}, & 1, & 6000 \end{bmatrix}, \quad
E_6 = \begin{bmatrix} 0, & 279.2, & 0_{1\times 3}, & -1, & -85506 \\ 0, & 0, & 0_{1\times 3}, & -1, & -3000 \\ 0, & -228.4, & 0_{1\times 3}, & 1, & 85506 \\ 0, & 0, & 0_{1\times 3}, & 1, & 6000 \end{bmatrix},
$$

$$
E_7 = \begin{bmatrix} 0, & 418.8, & 0_{1\times 3}, & -1, & -85506 \\ 0, & 0, & 0_{1\times 3}, & -1, & -3000 \\ 0, & -279.2, & 0_{1\times 3}, & 1, & 85506 \\ 0, & 0, & 0_{1\times 3}, & 1, & 6000 \end{bmatrix}, \quad
E_8 = \begin{bmatrix} 0, & 146, & 0_{1\times 3}, & 1, & -14785 \\ 0, & 0, & 0_{1\times 3}, & -1, & -3000 \\ 0, & -418.8, & 0_{1\times 3}, & 1, & 85506 \\ 0, & 0, & 0_{1\times 3}, & 1, & 6000 \end{bmatrix}.
$$

Here, zero columns in (5.6) are not shown in the *cell bounding matrices*. Then the *continuity matrices* are defined as $F_i = [E_i',\ I]'$.

Remark: It is always assumed that the equilibrium point is located at the origin, so the variable changing technique in (Khalil, 2002) must be applied to the system. Then, the same stability analysis methods are used to analyse the stability of the switched system with respect to an arbitrary equilibrium point x_e. This technique was mentioned in Chapter 2. According to this method, the hyperplanes in (5.6), *cell bounding matrices* and *continuity matrices* must be rearranged as a requirement of the stability theorem.

Here, the stability and $\mathcal{L}_2$-gain analysis are applied to two different cases of the ADMIRE model. In the first case, the dynamics of each cell are assumed to be consistent, so the dynamics are taken from each cell center. In the second case, it is assumed that the dynamics of the each cell belong to a polytopic system and they are convex combination of each of the cell vertices, thus the vertices of each cell are used.

First Case

In this case, we assumed that the system parameters of each cell are constant, so the data is taken from the center of each cell. To apply PQLF theories with the PWLTOOL package, at least one of the cells needs to contain the origin. Due to this, the PQLF theories have been solved eight times, with the center of one of the cells is moved to the origin each time.

The conditions in (4.5) and (4.6) for quadratic stability and the relaxed common quadratic Lyapunov function in Theorem 4.3.1 did not give a feasible solution for the stability of the switched system with the switched controller. By solving the LMIs in the theorems in Sections 4.4 and 4.5 with a Matlab toolbox (PWLTOOL) in (Hedlund and Johansson, 1999), the Piecewise Quadratic Lyapunov Function $V(t) = x(t)'P_i x(t)$ for $i = 1, \ldots, 8$ is found. The compression results are given in Table 5.9 where $\mathcal{L}_2$-gain is given in simple brackets.

	CQLF	CQLF (relaxed)	PQLF	$\mathcal{L}_2$-gain PQLF
Stability	✗	✗	✓	✓ (0.859)
Num. of LMIs	9	51	100	101
Num. of Var.	21	63	204	205
Solving Time (s)	0.34	0.84	1.37	3.39

Table 5.9: The stability analysis and $\mathcal{L}_2$-gain results for ADMIRE model

Second Case

In the first case, the assumption of consistent system parameters in the cells is not a realistic approach for the non-linear models. Hence, it is assumed that the system parameter of each cell is a convex combination of the vertices of each cell. The switched controller is now redesigned according to the system dynamics of each of the cell vertices. The Multi-Objective State-Feedback controller design function, $msfsyn$, is used to obtain an optimized controller for each of the polytopic cells. In addition to this, the stability analysis techniques are applied as in the first case, above. The results of this analysis are shown in Table 5.10 where $\mathcal{L}_2$-gain is given in simple brackets.

	CQLF	CQLF (relaxed)	PQLF	$\mathcal{L}_2$-gain PQLF
Stability	✗	✗	✓	✓ (0.8386)
Num. of LMIs	33	225	280	281
Num. of Var.	21	213	295	296
Solving Time (s)	0.51	0.91	5.76	18.36

Table 5.10: The stability analysis and $\mathcal{L}_2$-gain results for ADMIRE model

Although the piecewise theorems solve more inequalities in the second case than first, the results of the second case are the more accurate because of the assumption of a polytopic system. $\mathcal{L}_2$-gain results in both cases (given in Tables 5.9 and 5.10) are less than 1, meaning that both cases attenuate the wind disturbances.

5.4 Controller Design with Stability Analysis Methods

In this section, the switched state-feedback controller gains for the ADMIRE fighter aircraft model are computed by using the controller design methodologies mentioned in Sections 3.6 and 4.6. The advantage of using these methodologies is that they provide the stability of the system besides controller design.

5.4.1 Controller Design with Minimum Dwell Time Approach

The objective of this subsection is to design a switched state-feedback integral controller for the ADMIRE model using the methodologies in Section 3.6. According to the illustrative examples in Section 3.6, the parameter dependent Lyapunov function method computes a constant gain for each cell partition, and at the same time provides the smallest minimum dwell time constraint. Hence, the minimum dwell time is defined as $3\,s$, the prescribed scalar is chosen as $\beta = 0.04$ and Theorem 3.6.2 is solved with $Y_{i,h}$, and $S_{i,h}$ are free from h. Then, the constant controller gains for each subsystem are calculated as in Appendix A.1.

In addition to this, the state-feedback $\mathcal{H}_2-$optimal controller is computed by using Theorem 3.6.5, where the minimum dwell time is defined as $3\,s$, the prescribed scalar is chosen as $\beta = 0.04$ and the regulated output matrices are chosen just like LQR weight matrices in Section 5.2.3. The computed gains are listed in Appendix A.1.

5.4.2 Controller Design with Piecewise Quadratic Approach

In this subsection, the controller design method in Section 4.6 is used to obtain a switched state-feedback integral controller for the ADMIRE model. It is assumed that the dynamics of each cell do not vary significantly, so the data are taken in the center of each cell. Here, the weighting matrices are defined as the same as the LQR weights in Section 5.2.3. The same *cell bounding matrices* and the *continuity matrices* in Section 5.3.2 are defined for the controller design method. Then, the state-feedback controller gains are

found as in Appendix A.1.

In this section, the switched state-feedback integral controllers are computed based on the above approaches. According to these controllers, the closed-loop ADMIRE model will be simulated in the following section. Then, the simulation results will be compared with the switched LQR controller designed in Section 5.2.3.

5.5 Simulation Results and Discussions

The simulation results will be discussed in two cases. One is the advantages of the switched gain controller over the constant gain controller. The other is the comparison between the switched gain controller design methods and the LQR design approach. Before analysing the simulation results, it is worth to introduce some definitions.

The switched state-feedback integral controller is designed for the non-linear Simulink model in Figure 5.10. The actuators and initial conditions are also added to the model.

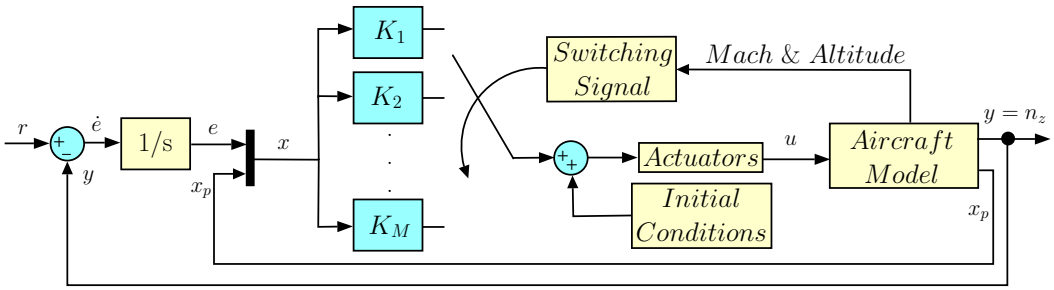

Figure 5.10: Non-linear simulink model with switched state-feedback controller

The states, Mach number and altitude are assumed to be observable. Based on these states, the state-dependent switching strategy is used in this model. The working principle of this strategy is that the switching occurs when the state parameters of system (Mach number and altitude) reach the cell boundaries in Figure 5.5. To ensure continuity of the control inputs during the switching instants, a constant is added to state-feedback law, such that

$$u = Kx + \upsilon, \quad \upsilon = u^+ - u^-.$$

The state-feedback controller gains are designed using different control design approaches in the previous sections.

Reference input selection for the longitudinal motion

The longitudinal motion of the aircraft happens around the lateral/ transverse axis. The lateral axis is an imaginary axis that extends crosswise from wing-tip to wing-tip, as shown in Figure 5.1 (right). The motion around this axis is called a pitch motion, and is controlled by the elevator and the canard surfaces as shown in Figure 5.1 (left). Most fighter aircraft are not equipped with canard surfaces so the effect of the canard on the longitudinal motion is disregarded in this chapter to generalize the simulation results.

The longitudinal motion of the aircraft occurs such that if the pilot pushes the control stick over, then the elevator surface deflects downward and the nose of the aircraft moves down, as illustrated in Figure 5.11 (left). On the other hand, if the pilot pulls the control stick up, then the elevator surface deflects upwards and the nose of the aircraft moves up, as illustrated in Figure 5.11 (right). In longitudinal control, the position of the control stick is used to generate a reference signal for the closed-loop system. This reference signal is converted to a required reference such as pitch angle, pitch rate or load factor. The load factor is a demanded input in this chapter. The range of the load factor varies from -3 g to 9 g in the ADMIRE model. Hence, load factor is defined as -3 g for full control stick push and conversely, as 9 g for full control stick pull. This definition will be used to move the aircraft around the flight envelope.

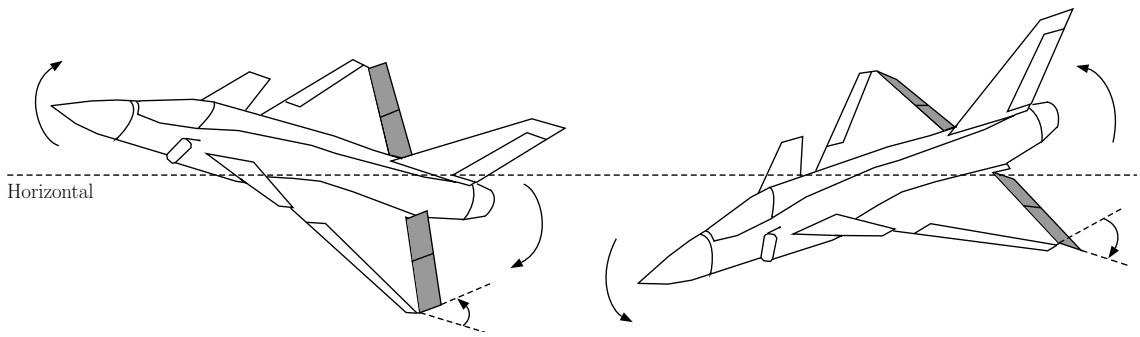

Figure 5.11: Longitudinal motion of the ADMIRE Aircraft

5.5.1 The Constant and The Switched gain Controllers Results

The aim of this subsection is to show that a switched gain controller can achieve better performance than a constant gain controller. Hence, to compare switched and constant gain state-feedback controllers, a constant state-feedback controller has been designed for a plant located at the center of the flight envelope. Two different simulation scenarios have been proposed for the system with these controllers. One is the short-term simulation for the different operating points. In this case, the simulation starts some operating points which are the linearised equilibrium point of the system. Although it allows us to compare the systems with defined controllers at these operating points, the system may deteriorate or give a different response while it is moving around the flight envelope. Hence, the other simulation (long-term simulation) is applied to observe the attitude of the system trajectories around the flight envelope.

For the short-term simulations, the center of each cell is chosen as an operating point. The load factor responses of these simulations are given in Figure 5.12. Here, 50% pull, full push and level positions of the control stick are, respectively, defined as required references.

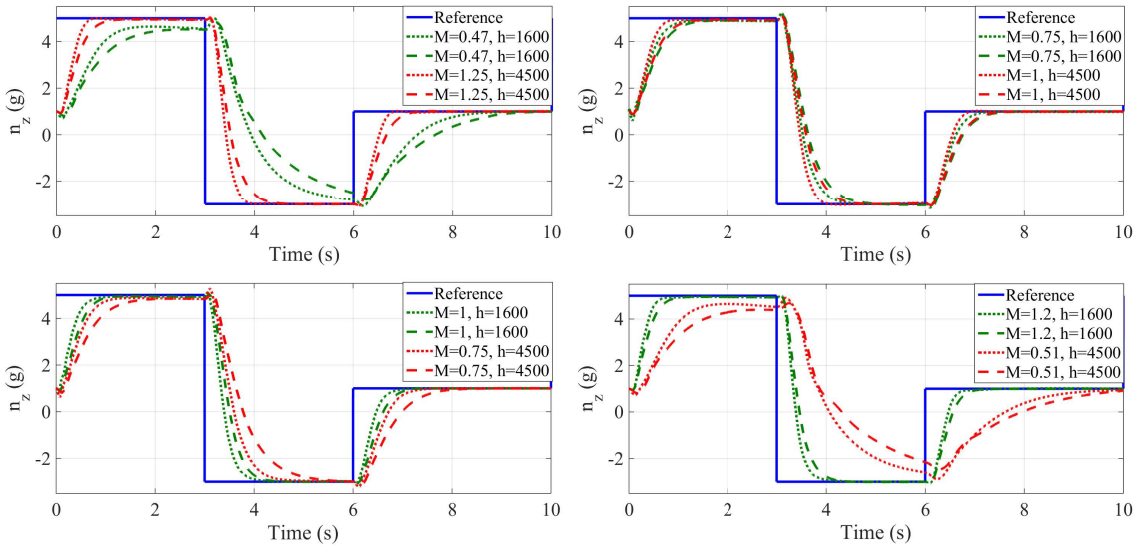

Figure 5.12: Constant gain (dash lines) and Switched gain (dotted lines) responses for the different operating points

For the long term simulation, load factor, n_z tracking performance throughout the flight envelope are compared. The simulation is applied twice to the non-linear system. One starts at $M = 0.4$ and $h = 100\,m$ and the other at $M = 0.38$ and $h = 4500\,m$. The output responses of these simulations are illustrated in Figures 5.13 and 5.15, where the switching instances and indices of the switched controller are also given. In addi-

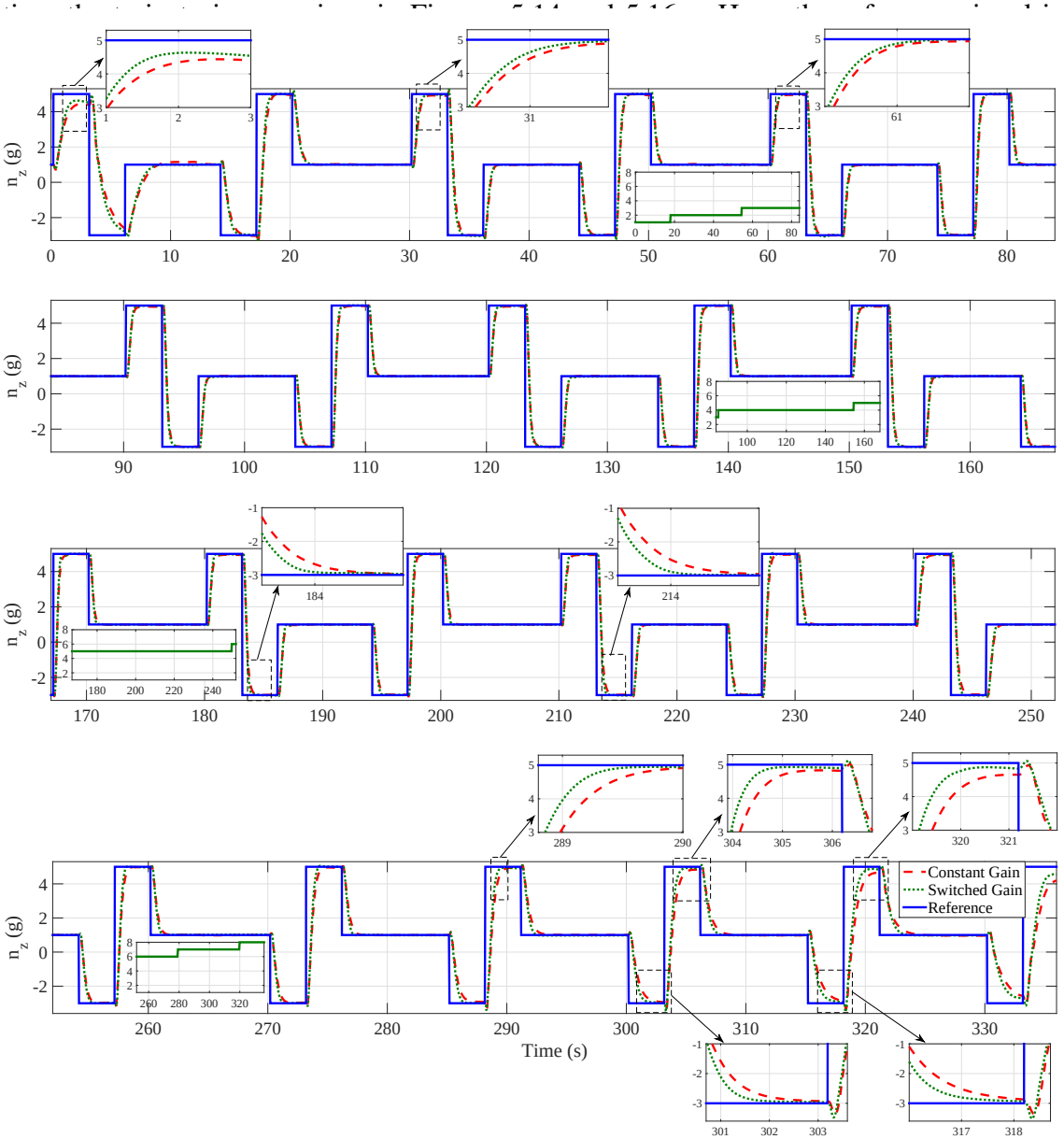

Figure 5.13: Load factor responses of the closed-loop systems, ($M = 0.4$ and $h = 100\,m$)

obtained using combination of the 50 % pull, full push and level position of the control

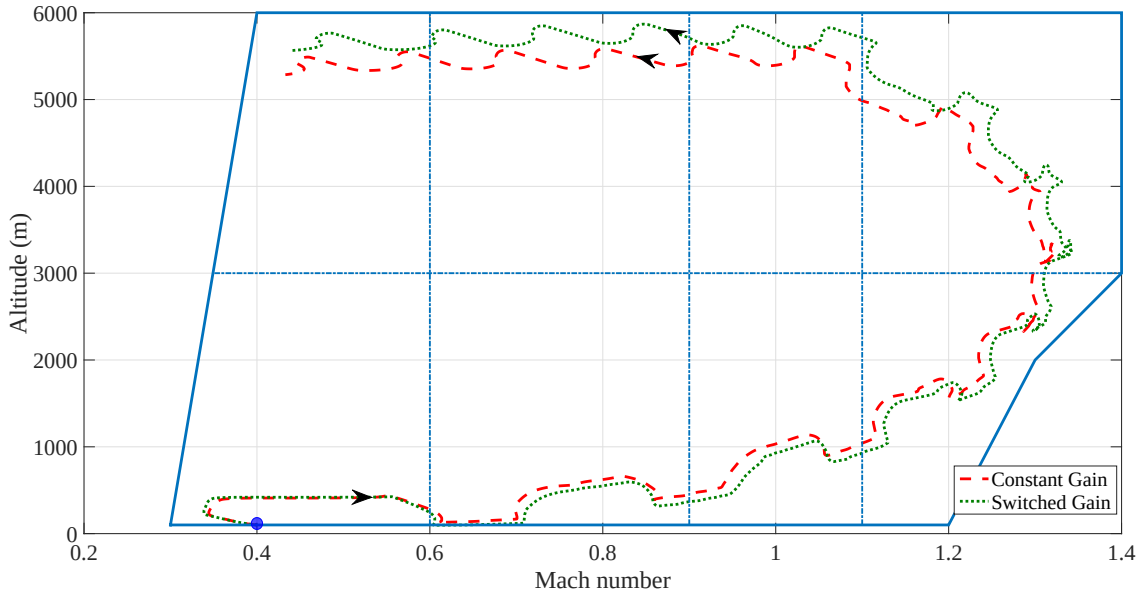

Figure 5.14: Envelope movement of the closed-loop systems, ($M = 0.4$ and $h = 100\,m$)

stick. The responses of the states and the input signals for these two simulations are given in Appendix A.2.

In the first simulation, aircraft moves around the edges of the flight envelope. Hence, the system parameters of the model change quickly and a switched gain controller gives better tracking performance.

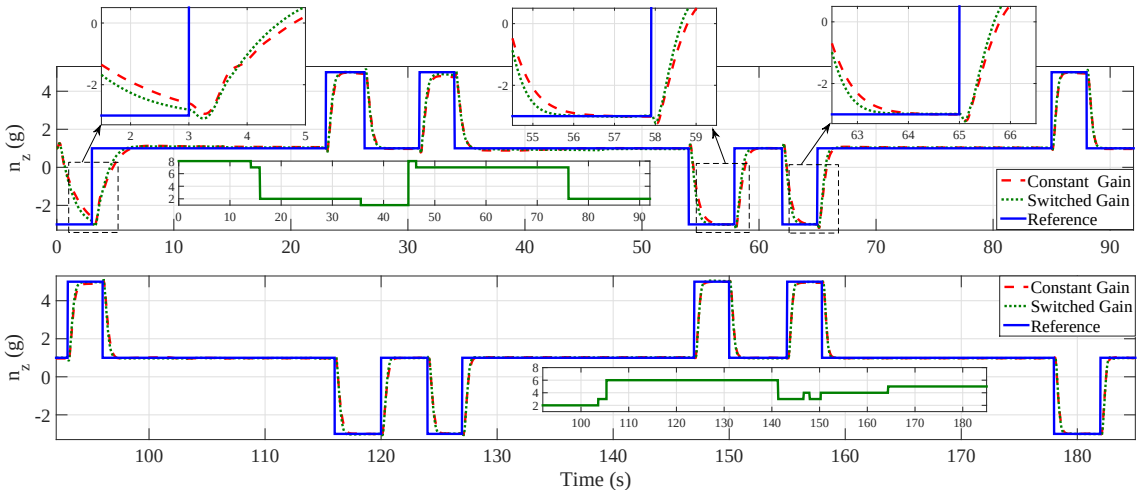

Figure 5.15: Load factor responses of the closed-loop systems, ($M = 0.38$ and $h = 4500\,m$)

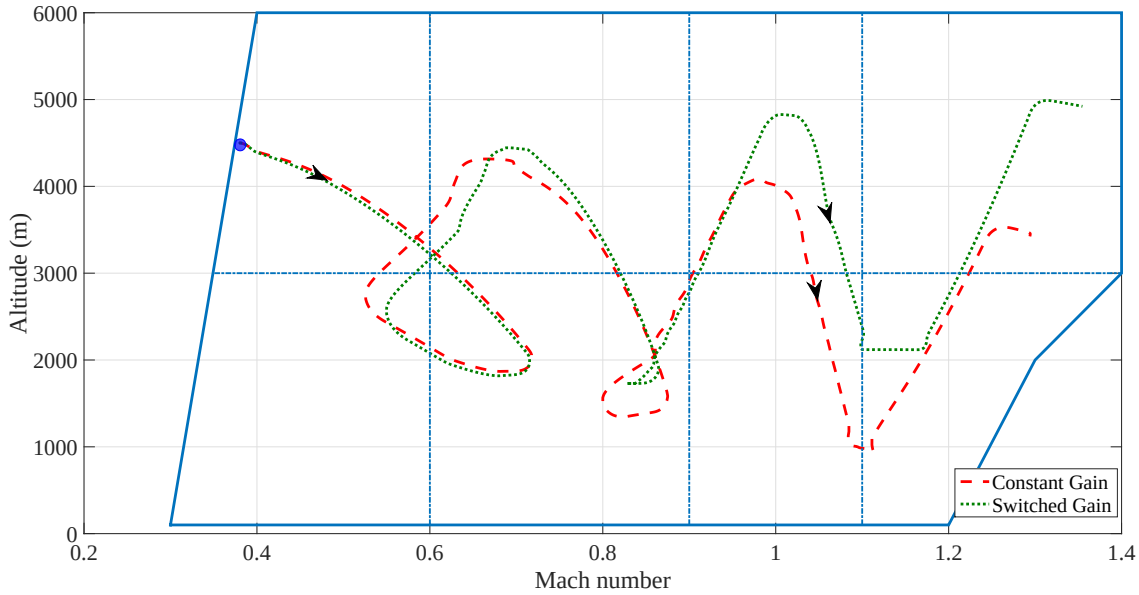

Figure 5.16: Envelope movement of the closed-loop systems, ($M = 0.38$ and $h = 4500\,m$)

In the other simulation, aircraft moves around the center of the flight envelope. In this case, more switching happens however tracking performance of a switched gain controller is nearly same as a constant gain controller. That is because the constant gain controller is designed for a plant located at the center of the envelope. Hence, it gives a good tracking performance around the center of the envelope.

From the results of the short-term simulations, the switched gain controller gives a lower settling time and quicker response than the constant gain controller (see Figure 5.12). From the results of the long term simulations, there is a small difference between the constant gain controller and the switched gain controller results whilst one of the cells 2, 3, 6 or 7 is active, however the differences between them is increased when one of the other cells is active (see Figures 5.15 and 5.13). As a result, the advantages of the switched gain controller over the constant gain controller is proven through the non-linear simulation.

5.5.2 Simulation Results for The Switched Controllers

In this subsection, the non-linear simulation results for the switched controllers are compared with the LQR approach. These controllers are designed by Theorem 3.6.2, Theorem 3.6.5 and the method reported in Section 4.6.

The switched closed-loop systems for each computed controller gain and LQR gain are simulated for $h = 2900\,m$ and $M = [0.5,\ 0.7,\ 1,\ 1.15]$, and the results are then given in Figure 5.17. The label, "Dwell H_2" in this figure indicates the switched gain controller responses which are designed by using Theorem 3.6.5. Although this controller gives nearly the same responses as the LQR method, it gives only a slightly reduced tracking performance at $M = 0.5$.

The label "Dwell L_2" in Figure 5.17 shows the responses of the switched gain controller designed by Theorem 3.6.2. In addition, the label "PWL" shows the responses of the switched gain controller calculated by the PWL approach in Section 4.6. Both switched system responses lack the tracking performance of the LQR method.

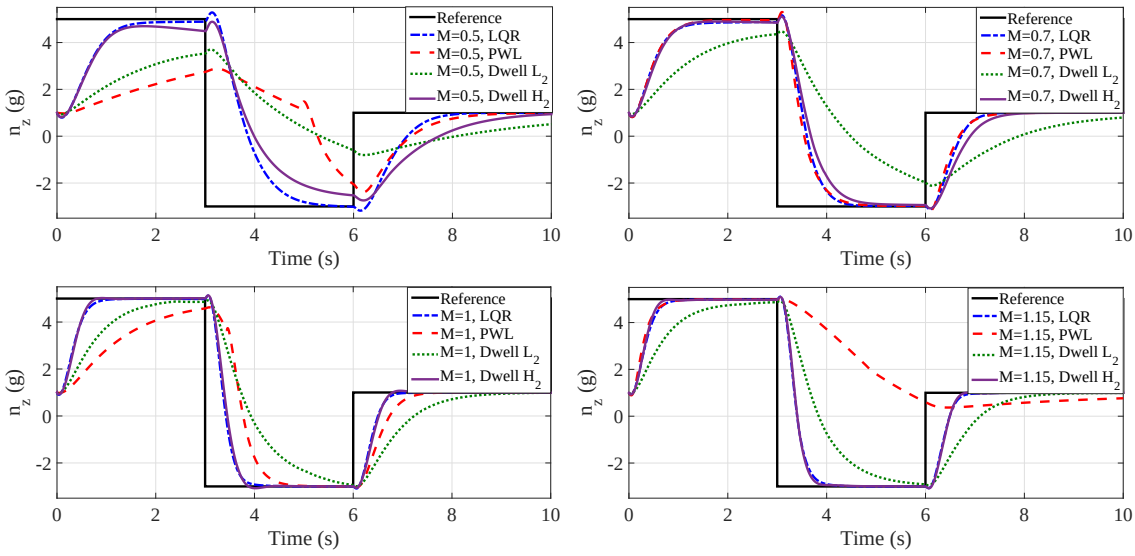

Figure 5.17: Load factor responses of the different switched controller

5.6 Summary

In this chapter, the ADMIRE aircraft model is introduced along with longitudinal control dynamics. The state-feedback integral controller is designed for the longitudinal motion of the ADMIRE model. The switched controller approach is applied to these closed loop systems. The controller gains are calculated with the LQR approach, and the data is taken from the center of each of the cells. Two switched system stability analysis methods - a minimum dwell time and piecewise quadratic stability mentioned, respectively, in Chapters 3 and 4 - are used to analyse the stability of the closed-loop switched system. In addition to this, the controller design techniques in these chapters are used to obtain the switched controller gains. At the end of the chapter, the closed-loop ADMIRE models with the constant gain and switched gain controllers are simulated, the results of which have been illustrated.

The simulation results verified that the switched controller with LQR gains performed better than the constant gain controller. It is noteworthy that the switched controller design techniques were expected to obtain better performance. They could not, however, give a good tracking performance except in one case. On the other hand, the controller design methods prove the stability of the switched system therefore we do not need to apply the stability analyse as in the LQR controller method.

CHAPTER 6

Conclusions and Future work

This thesis has presented the design of switched feedback controllers for load factor tracking and comprehensive stability analysis for a closed loop system with switched feedback controller. Indeed, the thesis has investigated the stability analysis of the switched systems proposed in previous studies, and has also studied how the state-feedback switched controller can be designed by using these studies.

The switched state-feedback controller design strategies have been applied to the ADMIRE model. The differences between the simulation results of these strategies are discussed, and they are also compared to the constant gain state-feedback controlled ADMIRE model. The benefits of the switched controller have been discussed with respect to the constant controller. The detailed contributions are summarized below.

6.1 Conclusions

The work described in this thesis built upon the idea that the switched controller can improve the performance of the system compared to the constant controller, particularly

when there exists large uncertainty. Additionally, detailed switched system stability analysis methods have been performed to prove the stability of the system and also examine how these techniques can be used to design a switched controller for fighter aircraft.

- To start with, the basic concepts and methods for the stability analysis have been given in Chapter 2. In addition to this, the switched systems' stability analysis has been introduced depending on arbitrary and constrained switching signals. $\mathcal{H}_2$, LQR controller design methodologies and state-feedback integral controller strategy are also given in this chapter. Time constraint switching analysis in Chapter 2 cannot be directly applied to the polytopic system, therefore the minimum dwell time theories for the switched systems have been mentioned from the perspective of the time dependent Lyapunov function in Chapter 3. From the definition of dwell time approaches, it is assumed that all subpolytopes are overlapping and asymptotically stable. The stability analysis theories in this chapter have been presented based on parameter independent / dependent Lyapunov functions, as mentioned in (Allerhand and Shaked, 2011) and (Allerhand and Shaked, 2013). Based on these Lyapunov functions, the new method for the state-feedback switched controller design has been proposed with $\mathcal{H}_2$-optimal control technique. The numerical analysis in the defined theorems was formulated, and illustrative examples have been solved by using a modelling and optimisation toolbox, YALMIP, in MATLAB (Lofberg, 2004). From the results of the examples, the constraints on dwell time have been discussed according to the size of the variable and LMIs in the theorems. It is found that a less minimum-dwell time for the switched systems with polytopic uncertainty can be achieved by using the parameter dependent Lyapunov function.

- The other constrained switching signal, state-dependent switching, has been mentioned with the piecewise quadratic stability techniques in Chapter 4. To relax stability conditions, firstly, the state-dependent constraints have been applied to the quadratic stability analysis technique. Additionally, the piecewise quadratic Lyapunov function is defined for the switched stability analysis, and the piece-

wise quadratic stability analysis method has thus been obtained for state-dependent switching. These methods have also been extended to $\mathcal{L}_2$ performance gain between disturbance inputs and outputs. Using the upper and lower bound theories, the state-feedback controller design has been mentioned. These theorems have been demonstrated with illustrative examples.

The main differences between the dwell time and the piecewise quadratic stability analysis is that stability with the minimum dwell time theory can be only achieved even each subsystem is individually stable. Conversely, the stability result with the piecewise quadratic stability analysis can be achieved when one or more subsystems are unstable. Thus, the piecewise quadratic stability analysis technique is more attractive than the minimum dwell time stability method. Assuming all subsystems as overlapping or disjointed cells is another difference between the piecewise stability and minimum dwell time stability analyses.

- The simulation model of the generic fighter aircraft model, ADMIRE, has been investigated in Chapter 5. The linearised system dynamics are reduced to the longitudinal dynamics to control the longitudinal movement of the ADMIRE model. Then, the state-feedback integral controller strategy and the switched controller approach have been applied. The effective controller design method, LQR, has been used to design the controller gains, where the data is taken from the center of each of the cells. The stability of the closed-loop switched system has been proved by using the stability analysis methods in Chapters 3 and 4. Therefore, the switched controller gains have also been designed using the techniques in these chapters. Finally, the closed-loop ADMIRE models with the constant gain and the switched gain controllers have been simulated. The results proved that the switched controller with LQR gains has performed better tracking performance than the constant gain controller. The short-term simulation responses of the switched controllers designed by LQR and stability analysis methods have been compared. The proposed switched controllers stabilise the system; however, only a controller designed by using the

dwell time approach with $\mathcal{H}_2$-optimal control technique can perform as good as the LQR method in terms of tracking performance.

The results of the stability analysis methods have proved the stability of the closed-loop switched system, and these methods are used to design the state-feedback switched controller at the same time. The results derived from the controller design techniques have been applied to the closed-loop ADMIRE model. Simulation results have shown that all three proposed switched controllers stabilise the system; however, only the second proposed switched controller can perform with as good a tracking performance as the LQR method. The simulation results have also proved that the switched controller with LQR gains has provided better tracking performance than the constant gain controller.

6.2 Future Work

The study presented can be further extended in several directions.

- **Stability Analysis:**

  In this thesis, the stability analysis methods are built on some assumptions. Hence, different stability analysis methods in the literature can be applied to find more accurate results with fewer assumptions (for example, non-linear stability analysis techniques).

  In real applications, sensors, actuators and computer delays cause a time-shift in the input signals that can affect the stability of the switched systems. Hence, the proposed methods in this thesis can be extended for the stability analysis of switched time-delay systems.

  Switched controllers are designed based on the state-feedback; one future research direction is to use output feedback for the switched controller design.

- **Application:**

  In this thesis, we use the state-dependent switching law for the ADMIRE aircraft model. Noise/ Disturbance dependent switching rules can be further applied to reduce effects on the performance. In addition, the performance can be increased using both switching rules with state-dependent and noise/ disturbance dependent.

  The LQR approach is used to compare the performance between switched and constant gain controlled system responses. One can apply the different robust control techniques to generalize the advantages of the switched gain controller over the constant gain controller.

  Switched state-feedback longitudinal control for the ADMIRE aircraft model is studied in this thesis. Additionally, lateral control can be designed and a full flight control system (FCS) can be achieved using both controllers.

APPENDIX A

Numerical & Simulation Results

A.1 Controller Gains for ADMIRE Model

$*$ The switched controller gains calculated by using the standard LQR approach:

$$K_1 = \begin{bmatrix} -1.2009 & -0.0623 & -12.5209 & -2.7394 & -0.4546 & 0.0009 \\ -0.2407 & 1.2201 & -4.0695 & -0.3735 & 1.5555 & 0.0001 \end{bmatrix},$$

$$K_2 = \begin{bmatrix} -0.9946 & 0.0186 & -13.5308 & -1.8310 & -0.1350 & 0.0002 \\ -0.1036 & 0.3126 & -3.3264 & -0.0551 & 2.7704 & -0.0000 \end{bmatrix},$$

$$K_3 = \begin{bmatrix} -0.9984 & -0.0184 & -13.8539 & -1.5738 & 0.0084 & 0.0001 \\ -0.0567 & 0.3120 & -0.6174 & -0.1022 & -0.4319 & 0.0000 \end{bmatrix},$$

$$K_4 = \begin{bmatrix} -0.9931 & -0.0236 & -14.2769 & -1.7266 & -0.1787 & 0.0001 \\ -0.1177 & 0.3141 & -2.8860 & -0.1170 & 1.7105 & -0.0000 \end{bmatrix},$$

$$K_5 = \begin{bmatrix} -0.9943 & -0.0268 & -12.8339 & -1.7756 & -0.0896 & 0.0001 \\ -0.1062 & 0.3141 & -2.0089 & -0.1512 & 0.7684 & -0.0000 \end{bmatrix},$$

$$K_6 = \begin{bmatrix} -0.9982 & -0.0160 & -12.0685 & -1.6543 & -0.0144 & 0.0001 \\ -0.0603 & 0.3119 & -0.8723 & -0.1124 & -0.1198 & 0.0000 \end{bmatrix},$$

$$K_7 = \begin{bmatrix} -0.9960 & 0.0075 & -12.1592 & -2.0000 & -0.1617 & 0.0003 \\ -0.0897 & 0.9974 & -2.1784 & -0.1842 & 0.7645 & 0.0000 \end{bmatrix},$$

$$K_8 = \begin{bmatrix} -0.9867 & -0.0150 & -10.8524 & -2.6837 & -0.3347 & 0.0008 \\ -0.1625 & 0.9970 & -3.3478 & -0.4030 & 0.8052 & 0.0001 \end{bmatrix}.$$

$*$ The constant controller gains calculated by using the standard LQR approach:

$$K = \begin{bmatrix} -0.9983 & 0.0110 & -14.1958 & -1.7067 & -0.0703 & 0.0002 \\ -0.0584 & 0.3115 & -1.9370 & -0.0700 & 1.3930 & 0.0000 \end{bmatrix}.$$

$*$ The switched controller gains calculated by using Theorem 3.6.2:

$$K_1 = \begin{bmatrix} -7.0012 & 0.0497 & 71.4976 & -8.0456 & -123.9549 & 0.3303 \\ -6.6028 & 0.0732 & -22.2104 & 1.0087 & 24.1061 & -0.0505 \end{bmatrix},$$

$$K_2 = \begin{bmatrix} 2.0265 & -0.0318 & 33.2071 & -2.2514 & -53.9825 & 0.1197 \\ -7.4051 & 0.0706 & 9.5513 & -1.0167 & -16.0243 & 0.0446 \end{bmatrix},$$

$$K_3 = \begin{bmatrix} -0.3281 & -0.0012 & 21.1361 & -1.1896 & -33.5404 & 0.0686 \\ -2.3864 & 0.0255 & -3.1770 & 0.1045 & 2.1633 & 0.0027 \end{bmatrix},$$

$$K_4 = \begin{bmatrix} -1.5095 & 0.0116 & 31.7415 & -1.5587 & -42.4383 & 0.0844 \\ -1.9361 & 0.0220 & -1.7372 & 0.2445 & 3.9458 & -0.0145 \end{bmatrix},$$

$$K_5 = \begin{bmatrix} -0.3069 & -0.0010 & 26.7588 & -1.5800 & -39.5003 & 0.0685 \\ -0.8257 & 0.0086 & 1.1554 & 0.0031 & -1.0842 & -0.0016 \end{bmatrix},$$

$$K_6 = \begin{bmatrix} -0.8870 & 0.0038 & 24.6798 & -1.4701 & -38.0784 & 0.0816 \\ -2.1644 & 0.0229 & -2.3099 & 0.0539 & 0.9090 & 0.0031 \end{bmatrix},$$

$$K_7 = \begin{bmatrix} 0.5631 & -0.0192 & 41.9903 & -2.9676 & -66.5081 & 0.1540 \\ -8.4315 & 0.0810 & 4.9162 & -0.8754 & -12.6452 & 0.0353 \end{bmatrix},$$

$$K_8 = \begin{bmatrix} -9.6410 & 0.0727 & 75.2097 & -7.5065 & -125.1077 & 0.3319 \\ -8.4839 & 0.0914 & -16.4999 & 0.5931 & 14.8969 & -0.0349 \end{bmatrix}.$$

$*$ The switched controller gains calculated by using Theorem 3.6.5:

$$K_1 = \begin{bmatrix} -3.5575 & 0.0299 & -51.1786 & -8.9018 & 11.5594 & -0.0130 \\ -0.3148 & 1.3193 & -6.1107 & -1.1478 & 0.1363 & -0.0023 \end{bmatrix},$$

$$K_2 = \begin{bmatrix} -10.4926 & -0.1159 & -198.3273 & -9.7432 & 124.7830 & -0.1527 \\ -0.5974 & 0.8712 & -13.5024 & -0.7063 & 8.0736 & -0.0129 \end{bmatrix},$$

$$K_3 = \begin{bmatrix} 1.2026 & -0.0533 & 23.6534 & -0.7210 & -16.4736 & 0.0204 \\ -0.0388 & 0.9438 & -3.8465 & -0.2715 & 2.4747 & -0.0063 \end{bmatrix},$$

$$K_4 = \begin{bmatrix} 1.3686 & -0.0317 & 40.6305 & -0.4977 & -29.4672 & 0.0358 \\ 0.2914 & 0.5518 & 7.3623 & 0.0688 & -5.2941 & 0.0056 \end{bmatrix},$$

$$K_5 = \begin{bmatrix} 0.5882 & -0.0427 & 16.8989 & -1.0843 & -12.2811 & 0.0154 \\ 0.6040 & 0.6065 & 13.8730 & 0.2562 & -9.9023 & 0.0107 \end{bmatrix},$$

$$K_6 = \begin{bmatrix} 0.2678 & -0.0635 & 1.8614 & -1.3783 & -1.5759 & 0.0026 \\ -0.0875 & 0.9270 & -4.8344 & -0.3297 & 2.8703 & -0.0070 \end{bmatrix},$$

$$K_7 = \begin{bmatrix} -12.4334 & -0.1847 & -217.0436 & -14.6079 & 124.8535 & -0.1469 \\ -1.8470 & 1.1209 & -34.3957 & -2.2778 & 19.1682 & -0.0263 \end{bmatrix},$$

$$K_8 = \begin{bmatrix} -2.6311 & -0.0062 & -36.9486 & -6.4338 & 10.3942 & -0.0090 \\ -0.2794 & 1.1471 & -6.0978 & -1.0966 & 0.4192 & -0.0031 \end{bmatrix}.$$

$*$ The switched controller gains found by using the method in Section 4.6.

$$
\begin{aligned}
K_1 &= \begin{bmatrix} -0.0392 & -0.0409 & -4.9994 & -0.3992 & -0.0804 & 0.0000 \\ -0.1399 & 0.9962 & -3.0109 & -0.2537 & 1.0561 & 0.0000 \end{bmatrix}, \\
K_2 &= \begin{bmatrix} -0.9581 & 0.0347 & -13.3054 & -1.6939 & -0.0235 & 0.0002 \\ -0.0256 & 0.9964 & -1.6281 & -0.1389 & 0.0673 & -0.0000 \end{bmatrix}, \\
K_3 &= \begin{bmatrix} -0.0781 & -0.0701 & -6.3235 & -0.7388 & 0.0073 & 0.0000 \\ -0.0026 & 0.9938 & -0.3941 & -0.0607 & -0.3433 & 0.0000 \end{bmatrix}, \\
K_4 &= \begin{bmatrix} -0.7811 & -0.0631 & -9.6619 & -0.8096 & -0.0745 & 0.0001 \\ -0.0737 & 0.9968 & -1.7194 & -0.0423 & 0.9245 & -0.0000 \end{bmatrix}, \\
K_5 &= \begin{bmatrix} -0.0160 & -0.0909 & -3.6252 & -0.4879 & -0.0394 & -0.0000 \\ -0.0138 & 0.9948 & -0.9703 & -0.0482 & 0.3787 & -0.0000 \end{bmatrix}, \\
K_6 &= \begin{bmatrix} -0.3722 & -0.0770 & -8.3080 & -1.1634 & -0.0098 & 0.0000 \\ -0.0313 & 0.9931 & -0.8979 & -0.1103 & -0.2272 & 0.0000 \end{bmatrix}, \\
K_7 &= \begin{bmatrix} -0.6744 & 0.0061 & -9.0164 & -0.8201 & -0.1055 & 0.0002 \\ -0.0924 & 0.9971 & -2.4056 & -0.1670 & 1.0519 & 0.0000 \end{bmatrix}, \\
K_8 &= \begin{bmatrix} -0.4974 & -0.0264 & -7.5636 & -1.1531 & -0.1838 & 0.0004 \\ -0.1413 & 0.9964 & -3.2211 & -0.3364 & 0.8435 & 0.0001 \end{bmatrix}.
\end{aligned}
$$

A.2 Long-term Simulation Results

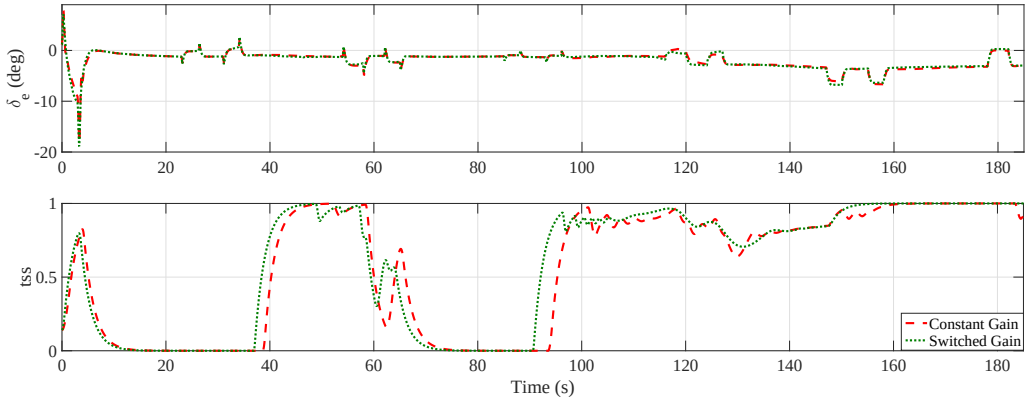

Figure A.1: Input responses of the switched systems for $M = 0.38$ and $h = 4500\,m$

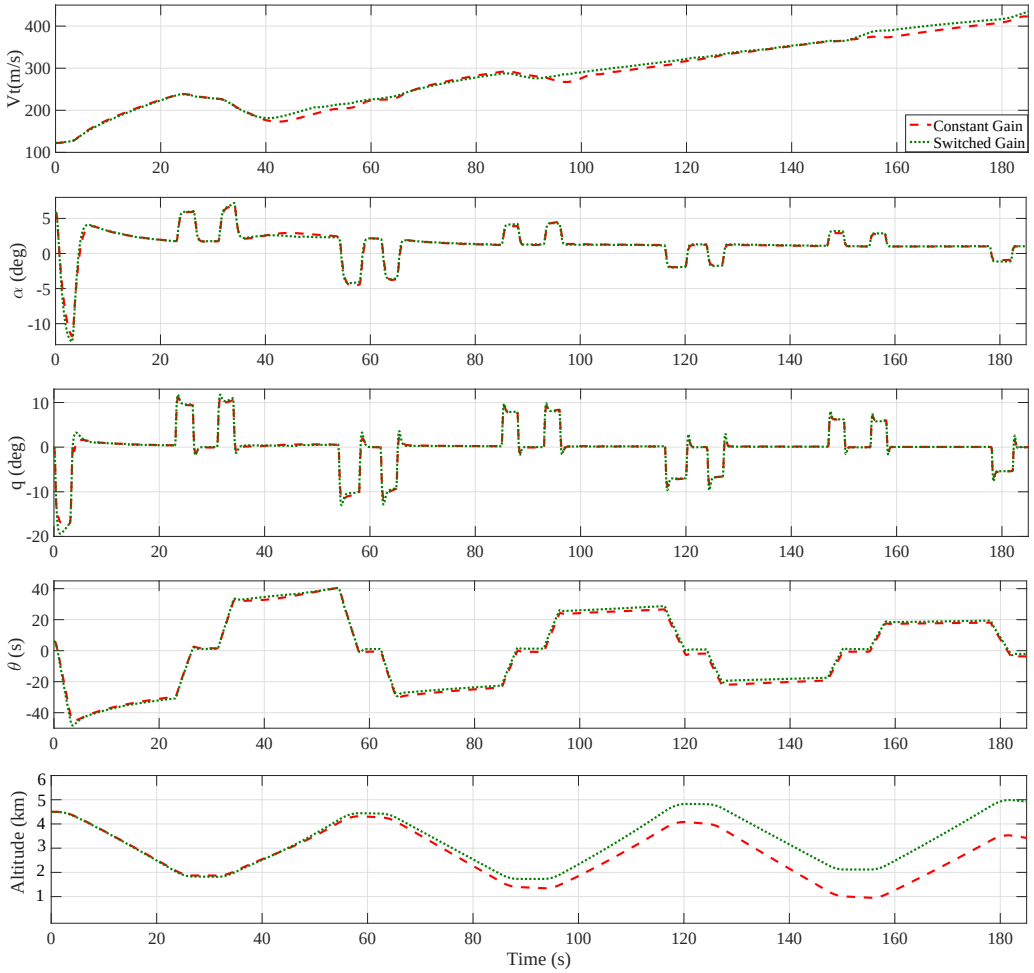

Figure A.2: State responses of the switched systems for $M = 0.38$ and $h = 4500\,m$

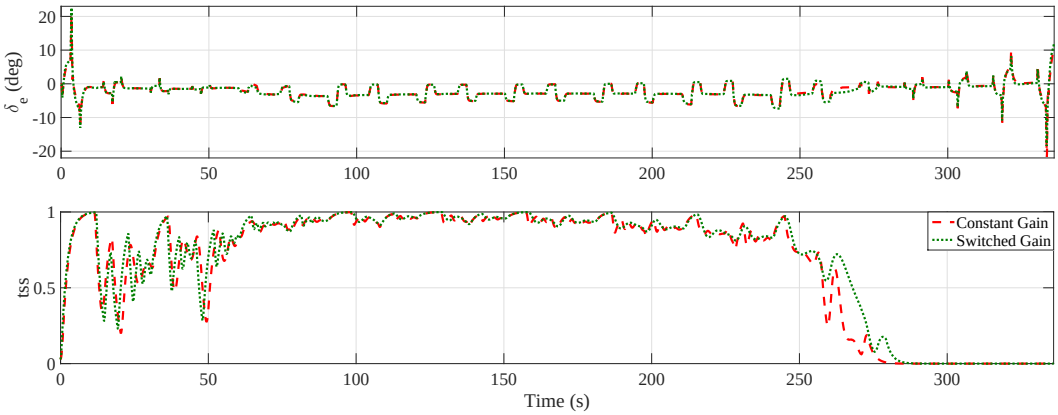

Figure A.3: Input responses of the switched systems for $M = 0.4$ and $h = 100\,m$

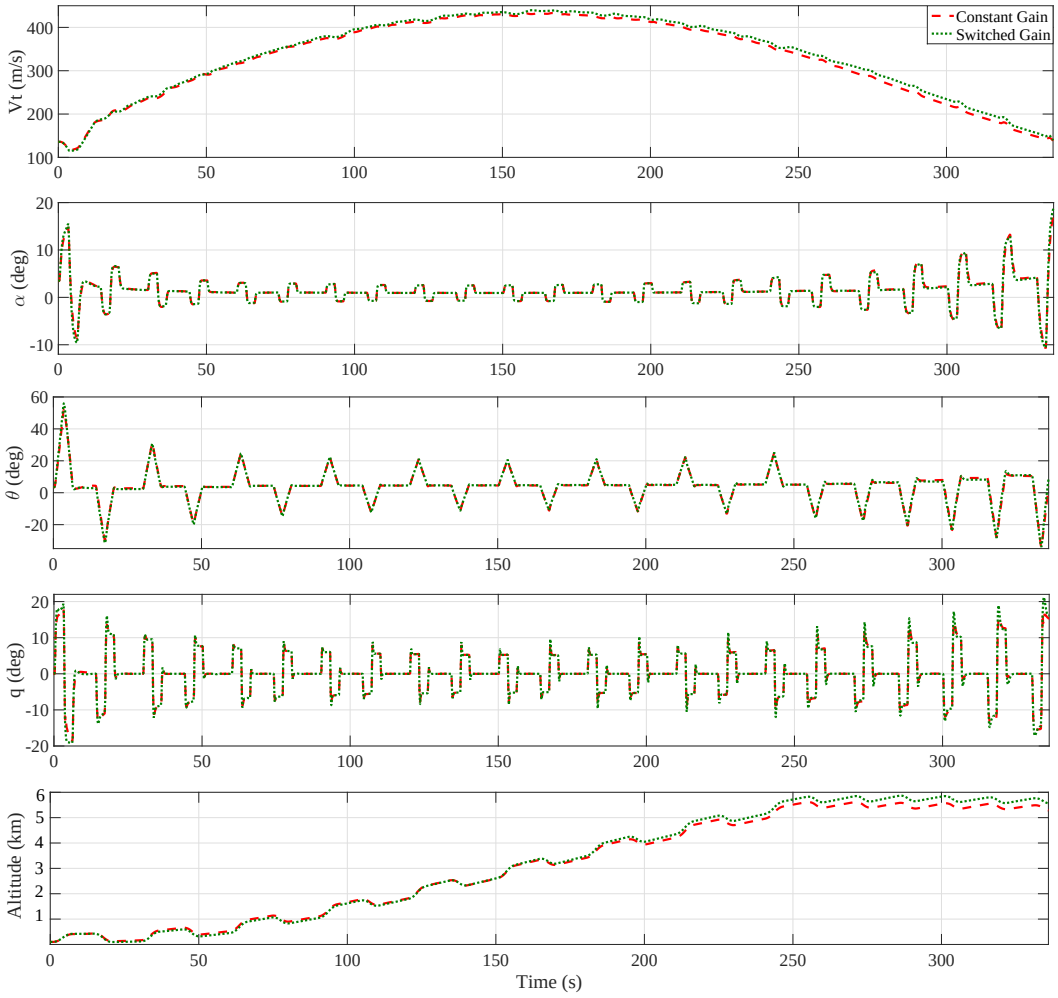

Figure A.4: State responses of the switched systems for $M = 0.4$ and $h = 100\,m$

Bibliography

L. I. Allerhand and U. Shaked. Robust control of switched linear systems with dwell time. In *IEEE 26th Convention of Electrical and Electronics Engineers in Israel*, pages 198–201. IEEE, 2010.

L. I. Allerhand and U. Shaked. Robust stability and stabilization of linear switched systems with dwell time. *IEEE Transactions on Automatic Control*, 56(2):381–386, 2011.

L. I. Allerhand and U. Shaked. Robust control of linear systems via switching. *IEEE Transactions on Automatic Control*, 58(2):506–512, 2013.

S. Boyarski and U. Shaked. Time-convexity and time-gain-scheduling in finite-horizon robust H_∞-control. In *Proceedings of the 48th IEEE Conference on Decision and Control, held jointly with the 28th Chinese Control Conference*, pages 2765–2770. IEEE, 2009.

S. P. Boyd, L. El Ghaoui, E. Feron, and V. Balakrishnan. *Linear Matrix Inequalities in System and Control Theory*, volume 15. SIAM, 1994.

M. S. Branicky. Stability of Switched and Hybrid Systems. In *Proceedings of the 33rd IEEE Conference on Decision and Control*, volume 4, pages 3498–3503. IEEE, 1994.

R. W. Brockett. *Hybrid models for motion control systems*. Springer, 1993.

G. Chesi, P. Colaneri, J. C. Geromel, R. Middleton, and R. N. Shorten. Computing upper-bounds of the minimum dwell time of linear switched systems via homogeneous polynomial Lyapunov functions. In *American Control Conference (ACC)*, pages 2487–2492. IEEE, 2010.

M. C. de Oliveira and R. E. Skelton. Stability tests for constrained linear systems. In *Perspectives in robust control*, pages 241–257. Springer, 2001.

R. A. DeCarlo, M. S. Branicky, S. Pettersson, and B. Lennartson. Perspectives and results on the stability and stabilizability of hybrid systems. *Proceedings of the IEEE*, 88(7): 1069–1082, 2000.

K. Derinkuyu and M. Ç. Pınar. On the S-procedure and some variants. *Mathematical Methods of Operations Research*, 64(1):55–77, 2006.

R. C. Dorf and R. H. Bishop. *Modern control systems*. Pearson, Twelfth edition, 2011.

G. R. Duan and H. H. Yu. *LMIs in Control Systems: Analysis, Design and Applications*. CRC Press, 2013.

P. Finsler. *Uber das Vorkommen definiter und semidefiniter Formen in Scharen quadratischer Formem*, volume 9. Commentarii Mathematici Helvetici, 1937.

L. Forssell and U. Nilsson. *ADMIRE the aero-data model in a research environment version 4.0, model description*. FOI-Totalförsvarets forskningsinstitut, 2005.

G. F. Franklin, J. D. Powell, and A. Emami-Naeini. *Feedback Control of Dynamic Systems*. Pearson Education Limited, Sixth (International Edition) edition, 2010.

P. Gahinet, A. Nemirovskii, A. J. Laub, and M. Chilali. The LMI Control Toolbox. In *Proceedings of the 33rd IEEE Conference on Decision and Control*, volume 3, pages 2038–2041. IEEE, 1995.

D. Gangsaas, K. R. Bruce, J. D. Blight, and U. L. Ly. Application of modern synthesis to aircraft control: three case studies. *IEEE Transactions on Automatic Control*, 31(11): 995–1014, 1986.

J. C. Geromel and P. Colaneri. Stabilization of continuous-time switched systems. In *Proceedings of the 16th IFAC World Congress*, 2005.

J. C. Geromel and P. Colaneri. Stability and stabilization of continuous-time switched linear systems. *SIAM Journal on Control and Optimization*, 45(5):1915–1930, 2006.

J. C. Geromel, M. C. de Oliveira, and L. Hsu. LMI characterization of structural and robust stability. In *Proceedings of the American Control Conference*, volume 3, pages 1888–1892. IEEE, 1999.

G. Hadley. *Linear algebra*. Addison-Wesley, Reading, MA, 1961.

M. Hagström. The ADMIRE benchmark aircraft model. *Nonlinear Analysis and Synthesis Techniques for Aircraft Control*, pages 35–54, 2007.

S. Hedlund and M. Johansson. PWLTOOL: A Matlab Toolbox for Analysis of Piecewise Linear Systems. 1999.

J. P. Hespanha. Root-mean-square gains of switched linear systems. *IEEE Transactions on Automatic Control,*, 48(11):2040–2045, Nov 2003.

J. P. Hespanha. Uniform stability of switched linear systems: extensions of Lasalle's Invariance Principle. *IEEE Transactions on Automatic Control*, 49(4):470–482, April 2004a.

J. P. Hespanha. Stabilization through hybrid control. *Encyclopedia of Life Support Systems (EOLSS)*, 2004b.

J. P. Hespanha. *Linear systems theory*. Princeton university press, 2009.

K. Hirata and J. P. Hespanha. $\mathcal{L}_2$-induced gain analysis for a class of switched systems. In *Proceedings of the 48th IEEE Conference on Decision and Control, held jointly with the 28th Chinese Control Conference*, pages 2138–2143. IEEE, 2009.

M. Johansson. *Piecewise Linear Control Systems*. PhD thesis, Lund Institute of Technology, Sweden, Department of Automatic Control, 1999.

M. Johansson. *Piecewise linear control systems*. Springer, 2003.

M. Johansson and A. Rantzer. Computation of piecewise quadratic Lyapunov functions for hybrid systems. Technical Report ISRN LUTFD2/TFRT-7459-SE, Department of Automatic Control, 1996.

M. Johansson and A. Rantzer. On the computation of piecewise quadratic Lyapunov functions. In *Proceedings of the 36th IEEE Conference on Decision and Control*, San Diego, California, Dec. 1997a.

M. Johansson and A. Rantzer. Computation of piecewise quadratic Lyapunov functions for hybrid systems. In *Proceedings of the European Control Conference*, Brussels, Belgium, July 1997b.

M. Johansson and A. Rantzer. Computation of piecewise quadratic Lyapunov functions for hybrid systems. *IEEE Transactions on Automatic Control*, 43(4):555–559, 1998.

F. Karlsson. Nonlinear flight control design and analysis challenge. *Nonlinear Analysis and Synthesis Techniques for Aircraft Control*, pages 55–65, 2007.

M. Kermani and A. Sakly. Stability analysis for a class of switched nonlinear time-delay systems. *Systems Science & Control Engineering: An Open Access Journal*, 2(1):80–89, 2014.

H. K. Khalil. *Nonlinear Systems*. Prentice-Hall, Inc., Third edition, 2002.

W. S. Levine. *Control System Advanced Methods*. USA: Taylor and Francis Group, 2011.

F. L. Lewis. *Applied optimal control and estimation*. Prentice Hall PTR, 1992.

D. Liberzon. *Switching in Systems and Control*. Boston: Birkhäuser, 2003.

D. Liberzon. Switched Systems. In *Handbook of Networked and Embedded Control Systems*, pages 559–574. Springer, 2005.

D. Liberzon and A. S. Morse. Basic problems in stability and design of switched systems. *IEEE Control Systems*, 19(5):59–70, 1999.

H. Lin and P. J. Antsaklis. Stability and stabilizability of switched linear systems: A survey of recent results. *IEEE Transactions on Automatic control*, 54(2):308–322, 2009.

J. Lofberg. YALMIP: A toolbox for modeling and optimization in MATLAB. In *IEEE International Symposium on Computer Aided Control Systems Design*, pages 284–289. IEEE, 2004.

A. M. Lyapunov. *The General Problem of The Stability of Motion*. PhD thesis, University of Kharkov. Published by Kharkov Mathematical Society, 1892.

M. Margaliot and J. P. Hespanha. Root-mean-square gains of switched linear systems: A variational approach. *Automatica*, 44(9):2398–2402, 2008.

A. N. Michel. Recent trends in the stability analysis of hybrid dynamical systems. *IEEE Transactions on Circuits and Systems I: Fundamental Theory and Applications*, 46(1): 120–134, 1999.

A. S. Morse. *Control using logic-based switching*. Springer, 1995.

R. M. Murray. Optimization-based control. *California Institute of Technology, CA*, 2009.

R. C. Nelson. *Flight stability and automatic control*, volume 2. WCB/McGraw Hill, 1998.

K. Ogata. *Modern Control Engineering*. Prentice-Hall International, Inc., Second edition, 1990.

K. Ogata. *Modern Control Engineering*. Prentice-Hall International, Inc., Fifth edition, 2010.

G. Papageorgiou, K. Glover, G. D'Mello, and Y. Patel. Taking robust lpv control into flight on the vaac harrier. In *Decision and Control, 2000. Proceedings of the 39th IEEE Conference on*, volume 5, pages 4558–4564. IEEE, 2000.

S. Pettersson. Synthesis of Switched Linear Systems. In *Proceedings of the 42nd IEEE Conference on Decision and Control*, volume 5, pages 5283–5288. IEEE, 2003.

S. Pettersson and B. Lennartson. Modelling, analysis & synthesis of hybrid systems. In *Preprints of Reglermöte '96*, 1996a.

S. Pettersson and B. Lennartson. Stability and robustness for hybrid systems. In *Proceedings of the 35th IEEE Conference on Decision and Control*, volume 2, pages 1202–1207. IEEE, 1996b.

S. Pettersson and B. Lennartson. Stability and robustness for hybrid systems. Technical Report CTH/RT/I-96/003, Control Engineering Laboratory, Chalmers University of Technology, July 1996c.

S. Pettersson and B. Lennartson. Exponential stability analysis of nonlinear systems using LMIs. In *Proceedings of the 36th IEEE Conference on Decision and Control*, volume 1, pages 199–204. IEEE, 1997a.

S. Pettersson and B. Lennartson. LMI for stability and robustness of hybrid systems. In *Proceedings of the American Control Conference*, volume 3, pages 1714–1718. IEEE, 1997b.

S. Pettersson and B. Lennartson. An LMI approach for stability analysis of nonlinear systems. *Proceedings of Europian Control Conference, Brussels, Belgium*, 1997c.

S. Pettersson and B. Lennartson. Exponential stability of hybrid systems using piecewise quadratic Lyapunov functions resulting in LMIs. In *IFAC, 14th Triennial World Congress, Beijing, PR China*. Citeseer, 1999.

S. Pettersson and B. Lennartson. Hybrid system stability and robustness verification using linear matrix inequalities. *International Journal of Control*, 75(16-17):1335–1355, 2002.

A. Y. Pogromsky, M. Jirstrand, and P. Spangeus. On stability and passivity of a class of hybrid systems. In *IEEE Conference on Decision and Control*, volume 4, pages 3705–3710. IEEE, 1998.

I. Queinnec, S. Tarbouriech, and G. Garcia. A state-space approach for stability analysis of a combat aircraft in presence of rate limits involving pilot-induced-oscillation. Technical report, 2002.

A. Rantzer and M. Johansson. Piecewise linear quadratic optimal control. In *Proceedings of the American Control Conference, Albuquerque, New Mexico*, 1997.

A. Rantzer and M. Johansson. Piecewise linear quadratic optimal control. *IEEE Transactions on Automatic Control*, 45(4):629–637, 2000.

A. V. Savkin, E. Skafidas, and R. J. Evans. Robust output feedback stabilizability via controller switching. *Automatica*, 35(1):69–74, 1999.

C. Scherer and S. Weiland. Linear matrix inequalities in control. *Lecture Notes, Dutch Institute for Systems and Control, Delft, The Netherlands*, 3, 2000.

H. R. Shaker, R. Wisniewski, and S. Tabatabaeipour. Switched controller order reduction. In *IEEE International Conference on Control and Automation*, pages 2237–2242. IEEE, 2009.

J.-Y. Shin, G. J. Balas, and M. A. Kaya. Blending methodology of linear parameter

varying control synthesis of f-16 aircraft system. *Journal of Guidance, Control, and Dynamics*, 25(6):1040–1048, 2002.

M. Sidoryuk, M. Goman, S. Kendrick, D. Walker, and P. Perfect. An LPV control law design and evaluation for the ADMIRE model. *Nonlinear Analysis and Synthesis Techniques for Aircraft Control*, pages 197–229, 2007.

E. Skafidas, R. J. Evans, A. V. Savkin, and I. R. Petersen. Robust stabilization via state feedback controller switching. In *2nd Asian Control Conference*, volume 3, pages 235–239, 1997.

E. Skafidas, R. J. Evans, A. V. Savkin, and I. R. Petersen. Stability results for switched controller systems. *Automatica*, 35(4):553–564, 1999.

J. J. E. Slotine and W. Li. *Applied Nonlinear Control*. Prentice Hall international Inc., Englewood Cliffs, New Jersey, 1991.

B. L. Stevens and F. L. Lewis. *Aircraft Control and Simulation*. John Wiley & Sons, 1992.

Y. Sun and L. Wang. On stability of a class of switched nonlinear systems. *Automatica*, 49(1):305–307, 2013.

Z. Sun and S. S. Ge. Analysis and synthesis of switched linear control systems. *Automatica*, 41(2):181–195, 2005.

M. Turner, N. Aouf, D. Bates, I. Postlethwaite, and B. Boulet. Switched control of a vertical/short take-off land aircraft: an application of linear quadratic bumpless transfer. *Proceedings of the Institution of Mechanical Engineers, Part I: Journal of Systems and Control Engineering*, 220(3):157–170, 2006.

F. Wirth. A converse Lyapunov theorem for linear parameter-varying and linear switching systems. *SIAM journal on control and optimization*, 44(1):210–239, 2005.

L. Wu and W. X. Zheng. Weighted H_∞ model reduction for linear switched systems with time-varying delay. *Automatica*, 45(1):186–193, 2009.

X. Zhao, L. Zhang, and P. Shi. Stability of a class of switched positive linear time-delay systems. *International Journal of Robust and Nonlinear Control*, 23(5):578–589, 2013.

K. Zhou, J. C. Doyle, K. Glover, et al. *Robust and optimal control*, volume 40. Prentice hall New Jersey, 1996.